AMRL-TR-78-50

LEVEL Ⅱ

ADA058040

OPTICAL POWER SPECTRUM ANALYSIS OF DISPLAY IMAGERY

RICHARD A. SCHINDLER

LOGISTICS SUPPORT AND SERVICES DIVISION
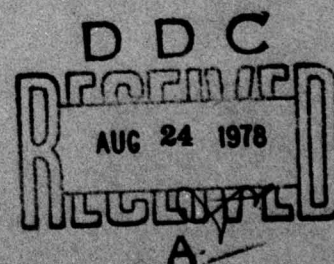*BOEING AEROSPACE COMPANY*
SEATTLE, WASHINGTON 98124

WAYNE L. MARTIN

AEROSPACE MEDICAL RESEARCH LABORATORY

JUNE 1978

DDC
RECEIVED
AUG 24 1978
A.

AEROSPACE MEDICAL RESEARCH LABORATORY
AEROSPACE MEDICAL DIVISION
AIR FORCE SYSTEMS COMMAND
WRIGHT-PATTERSON AIR FORCE BASE, OHIO 45433

78 08 21 029

NOTICES

When US Government drawings, specifications, or other data are used for any purpose other than a definitely related Government procurement operation, the Government thereby incurs no responsibility nor any obligation whatsoever, and the fact that the Government may have formulated, furnished, or in any way supplied the said drawings, specifications, or other data, is not to be regarded by implication or otherwise, as in any manner licensing the holder or any other person or corporation, or conveying any rights or permission to manufacture, use, or sell any patented invention that may in any way be related thereto.

Please do not request copies of this report from Aerospace Medical Research Laboratory. Additional copies may be purchased from:

> National Technical Information Service
> 5285 Port Royal Road
> Springfield, Virginia 22161

Federal Government agencies and their contractors registered with Defense Documentation Center should direct requests for copies of this report to:

> Defense Documentation Center
> Cameron Station
> Alexandria, Virginia 22314
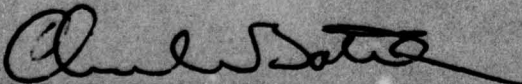
TECHNICAL REVIEW AND APPROVAL

AMRL-TR-78-50

This report has been reviewed by the Information Office (OI) and is releasable to the National Technical Information Service (NTIS). At NTIS, it will be available to the general public, including foreign nations.

This technical report has been reviewed and is approved for publication.

FOR THE COMMANDER

CHARLES BATES, JR.
Chief
Human Engineering Division
Aerospace Medical Research Laboratory

REPORT DOCUMENTATION PAGE		READ INSTRUCTIONS BEFORE COMPLETING FORM
1. REPORT NUMBER AMRL-TR-78-50	2. GOVT ACCESSION NO.	3. RECIPIENT'S CATALOG NUMBER
4. TITLE (and Subtitle) OPTICAL POWER SPECTRUM ANALYSIS OF DISPLAY IMAGERY		5. TYPE OF REPORT & PERIOD COVERED Final Report, 3 May 1976 - 31 March 1978
		6. PERFORMING ORG. REPORT NUMBER
7. AUTHOR(s) Richard A. Schindler (Boeing Aerospace Co.) Wayne L. Martin (Aerospace Medical Research Lab)		8. CONTRACT OR GRANT NUMBER(s) F33615-76-C-0030
9. PERFORMING ORGANIZATION NAME AND ADDRESS Logistics Support and Services Division Boeing Aerospace Company Seattle, Washington 98124		10. PROGRAM ELEMENT, PROJECT, TASK AREA & WORK UNIT NUMBERS 61102F; 2313-V1-15
11. CONTROLLING OFFICE NAME AND ADDRESS Aerospace Medical Research Laboratory Aerospace Medical Division (AFSC) Wright-Patterson AFB, Ohio 45433		12. REPORT DATE June 1978
		13. NUMBER OF PAGES 134
14. MONITORING AGENCY NAME & ADDRESS(if different from Controlling Office) 134 p.		15. SECURITY CLASS. (of this report) UNCLASSIFIED
		15a. DECLASSIFICATION/DOWNGRADING SCHEDULE

16. DISTRIBUTION STATEMENT (of this Report)

Approved for public release; distribution unlimited

410 375.

17. DISTRIBUTION STATEMENT (of the abstract entered in Block 20, if different from Report)

18. SUPPLEMENTARY NOTES

19. KEY WORDS (Continue on reverse side if necessary and identify by block number)

Diffraction Pattern Sampling
CRT Display Evaluation
Information Theory
Optical Power Spectrum
Observer Target Recognition

20. ABSTRACT (Continue on reverse side if necessary and identify by block number)

This report describes the approach, procedures and results of a series of studies to examine the use of a simple, rapid measurement technique for the quantitative evaluation of display imagery. This technique, diffraction pattern sampling, provides an estimate of the image optical power spectrum. The resulting values are used to calculate the image information density for CRT imagery under various levels of display operating

DD FORM 1 JAN 73 1473   EDITION OF 1 NOV 65 IS OBSOLETE

410 375

parameters. The resulting information density values are compared with observer target recognition performance under the same display conditions. The report considers the effectiveness, characteristics and limitations of the diffraction pattern sampling technique.

SUMMARY

PURPOSE

The effort reported here is concerned with the quantitative evaluation
of display imagery. Emphasis is on the use of image power spectral data
along with the concepts and formulations of information theory. Specifi-
cally, the effort is concerned with the feasibility and effectiveness of
a simple and rapid technique, diffraction pattern sampling, for obtain-
ing an estimate of the image optical power spectrum and the use of this
estimate in an information theory metric, i.e, information density.

APPROACH

The application of diffraction pattern sampling to the determination of
image information density was evaluated in a series of studies using CRT
displays. In these studies several display operating parameter values
were varied. The effects of this variation on the measured information
density values and on observer target recognition performance were
determined. The relationship between information density and observer
performance was then evaluated.

Display parameters treated in these studies were:

- display dynamic range

- bandwidth

- noise

- luminance quantization level using a
  matrix input and pulse coded
  modulation (PCM).

Target recognition performance was measured using a series of "zoom"
sequences of tactical military vehicles. The visual angle of the

vehicle at recognition was used as the measure of performance. Information density measures were made using standardized inputs (random dot and random bar patterns) as well as the vehicle images used in the performance tests. Since the measurement technique requires the use of photographic transparencies, the CRT images were recorded on film for the information density measurements.

RESULTS AND CONCLUSIONS

The information density values based on diffraction pattern sampling for the random dot and random bar patterns exhibit very strong positive relationships with CRT dynamic range and bandwidth. Product-moment correlation coefficients for the dot pattern, for example, are 0.997 with log dynamic range and 0.98 with log bandwidth. The random bar results are comparable. Information density values for the vehicle images correlate less strongly, 0.90 and 0.88 with log dynamic range and log bandwidth respectively. Differences due to noise levels and number of quantization levels used in these studies were too small to establish significant relationships.

The relationships between information density and observer target recognition performance are more variable than those with display parameters but are sufficiently strong to demonstrate a high degree of promise for the diffraction pattern sampling approach. Product-moment correlation coefficients across all three performance studies exceed 0.90. When the results are corrected for differences among the three studies in the film recording scale used, the correlation is increased to 0.97.

The results, however, indicate a number of problem areas that must be resolved if the full potential of this approach is to be realized. The most important are:

2

-   the measurements at low spatial frequencies are distorted
    by artifacts in the measurement techniques used in this
    study. The results, furthermore, suggest that these low
    frequency values are likely to be important correlates
    of observer performance.

-   the approach utilized here does not incorporate the
    effects of visual thresholds. A proper image evaluation
    must include considerations of the viewer's perceptual
    limitations.

-   techniques for the measurement of quantization noise
    in digitized imagery must be improved for evaluation of
    this image type.

Potential solutions for these problems are available and should be
considered in future applications of the diffraction pattern sampling
approach.

3

PREFACE

This report was prepared by the Crew Systems Technology organization, Logistics Support and Services Division of the Boeing Aerospace Company, Seattle, Washington. The work was done under USAF Contract F33615-76-C-0030, for the Visual Display Systems Branch, Human Engineering Division, of the Aerospace Medical Research Laboratory. Mr. Wayne Martin was the Technical Monitor for the Air Force.

The contract effort was initiated in May, 1976 and completed in March, 1978. Mr. D. Zipoy was Program Manager and Mr. R. Schindler was Principal Investigator for the Boeing Company.

Significant contributions to the research effort were made by Mr. C. Pyle for observer performance data collection and Mr. B. Wittman and Mr. E. Jones for display systems laboratory support. Special acknowledgement is made of the comments and suggestions by Capt. A. Ginsburg of AMRL.

TABLE OF CONTENTS

SECTION I
INTRODUCTION

The evaluation of imagery and imaging systems by means of spatial frequency analysis has become an important approach in many areas of application.

Frequency transformation has been found to be a valuable tool in several areas of research including: visual perception (Campbell, 1968; Blakemore et al, 1973), image quality metrics (Shaw, 1962; Feldgett and Linfoot, 1955; Harris, 1964), and in some procedures for determining the modulation transfer function (Swing and Shin, 1963; Vander Lugt and Mitchel, 1967). The term "optical power spectrum" (OPS) is used in this report to refer to the results of an image measurement process that describes the content of an image in terms of its spatial frequency components. This measurement process uses an optical analog of the familiar mathematical Fourier transform to translate image content from spatial dimensions (units of distance) to frequency dimensions (units of cycles per distance). An important application of interest in this report is the use of this transform in the information theory approach to the quantification of image content. The information theory approach for image evaluation has been developing rapidly in recent years and offers a valuable framework, particularly with the increasing interest in electro-optical and digitized imagery. Dainty and Shaw (1974) provide a good review of work in this area.

There are two basic approaches to the determination of an image Fourier transform. One technique utilizes a scanner to digitize the image and a computer to perform the Fourier transformation. The second involves the principles of coherent optical processing to form a pattern of light (Frauhofer diffraction pattern), whose amplitude distribution is proportional to the Fourier transform. Measurement of the diffraction pattern distribution allows the determination of the desired results.

The digitizing approach can provide an exact Fourier transform, (within the performance limits of the scanner), but the scanning process is very slow and, because of the large amount of data involved, the required computer processing is also slow and expensive. The coherent optical processing technique does not require digitization of the image and, because the Fourier transform is accomplished optically, the computer processing requirements are greatly reduced. Even with this technique, however, the precise determination of the Fourier transform is a very difficult and time-consuming process when dealing with complex two-dimensional imagery. The photometric resolution and sensitivity require-ments for precise measurement of the diffraction pattern light distri-bution are not insignificant. With either technique, the precise measure-ment of the Fourier transform involves data loads and time intervals that become prohibitive if large amounts of imagery are to be measured. If the OPS approach is to achieve a practical level of utility for routine display and image evaluation, simple, rapid, and inexpensive measurement techniques are highly desirable.

Lendaris and Stanley (1970) found that an estimate of the Fourier trans-form obtained by coarse sampling of the Fraunhofer diffraction pattern could be used for some automatic pattern recognition tasks. Since that time diffraction pattern sampling has been found to be effective for image quality determination, cloud cover analysis and a variety of additional pattern recognition tasks; Jensen (1973), Nill (1976), Leachtenauer (1977), Kasdan (1977), and Lukes (1977). All of these studies used a very small number of samples, (between 8 and 64) to characterize the diffraction pattern light distribution. This provides a data load reduction of many orders of magnitude. Furthermore, with the use of a segmented photodetector, the sampling can be accomplished in parallel, providing measurement times in fractions of a second rather than minutes or hours required for a precise Fourier transformation. The data processing requirements for many applications are reduced by the coarse sampling to levels easily handled by a desk calculator. These benefits of increased speed and reduced expense are very attractive for

7

the practical application of Fourier analysis to routine image evaluation.

A critical question is whether such an estimate can be used in conjunction with appropriate information theory metrics to provide a useful tool for display image evaluation.

It is the purpose of this study to evaluate such applications under conditions that are particularly severe with respect to the assumptions and artifacts involved in diffraction pattern sampling. This will be accomplished by using selected measurement procedures to obtain information density values under controlled variation in CRT display operating parameters, (i.e., dynamic range, bandwidth, noise, and quantization levels). Evaluation criteria will include the sensitivity and validity of variation in information density values as a function of changes in CRT parameter levels. In addition, the evaluation will include the correlation of information density values with observer target recognition performance under these display conditions.

The initial sections of this report describe the diffraction pattern sampling technique and applications to information theory metrics. This is followed by the development of specific measurement and data processing procedures with application to CRT imagery. The final sections describe the evaluation of the approach and procedures through a series of observer performance tests.

8

SECTION II
BACKGROUND

THE OPTICAL POWER SPECTRUM AND FRAUNHOFER DIFFRACTION

Dainty and Shaw (1974), define the optical power spectrum, $P(k_x, k_y)$, as,

$$P(k_x, k_y) = \lim_{A \to \infty} \left\langle \frac{\left| F(k_x, k_y) \right|^2}{A} \right\rangle \qquad (1)$$

where,

$\left| F(k_x, k_y) \right|^2$ is the squared modulus of the Fourier transform of an image distribution $t(x,y)$.

A is the area of the image, and the symbols "$\langle \; \rangle$" denote ensemble average.

There are several ways to obtain the Fourier transform of an image distribution. Armstrong and Thompson (1977), for example, provide a comparison of coherent and incoherent optical techniques. The work in this report is limited to the use of a coherent optical approach based on the principles of light diffraction.

The theoretical development of this approach has been treated extensively in the literature and will not be repeated here. Goodman (1968), Smith and Thompson (1971), and Ditchburn (1963), provide good sources for this material. If, as shown in Figure 1, a film transparency is

IMAGE PLANE

TRANSFORM LENS

FRAUNHOFER DIFFRACTION PLANE

PLANE WAVEFRONT

F
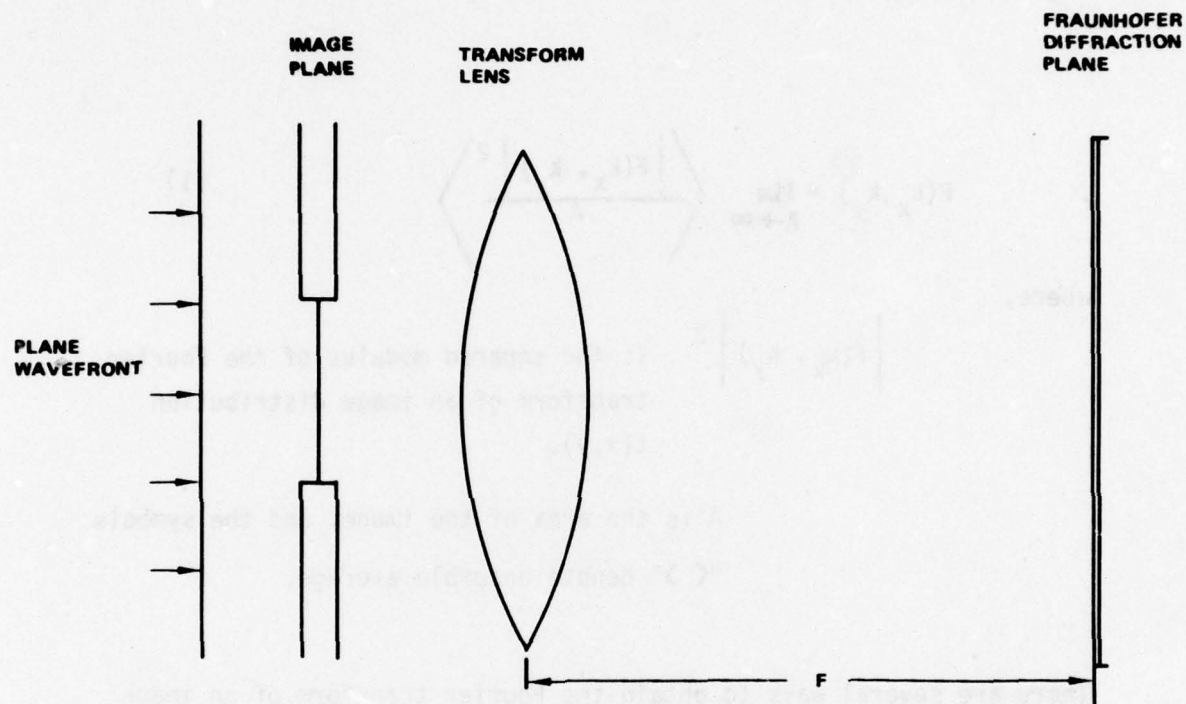
Figure 1. Optical Conditions for Fraunhofer Diffraction Pattern Sampling

illuminated with coherent, collimated light and the diffracted and non-diffracted light is collected by a lens, then a special pattern of light is produced at the back focal plane of the lens. This is the Fraunhofer diffraction pattern. The distribution of light intensity in this pattern is related to the image Fourier transform and is a function of the orientation, spacing, sharpness and contrast of the edges in the film transparency. After Goodman (1968), the intensity distribution, I (u, v), is described by,

$$I(u,v) = \frac{L^2}{\lambda^2 F^2} \left| \iint_{-\infty}^{\infty} t(x,y) \exp\left[-j \frac{2\pi}{\lambda F} (xu + yv) \right] dx\,dy \right|^2 \quad (2)$$

where,

L^2 is the intensity of the illuminating source,

λ is the wavelength of the source,

F is the focal length of the "transform" lens,

$t(x,y)$ is the light amplitude distribution immediately following the input film plane, and

j is $\sqrt{-1}$

The coordinates, (u, v), in the diffraction plane are related to coordinates in the frequency domain, (k_x, k_y), by,

$$k_x = u/\lambda F \quad (3)$$

$$k_y = v/\lambda F \quad (4)$$

Consequently, we can rewrite (2) as,

11

$$I(k_x, k_y) = \frac{L^2}{\lambda^2 F^2} \left| \iint\limits_{-\infty}^{\infty} t(x,y) \exp\left[-j2\pi(xk_x + yk_y) \right] dx\, dy \right|^2 \quad (5)$$

and from the definition of the Fourier transform,

$$I(k_x, k_y) = \frac{L^2}{\lambda^2 F^2} \left| F(k_x, k_y) \right|^2 \quad (6)$$

Combining equations (1) and (6),

$$P(k_x, k_y) = \lim_{A \to \infty} \left\langle \frac{\lambda^2 F^2}{L^2 A} I(k_x, k_y) \right\rangle \quad (7)$$

It will be convenient to consider equation (7) in terms of polar coordinates. Thus, if we define,

$$r = (k^2_x + k^2_y)^{\frac{1}{2}}, \quad \text{and} \quad (8)$$

$$\theta = \tan^{-1}(k_x/k_y) \quad (9)$$

equation (7) becomes,

$$P(r,\theta) = \lim_{A \to \infty} \left\langle \frac{\lambda^2 F^2}{L^2 A} I(r,\theta) \right\rangle \quad (10)$$

The limit and ensemble average operations are for the evaluation of images involving random processes, e.g., noise. A specific image can be evaluated without their implied requirements.

12

It should be noted that there is some disagreement in the literature concerning the definition of the optical power spectrum. See, for example, Nill (1976), and Shannon and Cheatham, (1976). The discrepancies, however, are restricted to the evaluation of the constants and, since the application in this study will involve only power ratios, the differences are only academic. For purposes of illustration we have chosen the definition by Dainty and Shaw (1974) because of its consistency with the analogous measures in electronics and with incoherent optical techniques.

To provide a simple example of a power spectrum consider the one-dimensional case of a slit of width a. The input function is,

$$t(x) = \begin{cases} 1 & \text{for } |x| \leq a/2 \\ 0 & \text{elsewhere} \end{cases}$$

From Goodman (1968), where illuminating intensity, $L^2 = 1$,

$$I(u) = \frac{a^2}{\lambda^2 F^2} \, \text{sinc}^2 \, \frac{au}{\lambda F}$$

Using equation (3)

$$I(k_x) = \frac{a^2}{\lambda^2 F^2} \, \text{sinc}^2 \, (ak_x)$$

In polar coordinates,

$$I(r) = \frac{a^2}{\lambda^2 F^2} \, \text{sinc}^2 \, (ar)$$

and from (10)

$$P(r) = \text{sinc}^2 \, (ar) \qquad\qquad (11)$$

where,
$$\text{sinc } (ar) = \frac{\sin (\pi ar)}{\pi ar}$$

Figure 2 is a plot of equation (11) for a slit where a = 1.5 millimeters.

DIFFRACTION PATTERN SAMPLING

Equation (10) shows that the optical power spectrum is determined by measuring the diffraction pattern intensity distribution. Exact measurement of this distribution is a formidable task because of the large dynamic range, (5 to 6 orders of magnitude is a typical range) and for patterns such as that represented by Figure 2, very high resolution is required. For example, with the 1016 millimeter focal length lens used in this study, the individual cycles in Figure 2 are less than one-half millimeter apart. In order to simplify the measurement and to significantly reduce the resulting data loads, the diffraction pattern distribution is sampled by integrating over large areas in the pattern. In this study, a segmented photodetector, configured as shown in Figure 3, is used. The detector consists of a series of ring elements to measure intensity as a function of radial distance, (and, hence, spatial frequency), and a series of wedge elements to measure intensity as a function of orientation. For purposes of optical power spectrum measurement, only the ring elements are used. This approach permits a very rapid measurement rate with minimum data loads. For example, the data reported in this study are the result of over 2000 individual power spectrum measurements, mostly from complex two-dimensional imagery. A sample of this size would not be possible with other techniques without expenditure of significant resources. The speed and simplicity, however, are at the expense of losing the fine detail in the true power spectrum. To illustrate the sampling effect, the spectrum in Figure 2 has been integrated over intervals corresponding to the detector configuration used here. The resulting spectrum, Figure 4, shows the effects of the "smoothing." It is clear that the resulting measurement provides
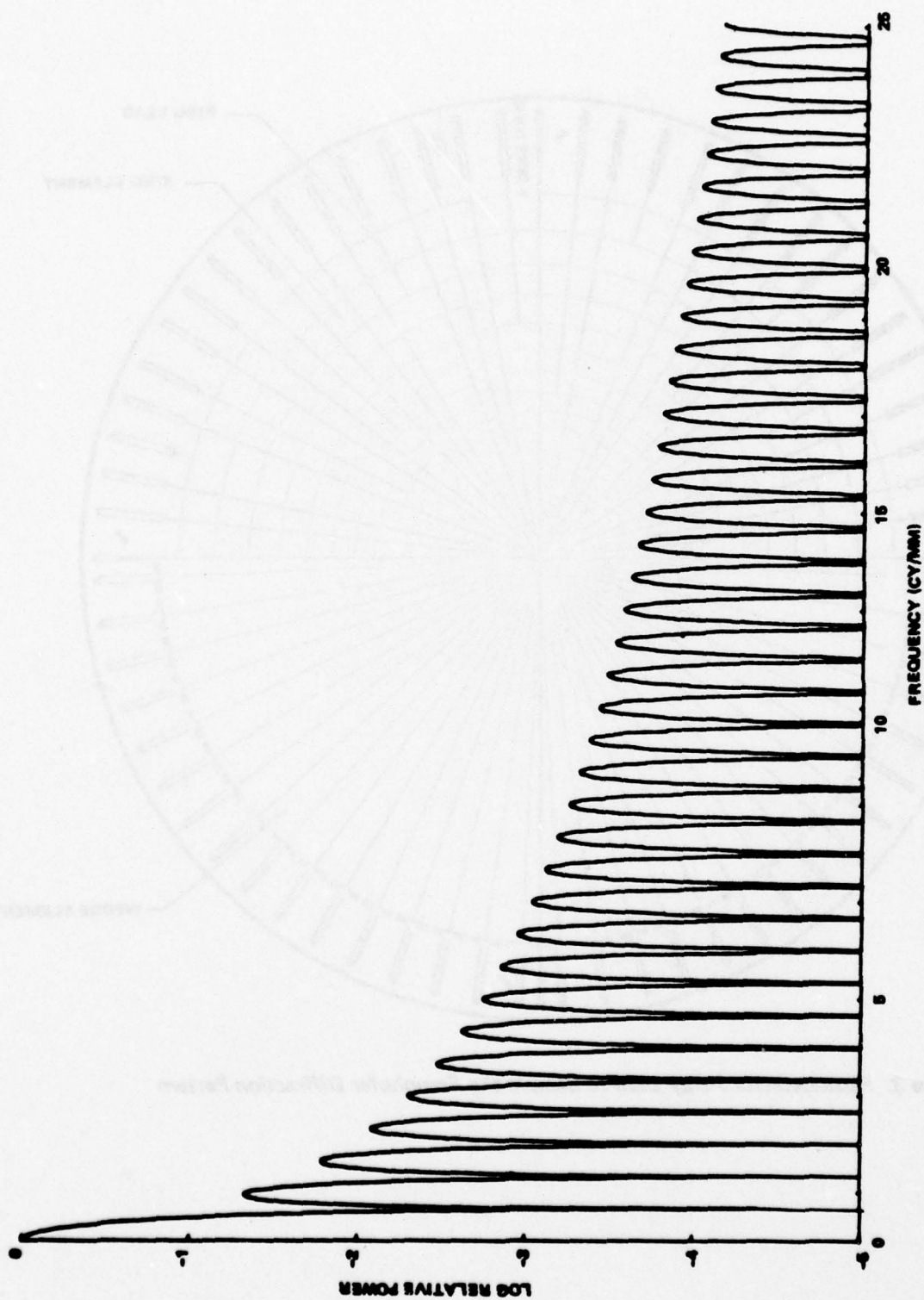
14

Figure 2. Theoretical Optical Power Spectrum for a 1.5 mm Wide Slit

FREQUENCY (CY/MM)

LOG RELATIVE POWER

15

RING LEAD

RING ELEMENT

WEDGE ELEMENT
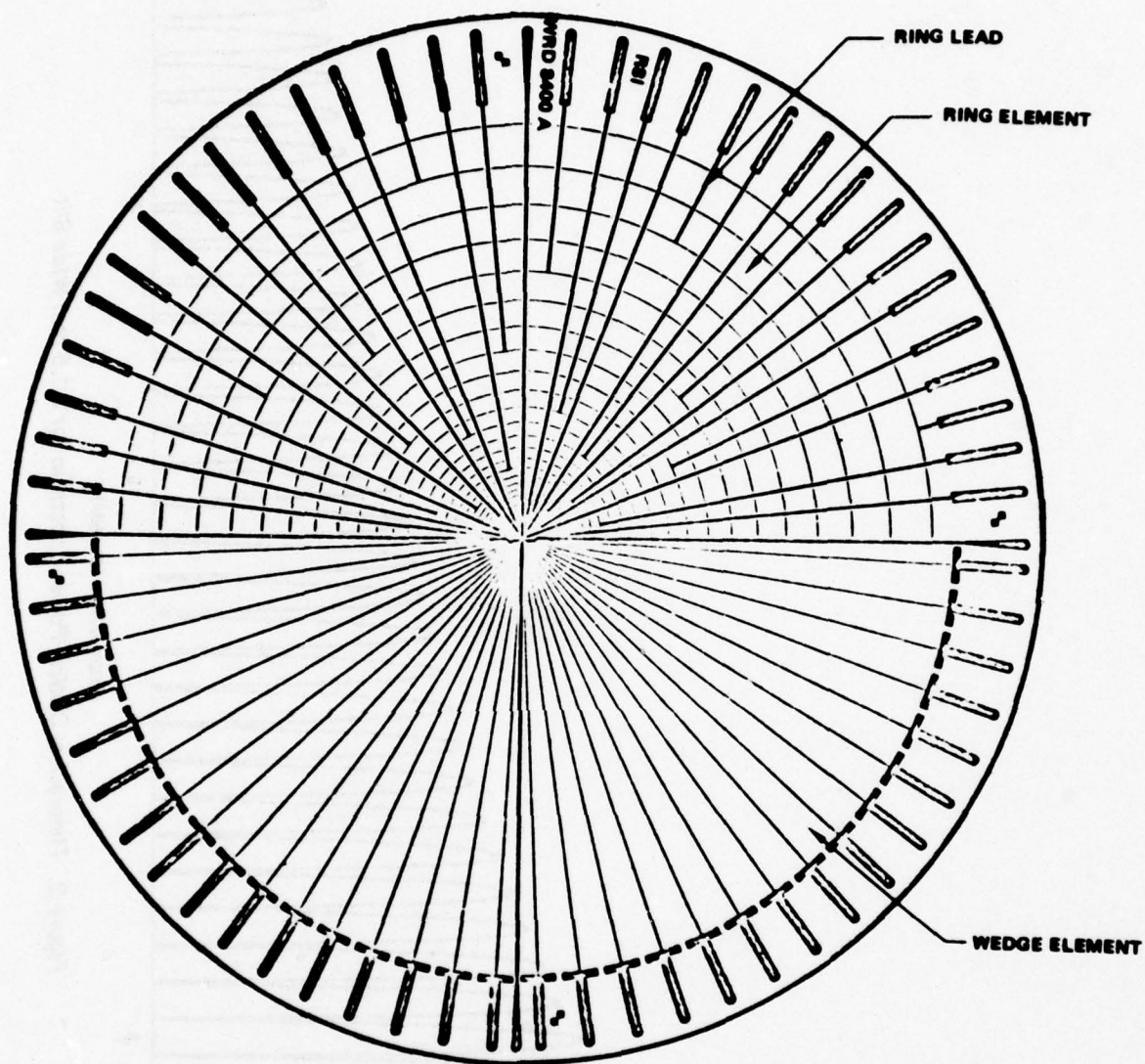
Figure 3. Photodetector Array Used to Sample the Fraunhofer Diffraction Pattern
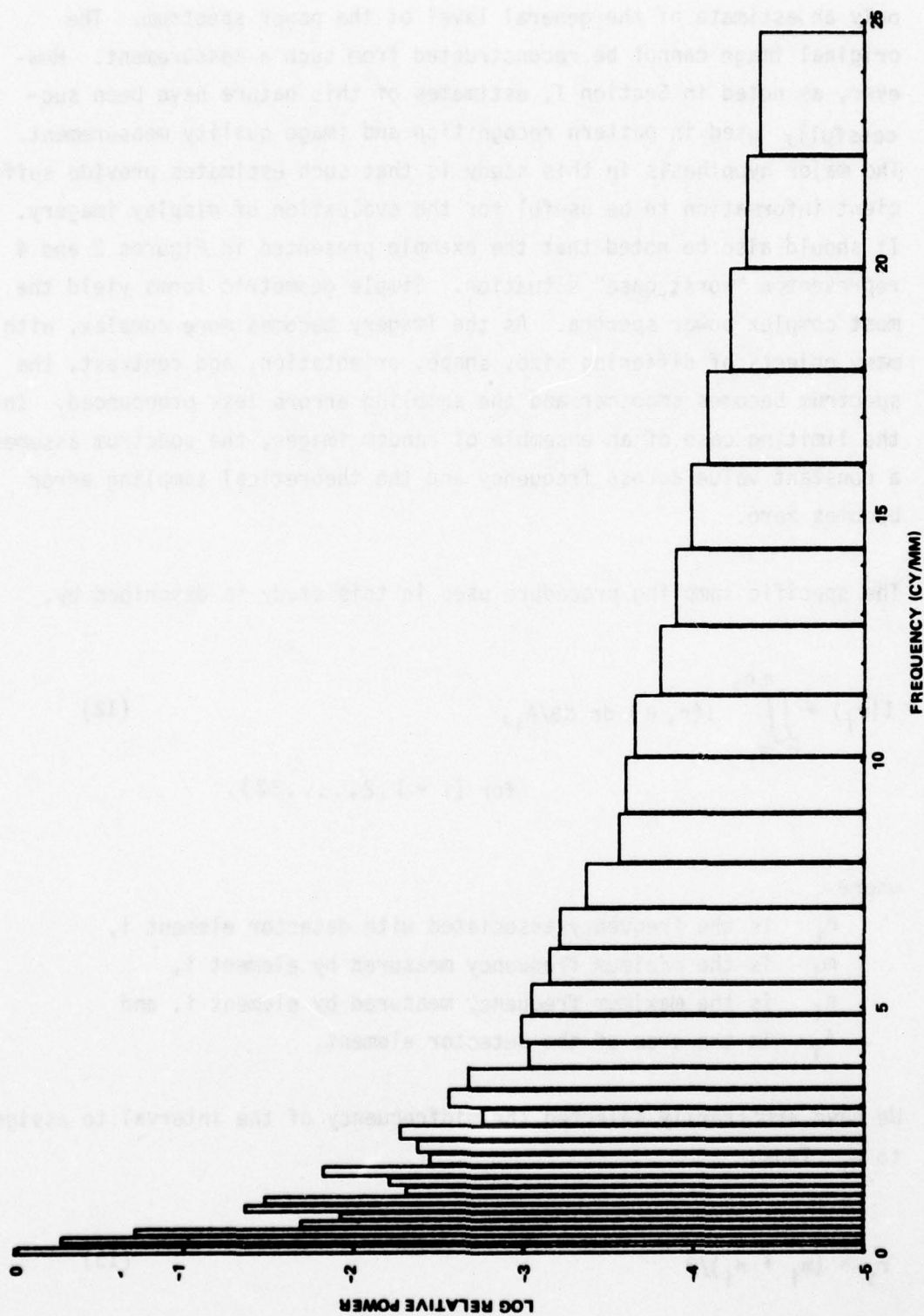
16

Figure 4. Effect of Diffraction Pattern Sampling on the Optical Power Spectrum Shown in Figure 2.

only an estimate of the general level of the power spectrum. The
original image cannot be reconstructed from such a measurement. How-
ever, as noted in Section I, estimates of this nature have been suc-
cessfully used in pattern recognition and image quality measurement.
The major hypothesis in this study is that such estimates provide suffi-
cient information to be useful for the evaluation of display imagery.
It should also be noted that the example presented in Figures 2 and 4
represents a "worst case" situation. Simple geometric forms yield the
most complex power spectra. As the imagery becomes more complex, with
many objects of differing size, shape, orientation, and contrast, the
spectrum becomes smoother and the sampling errors less pronounced. In
the limiting case of an ensemble of random images, the spectrum assumes
a constant value across frequency and the theoretical sampling error
becomes zero.

The specific sampling procedure used in this study is described by,

$$I(\overline{r}_i) = \iint\limits_{0 \ \ m_i}^{\pi \ \ n_i} I(r, \theta) \ dr \ d\theta / A_i , \qquad (12)$$

$$\text{for } (i = 1, 2, \ldots, 32),$$

where

$\overline{r}_i$ is the frequency associated with detector element i,

m_i is the minimum frequency measured by element i,

n_i is the maximum frequency measured by element i, and

A_i is the area of the detector element.

We have arbitrarily selected the midfrequency of the interval to assign
to $\overline{r}_i$. Thus,

$$\overline{r}_i = (m_i + n_i)/2 \qquad (13)$$

Specific values of r_i, m_i, n_i, and A_i as used in this study are presented in Section III.

As seen in equation (12) the individual elements integrate across the angle as well as across discrete frequency intervals. The integration is from 0 to π representing only one-half of the total circle. This is acceptable because a two-dimensional image distribution produces a diffraction pattern that is bilaterally symmetric, Kasdan (1977). The implications of the annular integration are very significant when measurements are made of two-dimensional imagery. The capability to determine individual power spectra as a function of angular orientation is lost. The radial integration is strictly valid only if the diffraction pattern is radially symmetric, i.e., if the input image distribution is radially symmetric (isotropic). For most practical measurement situations, the assumption of a radially symmetric image distribution will not be true. The symmetry of the distribution is affected by the image content and by the nature of the imaging process. Conventional photographic systems are approximately radially symmetric in response but the CRT display systems of interest in this study are not likely to behave in this fashion. The potential errors introduced by non-symmetric (anisotropic) image distributions is of major concern throughout this study.

The annular integration does have advantages, however. The result represents the ensemble average of all possible one-dimensional spectra for the image of interest. This contributes greatly to the data load reduction and to the stability of the resulting power spectrum data.

MEASUREMENT ARTIFACTS
In addition to the effects of the sampling technique described above, there are a number of error sources inherent in the diffraction pattern sampling process that may reduce the accuracy of the resulting optical power spectrum estimates.

19

Linearity and Additivity

The optical power spectrum is a function of the complex amplitude distribution of the input image.

Image distributions are most commonly expressed in units of intensity transmittance or optical density. Amplitude transmittance, as the square root of intensity, will not have the same properties as the more common units. This is particularly relevant to assumptions about linearity and additivity in the subsequent applications of the power spectrum data.

Phase Effects

Because of dependence on complex amplitude, the power spectrum is sensitive to phase effects introduced by irregularities in film thickness. There are two sources for these irregularities; random variations due to the manufacturing process and subsequent film handling operations, and signal-dependent variations in the emulsion caused by the developed image (image relief). These effects can be removed by immersing the film sample in a liquid of similar refractive index contained in a glass cell with optically flat sides (liquid gating). This is a very cumbersome process however, and reduces the speed and convenience advantages of the diffraction pattern sampling technique.

The phase effects have been found to contribute significantly to the measured power spectrum; Thiry (1963), and Vander Lugt and Mitchel (1967). Evaluations by the author in Phase I of this work and in a subsequent effort (Schindler 1976, 1977) have indicated that the signal dependent portion of the phase effect is a very small part (2% to 3%) of the total contribution. On this basis, we assume in this study that phase effects behave essentially as random film noise and that the subsequent calculation of signal-to-noise ratios at least partly corrects for these effects.

Measuring Aperture Effects

The optical power spectrum is a function of the total input amplitude distribution. This includes the distribution of the measuring system limiting aperture as well as the image distribution. Theoretical treatments of this effect will be found in Stark, et al (1969), Nill (1976), and Armstrong and Thompson (1977). These authors demonstrate that the aperture effect is convolved with the image contribution in the total power spectrum. From the practical point of view, this convolution is seen as two distinct effects. First, the aperture acts as a "point spread function" and serves to smooth the resulting power spectrum. Smoothing also results from frequency interval sampling as discussed above. If the "point spread" of the aperture is significantly smaller than the frequency sampling intervals, the error contribution of this effect is not very great. Stark, et al (1969) considers this aspect in detail. The sampling intervals used in this study are not constant, (interval width increases with frequency), and, consequently, an evaluation of the relative effect on smoothing, of aperture vs. interval, is not easily accomplished. Such an evaluation is complicated by the "second effect" of the measuring aperture. In the formation of the Fraunhofer diffraction pattern, the non-diffracted light is focused at a point in the center of the pattern. Typically, the non-diffracted light represents 70% or more of the total. The remaining light is spread over the "meaningful" area of the diffraction pattern. Theoretically, the non-diffracted light exists as an infinitely small spot at the center of the diffraction pattern. Practically, this spot is spread by two mechanisms. The optical system used (including such factors as dust and scratches) spreads this point source of light. Secondly, the aperture "point-spread" is operating here to produce the same effect. The result is that the zero frequency or "center spot" energy is spread over the adjacent low frequency areas of the diffraction pattern. As a consequence, the diffraction pattern measurement technique, contrary to most all other procedures, is much more accurate at high frequencies than at low frequencies.

21

The solution to this problem is not simple. The measuring aperture
effects can, theoretically, be removed by deconvolution or by other less
complicated techniques (Nill 1976, Armstrong and Thompson 1977). However,
the practical implementation of such procedures is seriously hampered by
interactions with other low-frequency error contributions, e.g., optical
scatter or spread of the center spot energy, and low frequency phase
effects. The contribution of the measuring aperture is inversely propor-
tional to the diameter of the aperture. It is good practice, therefore,
to maximize the measuring aperture size but this strategy must be balan-
ced with the requirement to limit the image measurement to areas of
interest as determined by the intended application of the measurements.
An evaluation of the measuring aperture effect is included in Appendix
A.

NORMALIZATION

The power spectrum values as shown by the denominator in equation (10)
are proportional to the total light energy transmitted through the image
during measurement. This includes the effect of the illumination source
as well as the image transmission function. A common technique in
frequency domain measures is to normalize the results such that zero
frequency has a value of 1.0. This is a questionable approach for
diffraction pattern sampling because, as indicated above, accurate
measurement of the zero frequency value is difficult. An alternate
technique is to normalize directly by the total transmitted energy. This
technique, discussed further in Appendix A is much more stable than zero
frequency normalization. Subsequent work by the author (Schindler, 1977)
indicates that total energy normalization is also a more valid approach
for the determination of power signal-to-noise ratios as used in this
study.

INFORMATION THEORY

The term "power" in the applications considered in this report has been
borrowed from the field of electronics and its meaning when applied to
imagery is difficult to understand. A transformation of "power" into

22

units that are more descriptive of image content is a desirable goal. Information theory provides the framework for such a transformation.

Although information theory was developed for the analysis and evaluation of communications systems, its application to pictorial displays has become increasingly common in recent years. Dainty and Shaw (1974) provide a good review of the work in this area. A detailed treatment of basic information theory is found in Shannon and Weaver (1949).

The basic unit of information is the "bit," (short for binary digit). The number of bits in an image is a function of the number of resolvable elements or "cells" in the image and the number of discriminable light levels that each element can assume. In its simplest form, this definition is expressed as,

$$C = N \log_2 L, \tag{14}$$

where,

C = information content,
N = number of independent display elements, and
L = number of element response levels.

A more useful measure, "information density," is defined as,

$$D = \frac{C}{A} \tag{15}$$

where,

D = information density (bits per unit display area), and
A = measured display area.

23

There are two important considerations in the interpretation of measurements of information density. First, most images of interest will vary over the image area in complexity or amount of information. The information density value represents an average of the total image area measured. Secondly, the formal theoretical definition of "information" represents discriminable differences in display response. This definition does not consider the meaning or significance of this "information." The significance of image content depends largely on the requirements of the observer's specific task. This distinction is especially important when considering the relationship between information density and observer task performance.

Equation (14) is strictly valid only for discrete element displays. For more complex displays with frequency dependent response characteristics, e.g., photographic transparencies or CRT displays, information density is related to the optical power spectrum. Dainty and Shaw (1974) derive the following expression for information density.

$$D = \pi \int_0^\infty \log_2 \left(1 + \frac{P_S(r)}{P_N(r)}\right) r \, dr \qquad (16)$$

where

$P_S(r) =$ signal image power for frequency r (in polar coordinates), and

$P_N(r) =$ noise image power for frequency r .

This equation, like the annular integration of diffraction pattern intensity, assumes a radially symmetric image. It also assumes a spatially continuous imaging system such as conventional photography. For sampled systems, the upper limit of integration should be restricted to the Nyquist limit, (i.e., one-half of the sampling frequency). As pointed out by Shannon and Weaver (1949), this is sufficient for a complete evaluation of the image content. Furthermore, the use of this

24

limit minimize the inclusion of extraneous values such as those resulting from the sampling raster itself. With this change,

$$D = \pi \int_0^R \log_2 \left(1 + \frac{P_S(r)}{P_N(r)} \right) r \, d \, r \qquad (17)$$

where

$$R \quad = \quad \text{maximum useful frequency or Nyquist limit.}$$

It will be convenient to consider the distribution as a function of frequency.

$$D(r) = \log_2 \left(1 + \frac{P_S(r)}{P_N(r)} \right), \qquad (18)$$

where D (r) is in units of bits per cycle. This distribution, called "information spectrum" in this report, describes the contribution, by frequency, to the total information density.

Therefore,

$$D = \pi \int_0^R D(r) \, r \, d \, r, \qquad (19)$$

IMAGE NOISE

Equations (17) and (18) involve several assumptions about the nature of the image noise. The formulation,

$$1 + \frac{P_S(r)}{P_N(r)},$$

requires that the noise be isotropic, Gaussian, additive in amplitude and independent of the signal level. While these assumptions are generally accepted for photographic imagery, Shaw (1962), they are questionable for CRT image displays and totally unacceptable for quantized imagery.

25

The latter class represents those images whose luminance or transmission values have been divided into a number of discrete levels. Figure 5 is a transfer function for quantizing an image into 16 levels. The quantizing process introduces errors related to the width of the quantizing interval. This "quantization noise" is not Gaussian but is more nearly rectangular in distribution. Better treatment of this noise is derived if we assume that the quantization is uniform in amplitude as a function of frequency and signal level, and that the "quantization noise" is significantly greater than other sources of noise in the image. Under these conditions the number of levels, L, is found to be,

$$L = 1 + \frac{S_{MAX} - S_{MIN}}{\Delta S} \qquad (20)$$

where,

S_{MAX} = maximum signal amplitude,

S_{MIN} = minimum signal amplitude, and

ΔS = amplitude of one quantization level.

In the frequency domain,

$$L(r) = 1 + \frac{F_S(r)}{F_{\Delta S}(r)} \qquad (21)$$

where, $F_S(r)$ = Fourier transform of the signal, and

$F_{\Delta S}(r)$ = Fourier transform of a random signal input with a maximum amplitude of one step.

In terms of power spectra,

$$L(r) = 1 + \left(\frac{P_S(r)}{P_{\Delta S}(r)} \right)^{\frac{1}{2}} \qquad (22)$$

With this approach, equations (17) and (18) become,

$$D = 2\pi \int_0^R \log_2 \left[1 + \left(\frac{P_S(r)}{P_{\Delta S}(r)} \right)^{\frac{1}{2}} \right] r \, d \, r \qquad (23)$$
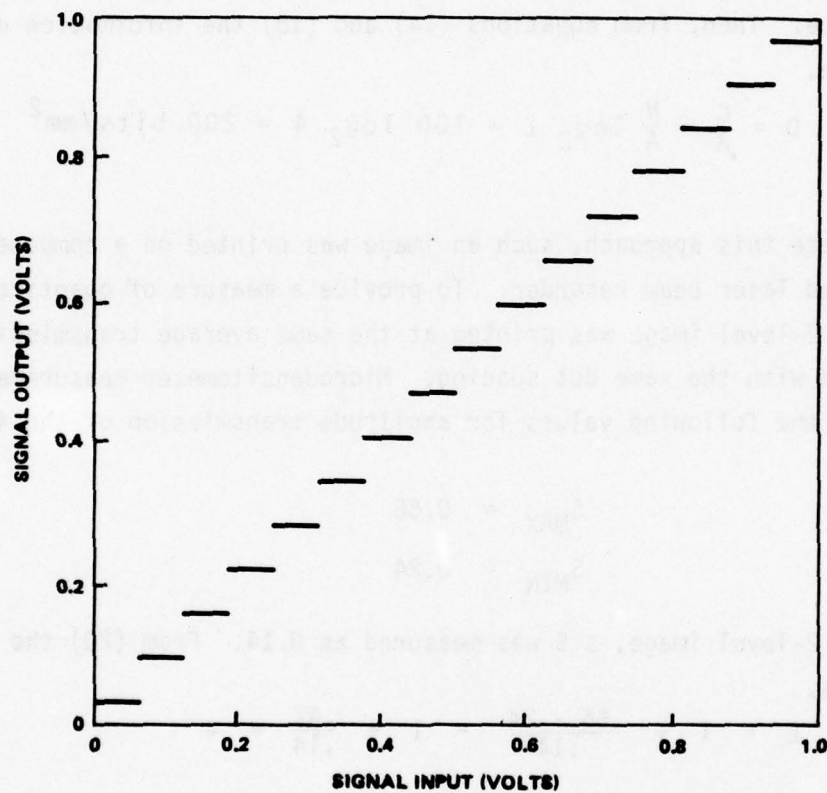
26

Figure 5. Transfer Function for 16-Level (4 Bit) Quantization

and,

$$D(r) = 2 \log_2 \left[1 + \left(\frac{P_S(r)}{P_{\Delta S}(r)} \right)^{\frac{1}{2}} \right] \tag{24}$$

As an example, consider an image composed of dots spaced as 10 dots per millimeter. Each dot is at one of four levels of amplitude transmission, selected at random such that each dot has an equal probability of occurrence. Then, from equations (14) and (15) the information density should be,

$$D = \frac{C}{A} = \frac{N}{A} \log_2 L = 100 \log_2 4 = 200 \text{ bits/mm}^2$$

To evaluate this approach, such an image was printed on a computer-controlled laser beam recorder. To provide a measure of quantization noise, a 2-level image was printed at the same average transmission level and with the same dot spacing. Microdensitometer measurements provided the following values for amplitude transmission of the 4-level image.

$$S_{MAX} = 0.66$$
$$S_{MIN} = 0.24$$

From the 2-level image, ΔS was measured as 0.14. From (20) the number of levels,

$$L = 1 + \frac{.66 - .24}{.14} = 1 + \frac{.42}{.14} = 4$$

For a random image of this nature, the Fourier transform should be a constant for all frequencies out to the Nyquist limit. That limit is one-half the sampling or dot frequency. Thus,

$$R = \frac{10 \text{ dots/mm}}{2} = 5 \text{ cycles/mm}$$

28

Therefore (21) yields,

$$L(r) = 1 + \frac{.42}{.14} = 4, \text{ for } 0 \leq r \leq 5, \text{ and}$$

from (24), the information spectrum should be,

$$D(r) = 2 \log_2\left[1 + (.18/.02)^{\frac{1}{2}}\right] = 4 \text{ bits/cycle}, \quad \text{for } 0 \leq r \leq 5.$$

Power spectrum measurements were made of the two images and $D(\bar{r}_i)$ values determined from equation (24). Figure 6 illustrates those results compared with the theoretical values determined above. Above 1.5 cycles/mm, there is a small underestimation of the theoretical values. Below this point, however, the discrepancy becomes very large. This illustrates the difficulties of the diffraction pattern sampling approach for low frequency measurement. A number of the problems noted earlier are undoubtedly contributing to these errors, e.g., center spot spread, measuring aperture convolution and film phase effects. The calculation of the information density using equation (23) provides a value of 176 bits/mm^2; this is an underestimation of about 12%. The contribution of the discrepancies below 1.5 cycles/mm is reduced because of the frequency weighting provided by equation (23), but the major component in the 12% error still comes from this source. This problem is perhaps even more significant because of the findings of a number of researchers that low frequency information is most critical to human perception, e.g., Ginsburg (1971). This problem clearly warrants special attention in the evaluation of the effectiveness of the diffraction pattern sampling approach.

VIEWER INTERACTION

The previous discussions have considered measurements in units of image dimensions. For applications involving human observers the measurement units should be expressed in terms of visual angle at the observer's eye. This transformation can be made as,

29
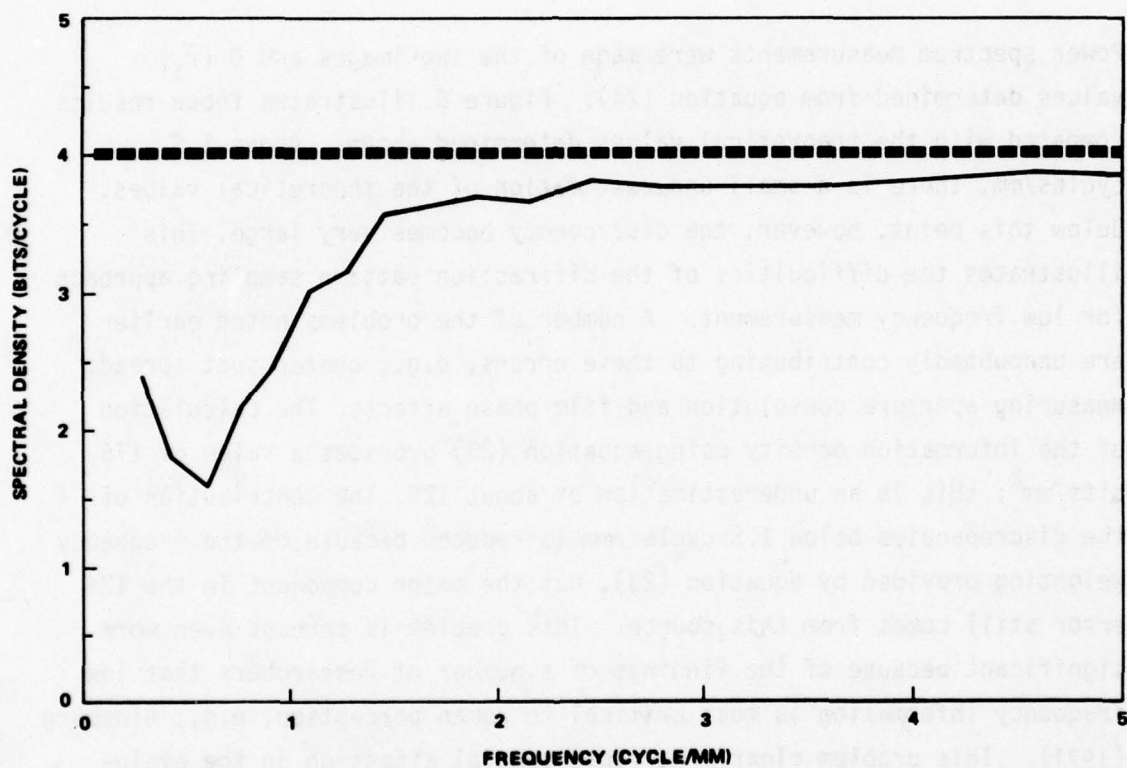
Figure 6. *Comparison of a Measured Information Spectrum With the Theoretical Spectrum for a Four-Level Random Pattern*

$$\nu = 2 \tan^{-1}\left(\frac{x}{2D}\right), \tag{25}$$

where

    X   =   distance in the image,

    D   =   viewing distance

It should be noted that for CRT evaluation an intermediate step is required that involves recording the CRT image on film. In this case,

$$\nu = \frac{2}{S} \tan^{-1}\left(\frac{x'}{2D}\right), \tag{26}$$

where

    ν =   visual angle at the CRT display

    S   =   photographic scale used to record the image

    x'   =   distance in the photograph

Similarly, spatial frequency is transformed by

$$\rho = \frac{r}{2 \tan^{-1} (1/2D)}, \tag{27}$$

where

    ρ =   frequency in units of cycles per unit visual angle, and

    r   =   frequency in units of cycles per unit distance.

31

Also, where intermediate film recording is used,

$$\rho = \frac{r'}{(2/S)\tan^{-1}(1/2D)} \qquad (28)$$

With this transformation, equation (18) becomes,

$$D(\rho) = \log_2\left[1 + \frac{P_S(\rho)}{P_N(\rho)}\right] \qquad (29)$$

and, for quantized imagery, from equation (24),

$$D(\rho) = 2\log_2\left[1 + \left(\frac{P_S(\rho)}{P_{\Delta S}(\rho)}\right)^{\frac{1}{2}}\right] \qquad (30)$$

From (17) or (23), information density, D, therefore is,

$$D = \pi\int_0^P D(\rho)\,\rho\,d\rho \qquad (31)$$

With the sampled power spectrum, equations (29) and (30) become,

$$D(\bar{\rho}_i) = \log_2\left(1 + \frac{P_S(\bar{\rho}_i)}{P_N(\bar{\rho}_i)}\right) \qquad (32)$$

and,

$$D(\bar{\rho}_i) = 2\log_2\left[1 + \left(\frac{P_S(\bar{\rho}_i)}{P_N(\bar{\rho}_i)}\right)^{\frac{1}{2}}\right] \qquad (33)$$

32

Equation (31) is approximated by,

$$D = \pi \sum_{i=1}^{I} D(\bar{\rho}_i)\, \bar{\rho}_i\, \Delta_i , \qquad (34)$$

where,

I = ring number, i, at the Nyquist frequency, and

Δ_i = width of ring i in units of cycles per unit visual angle.

There are other important aspects of viewer interaction. A most important consideration involves the effects of the viewer's perceptual thresholds. No attempt is made in this study to incorporate such threshold effects. The assumption made here is that performance is limited by display noise rather than viewer thresholds.

33

SECTION III
INFORMATION DENSITY MEASUREMENT OF CRT IMAGERY

INTRODUCTION

All of the observer performance tests reported in this study used CRT displays for image presentation. There are a number of special problems that arise because of the characteristics of these displays.

Film Recording

The CRT image cannot be measured directly. It must be recorded on film and the film transparency used for the OPS measurement. The fidelity of the film recording is therefore a critical factor in the accuracy of the resulting measurements. Because of possible degradations introduced in this step and because the film medium itself is a source of noise in the optical power spectrum measurement, additional errors are introduced at this point. Careful photometric calibration and control of processing conditions were used to keep such errors as constant as possible across all testing conditions.

In order to minimize the degradations in film recording, the original negative was used for measurement. The justification for this decision lies in the application of Babinet's principle which suggests that the diffraction patterns produced by a negative and by a positive should not differ. Ditchburn (1963) and Lipson and Walkley (1968) show that this is only approximately true and that the major error results from the interaction with measuring aperture diffraction patterns. As indicated in the previous section, the aperture interaction problem exists for all measurements and would remain even if a positive image were used. Somewhat arbitrarily, the decision was made to accept the approximation of Babinet's principle rather than risk the additional degradation of another processing step. Details of the specific film recording procedures used are presented later in this section.

34

Integration Time

The CRT is a dynamic display and, even with the presentation of a static image, the dynamics of scanning and of noise must be considered with respect to the visual integration time of the observer. It is desirable in the film recording process to use exposure times that approximate the integration time of the human visual system. Further details concerning integration time are presented in the evaluation of procedures in Appendix A of this report.

Cut-off Frequency

The maximum frequency used in the integration for the calculation of information density is defined in the previous section as the maximum useful frequency in the image. In sampled systems this frequency is defined as one-half of the sampling frequency (Nyquist limit). With a CRT display, this limit is generally one-half of the scan line frequency. This frequency is easily determined by the location of a distinctive spike in the optical power spectrum (see Figure 7). The measurement shown in the figure was made with a uniform signal input. The broad spike at the line frequency illustrates the effect of the diffraction pattern sampling interval and the interaction with the measuring aperture. This spike should be very narrow, depending on the uniformity of the scan line spacing.

CRT Noise

The noise model for information density presented as equation (29) assumes that the display noise is independent and additive. Several possible sources of CRT noise clearly violate these assumptions, i.e., "patterned" interference, ghost images, and raster noise. Fortunately, the first two sources are easily eliminated in closed circuit TV systems as used in this study. The effect of the latter source is primarily limited to the scan line frequency. This frequency is well beyond the range used for information density calculations. The remaining sources, video signal noise and phosphor noise, probably do not seriously violate the assumptions of independence and additivity. Although the noise
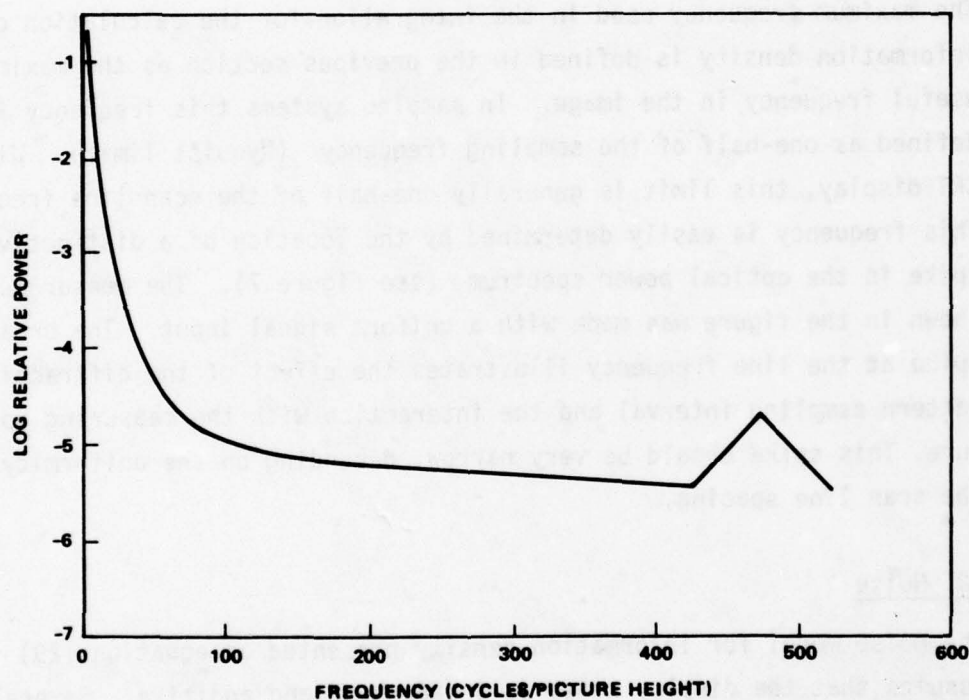
35

LOG RELATIVE POWER

FREQUENCY (CYCLES/PICTURE HEIGHT)

Figure 7. Sampled Optical Power Spectrum of CRT With a Uniform Signal Input

assumptions are reasonable, the effects of deviations cannot be evaluated and some question exists as to the absolute accuracy of the resulting information density values. If the input signal has been quantized equation (30) should be used.

Observer-Display Interaction

The primary concern of this study is the relationship between information density measurements and observer performance. The impact of the observer on perceived information density must be considered. If the display system is limited by the visual capabilities of the observer, then a visual threshold function should be used to define the just discriminable signal difference in the information density calculations. In the studies reported here, viewing conditions were selected to permit the assumption that all display systems were display noise limited.

Since the information density values are to be related to visual performance, units of display area relating to visual angle are preferred. This is accomplished by transforming area on the display surface to square degrees of visual angle at the appropriate viewing distance. The specific procedures are discussed as a part of the data calculation procedures.

EQUIPMENT

All optical power spectrum measures in this study were made with a Recording Optical Spectrum Analyzer (ROSA) manufactured by Recognition Systems Inc. This equipment, shown in Figure 8, is a general purpose instrument designed for ease and flexibility of optical set-up. The optical components, all with magnetic mounts, are positioned on a 72 x 44 inch optical table. A fiberglass shroud covers the table and components to protect against stray light.

For this work, the equipment is configured generally as shown in Figure 9. The illumination source is a 7 mw He-Ne laser. Illumination is controlled with a variable attenuator. The attenuator consists of two opposing glass wedges that are positioned for the desired transmission
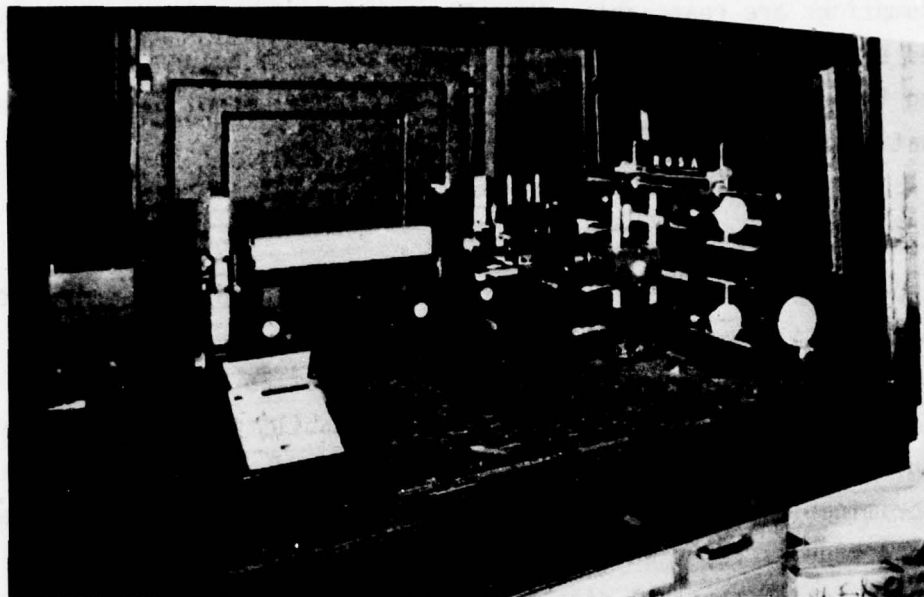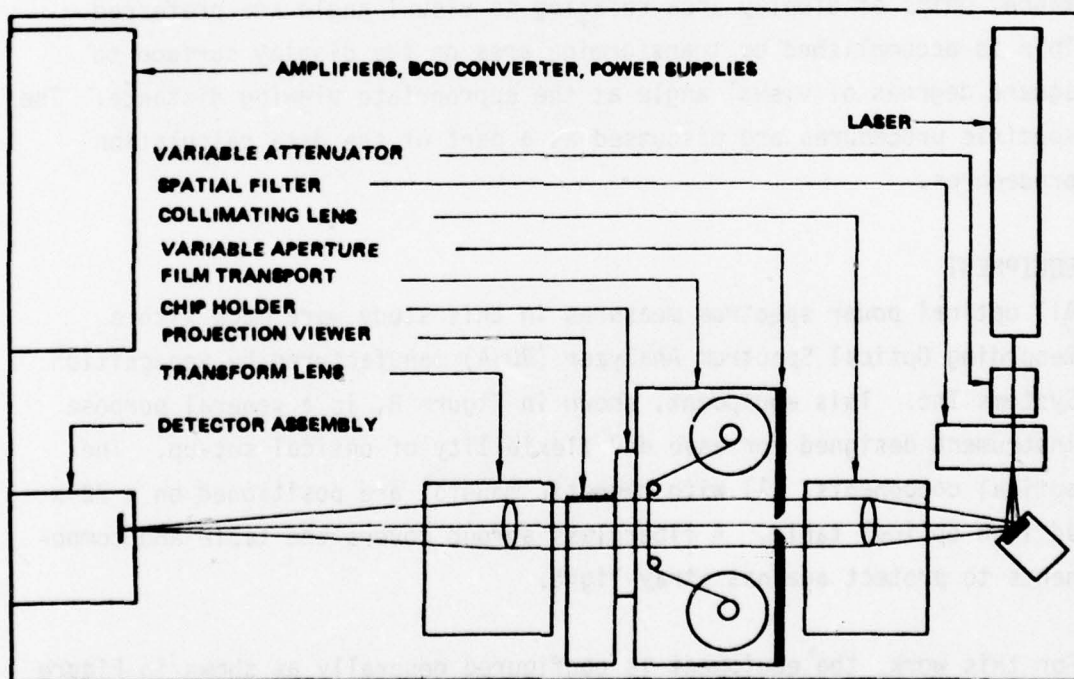
37

Figure 8. Recording Optical Spectrum Analyzer

AMPLIFIERS, BCD CONVERTER, POWER SUPPLIES

LASER

VARIABLE ATTENUATOR
SPATIAL FILTER
COLLIMATING LENS
VARIABLE APERTURE
FILM TRANSPORT
CHIP HOLDER
PROJECTION VIEWER
TRANSFORM LENS
DETECTOR ASSEMBLY

Figure 9. Typical Configuration for Diffraction Pattern Sampling.

38

without imposing a significant deviation in the laser light path. The laser beam is expanded with a microscope objective. The magnification of the objective controls the degree of expansion which, in turn, is determined by the desired area of illumination at the input plane. A 25 μm pinhole is placed at the focal point of the microscope objective to "clean up" the laser beam. The laser and microscope objective can be considered as a crude spectrum analyzer. The pinhole is placed at the Fraunhofer diffraction plane of the objective and thus passes only the uniform energy in the laser beam. It acts as a spatial filter that blocks the high frequency variation in the beam. The expanding beam is then collimated with a lens placed at a distance from the pinhole equal to its focal length. During alignment, collimation is assured by inserting an optical flat in the beam "downstream" from the collimating lens and adjusting the lens focus until the resulting interference fringes are minimized.

From the collimating lens, the beam passes through the film holder. This holder is designed to accept roll film up to 9 inches in width as well as slides or film "chips." It is equipped with a variable aperture to control the image area illuminated. A series of discrete circular apertures with diameters from 1/8 inch to 2 and 1/2 inches is available. The holder includes a projection unit for viewing the illuminated image. This unit is used to aid in positioning the image in the laser beam.

The light diffracted by the input image is collected by the transform lens and focused on the photodetector. The lenses used are simple spherical telescope objectives. The transform lens focal length determines the distance between the lens and detector and hence the "scale" of the diffraction pattern.

The ROSA uses a 64 element photodetector array for measurement of the diffraction pattern intensity values. Each element is a diffused silicon photodetector on a common substrate. The array as shown earlier in Figure 3 consists of 32 "rings" and 32 "wedges." The diffraction pattern is symmetric so the array is split essentially in half, each half measuring a different "characteristic" of the pattern. The rings measure

39

intensity as a function of frequency integrated over orientation and the wedges measure intensity as a function of orientation integrated over frequency. The central ring (Ring 1) is a complete circle and is intended to provide a measure of the zero frequency or non-diffracted energy. The succeeding rings are nearly half circles and provide measures of intensity integrated over a frequency band.

Dimensions for the individual detector rings are listed in Table 1. A 0.8 mil wide conductor strip is incorporated in each ring. The effect of this strip on total ring effective area is included in the tabled values. Table 2 shows the corresponding spatial frequency values for the 1016 mm focal length transform lens used for all measurements in this study.

The outputs from the individual elements are fed into a pre-amp/multiplexer, then each signal is fed into an auto-ranging amplifier where it is converted to the proper range for the binary-coded decimal converter. The signals, converted into 3 digit binary-coded decimals, are then recorded on a tape cassette. Time for a single measurement sequence, after film positioning, is about 10 seconds. Control of the measurement procedure and recording is accomplished by a Hewlett-Packard Model 9821 calculator. A similar model, equipped with an expanded tape memory, plotter and typewriter is used for information density calculations and data output.

MEASUREMENT PROCEDURES
The following discussion defines the specific steps used in the measurement of information density. These steps are the result of theoretical and experimental evaluations performed in Phase I of this study (Schindler, 1976) and a number of additional evaluations that are described in Appendix A. These steps represent the best approach within our present state of knowledge with respect to accuracy, reliability, and convenience. Further developments, including the results of observer testing in this study, are likely to suggest future improvements. The following steps are divided into several areas.

Table 1: Detector Ring Dimensions

Ring No.	Minimum Radius (mils)	Maximum Radius (mils)	Ring Angle (degrees)	Total Effective Area (sq. mils)
1	0	3.5	360.0	38.5
2	5.8	8.6	180.0	43.5
3	9.6	12.5	180.0	69.1
4	13.5	16.4	180.0	93.5
5	17.4	20.4	180.0	122.7
6	21.4	24.6	166.3	148.6
7	25.6	29.0	168.5	190.0
8	30.0	33.7	170.1	245.0
9	34.7	38.8	171.4	318.7
10	39.8	44.4	172.5	417.4
11	45.4	50.6	173.4	548.7
12	51.6	57.5	174.2	722.0
13	58.5	65.2	174.9	948.7
14	66.2	74.0	175.5	1279.6
15	75.0	83.9	176.0	1688.8
16	84.9	95.1	176.5	2237.0
17	96.1	107.8	176.9	2963.6
18	108.8	122.1	177.3	3884.7
19	123.1	138.3	177.6	5114.3
20	139.3	156.6	177.9	6697.1
21	157.6	177.2	178.1	8715.4
22	178.2	200.2	178.3	11209.0
23	201.2	225.9	178.5	14385.5
24	226.9	254.7	178.7	18473.4
25	255.7	286.7	178.8	23448.5
26	287.7	322.2	179.0	29630.1
27	323.2	361.6	179.1	37361.6
28	362.6	405.0	179.2	46614.1
29	406.0	452.8	179.3	57988.0
30	453.8	505.4	179.3	71889.4
31	506.4	563.0	179.4	88448.7
32	564.0	626.0	179.5	108409.8

Table 2: Detector Spatial Frequency Values

40 inch Focal Length

Ring No.	Minimum Frequency (cy/mm)	Maximum Frequency (cy/mm)	Center Frequency (cy/mm)	Bandwidth (cy/mm)
1	0.00	0.14	0.07	.14
2	0.23	0.34	0.28	.11
3	0.38	0.49	0.43	.11
4	0.53	0.65	0.59	.12
5	0.69	0.80	0.75	.11
6	0.85	0.97	0.91	.12
7	1.01	1.15	1.08	.14
8	1.18	1.33	1.26	.15
9	1.37	1.51	1.44	.14
10	1.57	1.75	1.66	.18
11	1.79	2.00	1.89	.21
12	2.03	2.27	2.15	.24
13	2.31	2.57	2.44	.26
14	2.61	2.92	2.76	.31
15	2.96	3.31	3.13	.35
16	3.35	3.75	3.55	.40
17	3.79	4.25	4.02	.46
18	4.29	4.81	4.55	.52
19	4.85	5.45	5.15	.60
20	5.49	6.17	5.83	.68
21	6.22	6.99	6.60	.77
22	7.03	7.90	7.46	.87
23	7.93	8.91	8.42	.98
24	8.95	10.05	9.49	1.10
25	10.08	11.31	10.69	1.23
26	11.34	12.70	12.02	1.36
27	12.75	14.26	13.50	1.51
28	14.30	15.97	15.13	1.67
29	16.01	17.85	16.93	1.84
30	17.89	19.93	18.91	1.96
31	19.97	22.20	21.08	2.23
32	22.24	24.68	23.46	2.44

42

- CRT Inputs and Adjustments

- Film Recording

- Optical Power Spectrum Measurement

- Information Density Calculation

CRT Inputs and Adjustments

1. The CRT video transfer function is adjusted to the desired conditions.

2. The test targets (dot and bar patterns) are imaged at a scale such that the target sampling frequency is slightly higher than the CRT scan line frequency.

3. Uniform signal inputs for noise measurements are provided at levels equal to the average signal levels of the images to be measured.

Film Recording

1. The camera distance is selected to provide the proper image scale. The recommended scale is such that the frame height of a 525 line CRT is 0.9 inches on the film.

2. The camera is positioned at the selected distance with its optical axis centered and perpendicular to the display screen.

3. Exposure time is selected to provide the desired integration time.

4. Film type is selected to provide sufficient speed for expected levels of display luminance and the selected exposure time. The film speed should allow lens f-stop settings that will provide adequate depth of field.

43

5.   Exposures are made of the desired imagery and appropriate uniform
     signal inputs for noise determinations.

6.   The film is processed to a gamma value near unity. Calibration
     grey steps should be included to verify the gamma value and to
     assure that the display dynamic range is linearly recorded.

Optical Power Spectrum Measurement

1.   After equipment set-up and alignment, an initial reading is made
     with the detector covered to determine system bias levels for each
     detector element. These readings are repeated periodically through-
     out the session as a check and correction for system drift.

2.   The image area of interest is positioned in the measuring aperture
     and a diffuser in the optical path. This measurement is used to
     determine the total diffraction pattern energy for normalization.

3.   The diffuser is removed and the measurement repeated.

4.   The power spectrum is estimated by calculating the power level for
     each sampling interval, i.

$$P(\overline{r}_i) = \lambda^2\ F^2\ \frac{V_i - B_i}{A_i} \Bigg/ \frac{V_d - B_{32}}{A_{32}}\ ,$$

for i = 1, 2, ... 31,

where,

$\quad P(\overline{r}_i) \quad = \quad$ power value at frequency, r , where r is the
center frequency of ring i,

$\quad \lambda \quad = \quad$ laser wavelength, (6.28×10^{-4} mm/cycle for all
measurements in this report),

44

F   = transform lens focal length, (1016 mm for all measurements in this report),

V_i = ROSA output voltage for ring i,

V_d = ROSA output voltage for ring 32 from the diffuser reading,

B_i = system bias value for ring i, and

A_i = detector element area for ring i.

Information Density Calculation

1. The line frequency sampling spikes are identified and the Nyquist limit for the image set is specified, (Nyquist limit equals one-half the line frequency). Direct measurement of line spacing on the film can be used to verify the above or to provide greater accuracy if required.

2. For the vehicle images, the power values, $P(\bar{r}_i)$, are averaged across all images within a display condition to provide a power spectrum ensemble average, $\langle P(\bar{r}_i) \rangle$.

3. Spatial frequency units, r are transformed into units of cycles per unit visual angle, ρ as described by equation (28).

4. The information spectrum values are calculated for each sampling interval by equation (32) or (33) or determined by display noise characteristics.

5. The information density value is then estimated through the use of equation (34).

MEASUREMENT ACCURACY AND REPEATABILITY

Accuracy is defined as the level of agreement between the measured value and the true value. This attribute is, however, determined here as the magnitude of the discrepancies between the two values or the measurement error level. Specifically, error is measured as the root mean square (RMS) deviation,

$$\text{RMS Error} = \left[\frac{\Sigma (X - T)^2}{N} \right]^{\frac{1}{2}} \quad ,$$

where,

X = the measured value,

T = the true value, and

N = the number of measurements.

Evaluations of the basic optical power spectrum measurement capability were made in Phase I of this study and the details are reported in Schindler (1976). These evaluations consisted of comparisons of measured values of clear circular apertures with predicted values determined by integrating the theoretical diffraction pattern over intervals corresponding to the sampling element widths. The results indicated an RMS error level of 10% to 11% over a range of 6 orders of magnitude.

A partial evaluation of the measurement procedures outlined above was made using the laser-generated random-dot test imagery. Ten measurements were made with a 1 inch diameter aperture. Values of $D(\overline{r}_i)$ were calculated and deviations from the theoretical level of 4 bits/cycle were determined. The RMS error values, as a function of frequency, are shown in Figure 10. The aperture effect is seen in the increased error levels at low frequencies. The RMS error for the information density values, as deviations from the theoretical value of 200 bits/mm^2, was found to be 17.2 bits/mm^2, an error of about 9%.

The evaluations above do not include the special problems of CRT measurement. Assessment of these values is not possible at the present time because of the lack of a comparison standard or "true" density value.

46

RMS ERROR (1/CYCLE)

FREQUENCY (CYCLES/mm)
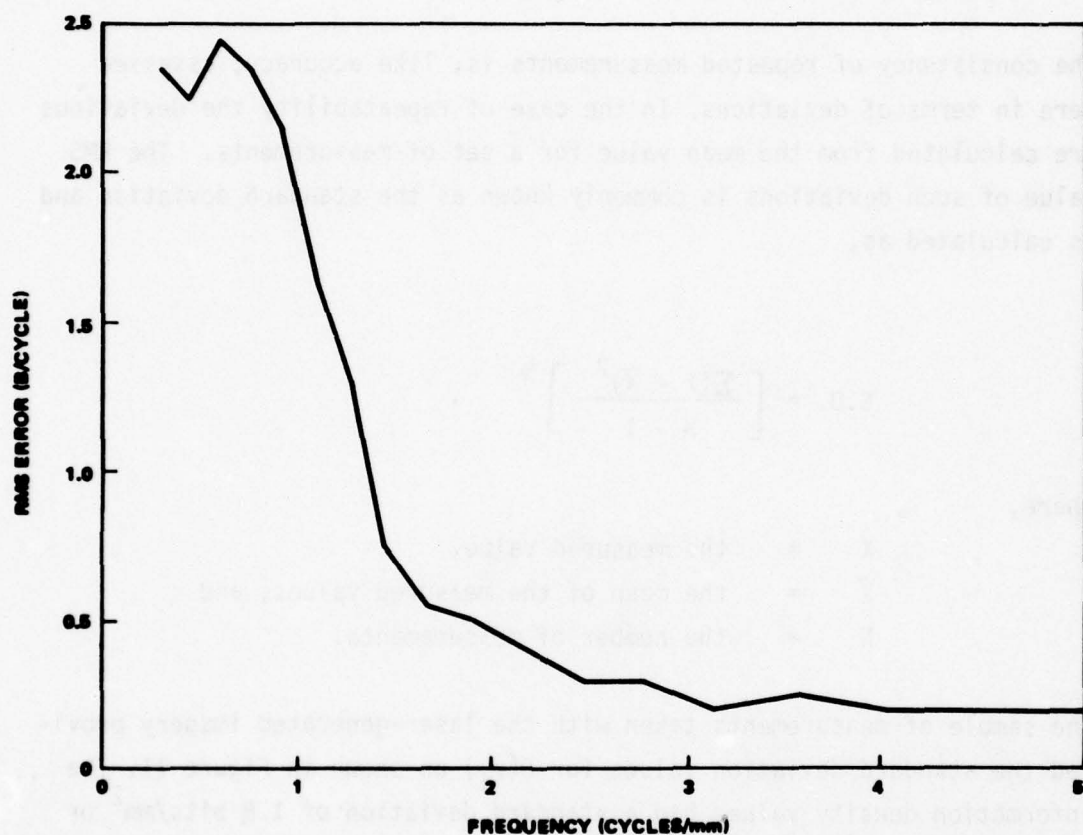
Figure 10. Root-Mean-Square Errors as a Function of Frequency for the Laser Printed Random Dot Pattern. Based on a Sample of 10 Measurements.

47

Neither theoretical levels nor independent measurements of such levels are available. Because of this limitation and because of uncertanties about the adequacy of the noise assumptions and the possible distortions in the film recording process, no claim can be made for the absolute accuracy of the information density measures.

The consistency of repeated measurements is, like accuracy, assessed here in terms of deviations. In the case of repeatability the deviations are calculated from the mean value for a set of measurements. The RMS value of such deviations is commonly known as the standard deviation and is calculated as,

$$S.D. = \left[\frac{\sum (X - \overline{X})^2}{N - 1} \right]^{\frac{1}{2}} ,$$

where,

X = the measured value,
$\overline{X}$ = the mean of the measured values, and
N = the number of measurements.

The sample of measurements taken with the laser-generated imagery provided the standard deviation values for $D(\overline{r}_i)$ as shown in Figure 11. The information density values had a standard deviation of 1.9 bits/mm^2 or about 1% of the mean. Repeatability of the total CRT measurement procedure was assessed by a series of measurements with the random-dot test pattern displayed on a CRT. Ten measurements, individually photographed and processed were made over a period of several days. Standard deviations for the resulting $(D\overline{\rho}_i)$ values are shown in Figure 12. The differences between Figure 11 and Figure 12 are largely due to the film recording process. The standard deviation for the information density values was about 8% of the mean.
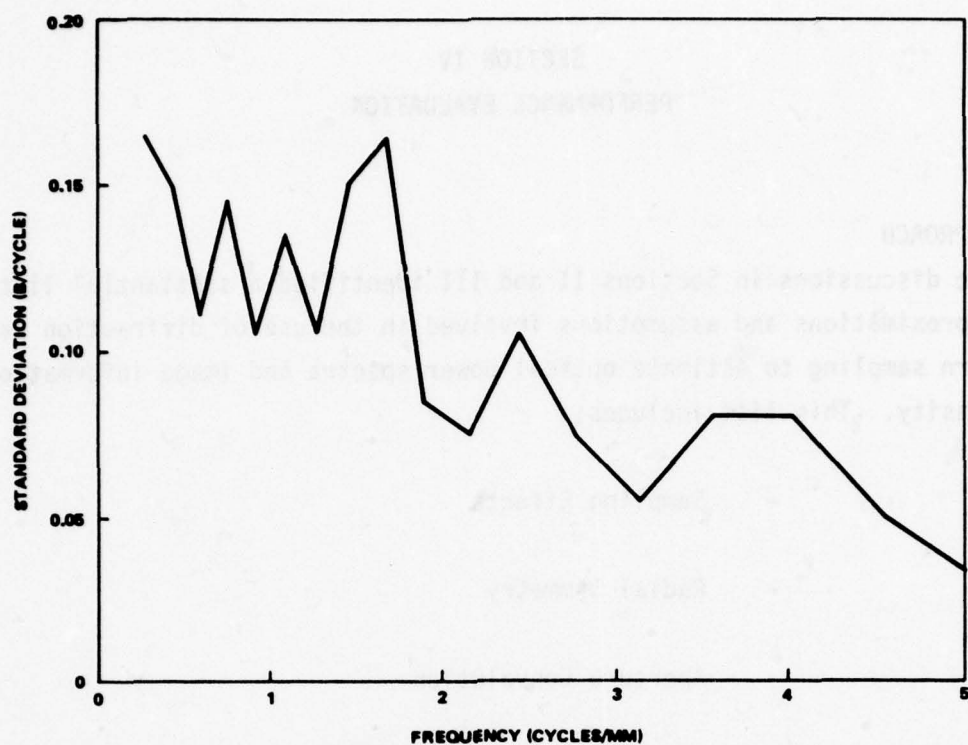
Figure 11. *Repeatability Evaluation Using the Laser Printed Random Dot Pattern. Based on a Sample of 10 Measurements.*
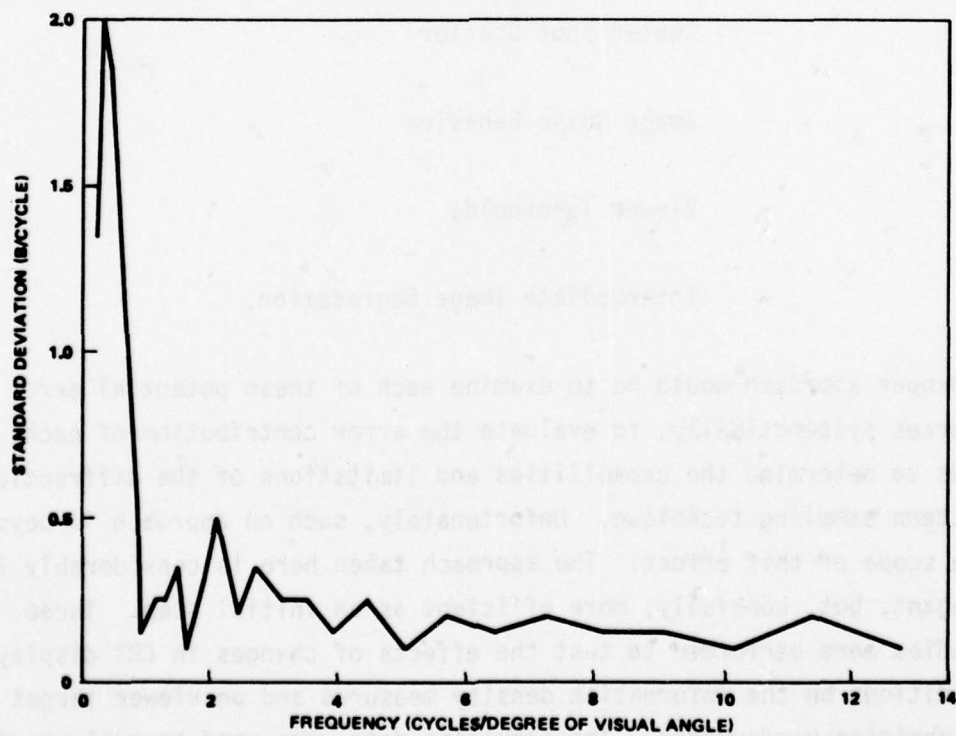
Figure 12. *Repeatability Evaluation Using CRT Display of a Random Dot Pattern. Based on a Sample of 10 Measurements.*

49

SECTION IV
PERFORMANCE EVALUATION

APPROACH

The discussions in Sections II and III identified a substantial list of
approximations and assumptions involved in the use of diffraction pat-
tern sampling to estimate optical power spectra and image information
density. This list includes;

- Sampling Effects

- Radial Symmetry

- Aperture Convolution

- Phase

- Center Spot Scatter

- Image Noise Behavior

- Viewer Thresholds

- Intermediate Image Degradation.

A proper approach would be to examine each of these potential error
sources systematically, to evaluate the error contribution of each, and
thus to determine the capabilities and limitations of the diffraction
pattern sampling technique. Unfortunately, such an approach is beyond
the scope of this effort. The approach taken here is considerably less
elegant, but, hopefully, more efficient as an initial step. Three
studies were performed to test the effects of changes in CRT display
conditions on the information density measures and on viewer target
recognition performance. The resulting data were used to evaluate the

50

relationship between information density and recognition performance across the various display conditions tested. The display conditions were selected to provide an especially difficult test for the validity of the diffraction pattern sampling technique. The use of CRT displays with the attendant requirement for intermediate image recording places a severe load on the ability of the measurement technique to provide meaningful and useful values of information density. The intent of these tests was to identify the limits of application of the procedures used here, to indicate the most critical problem areas, and suggest approaches for improving the application of the diffraction pattern sampling technique.

Table 3 lists the display conditions (independent variables) used in each of the three studies.

Table 3:   Display Conditions Tested

Study	Display Condition	Levels Tested
I	- CRT Dynamic Range	37.5:1, 10.1, 5.4:1, 2.5:1
	- Target Orientation	Diag. (upper left, lower rt.)
II	- CRT Bandwidth	4.0, 1.0, 0.4 MHz
	- CRT Noise	S/N = 43 db, S/N = 15 db
	- Target Orientation	Horiz., Vert., Diag.
III	- Number of Commanded Grey Levels	8, 5, 4 bits
	- Target Orientation	Diag. (lower left, upper rt.)

The basic stimulus materials, the performance task (dependent variable), and the test procedures were identical for all three studies and were based on work performed by the USAF Aerospace Medical Research Laboratory (Martin and Task, 1976, and Task and Verona, 1976).

In all of the performance evaluation studies reported here, three classes of information density measures are considered. These classes differ in the characteristics of the image content used for evaluation.

Class 1: Random Dot Pattern - This pattern, shown in Figure 13, represents the theoretical maximum "information" input. It provides a measure of display response, independent of the specific image content used in the viewer performance tasks. This pattern has advantages because it is simple to construct and its statistical properties are well known. Since it provides the highest level of content, it results in a high signal-to-noise ratio in the optical power spectrum measurement.

Class 2: Random Bar Patterns - The random bar pattern, Figure 14, is the one-dimensional analog of the random dot. It has the advantage of providing measures of information display performance at any selected orientation. In these studies, measurements are made with a vertical, horizontal, and diagonal orientation.

Class 3: Recognition Target Images - Information density measures of the actual images as they are displayed in the performance tests have the advantage of direct applicability to the specific test and class of imagery used. This imagery, as shown in Figure 15, is clearly not radially symmetric in content. The random dot pattern, because of the sampling geometry used, is not truly symmetric but the deviation is much smaller than the target images. An additional problem results because of a much lower signal-to-noise ratio in the vehicle imagery. This could reduce the stability and accuracy of the resulting measurements as compared with the random

52
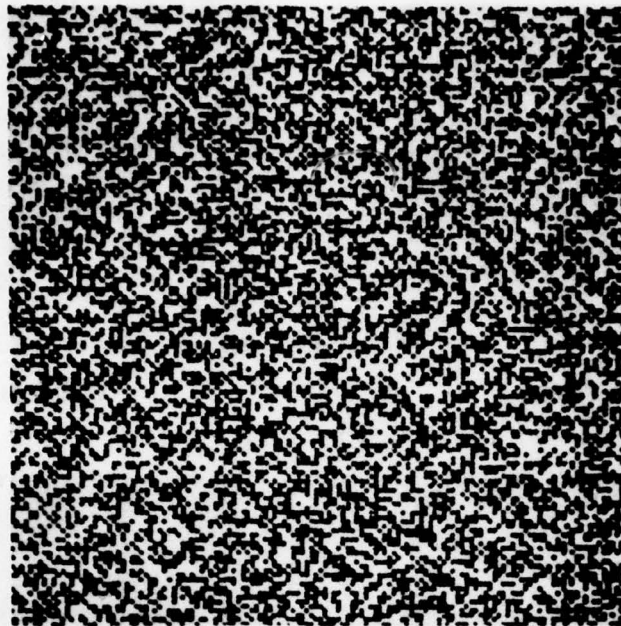
Figure 13. *The Random Dot Pattern as Used for CRT Information Density Measures.*
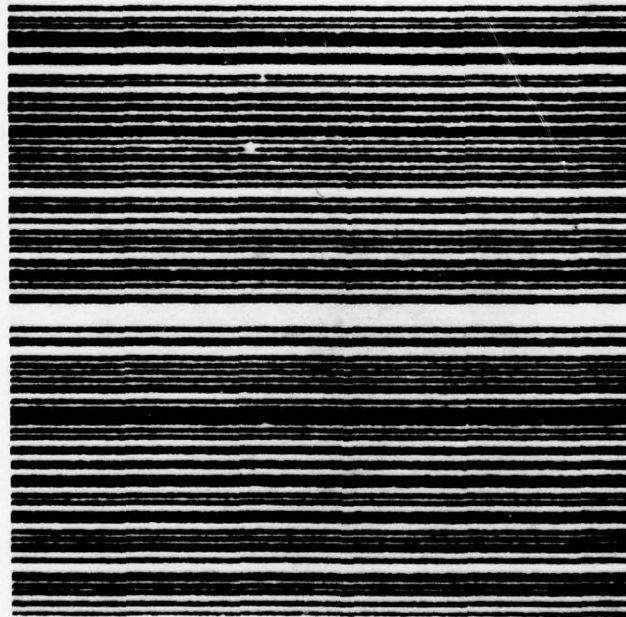
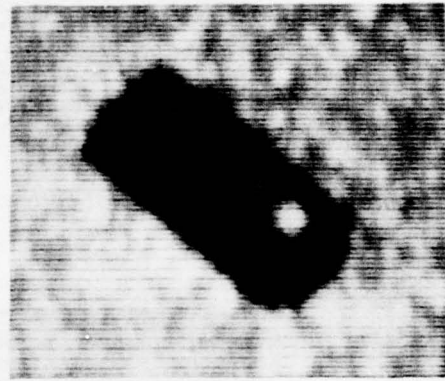**Figure 14.** *The Random Bar Pattern as Used for CRT Information Density Measures.*
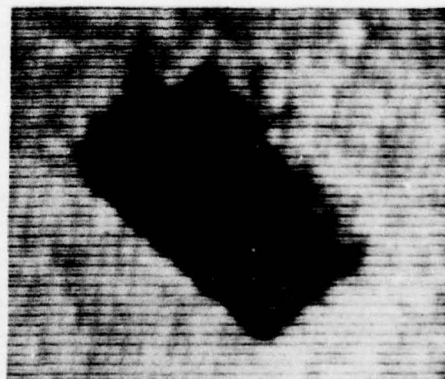
53
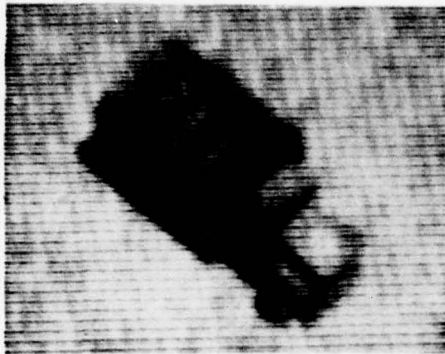
COVERED TRUCK

OPEN TRUCK

TANK

HALF-TRACK

MOBILE GUN

*Figure 15. The 5 Target Vehicles As They Appeared At Maximum Dynamic
Range*

dot targets. Partly for this reason, but primarily as defined by
Shannon and Weaver (1949), and Dainty and Shaw (1974), the calcu-
lation of information density for the recognition target images
uses the ensemble average of the power spectra for all target
images within a given display condition. This means that the power
values for all targets and orientations are averaged before the
calculation of the information density for this class of imagery.

STUDY I - CRT DYNAMIC RANGE

Objective

The first study in this series uses CRT display conditions that are in
best agreement with the assumption of radial symmetry. At best, this is
difficult with a CRT display. The imaging mechanisms are very different
along the two major display axes. Along the vertical axis the image is
discretely sampled by the scan lines. Along the horizontal axis the
image is continuously sampled by variation in spot brightness. Neverthe-
less, it is a standard practice to design the CRT display to yield
comparable performance in both axes. We assume, at least initially,
that this is the case. The use of dynamic range as a primary variable
is also an important test. The optical power spectrum is directly
related to image contrast (Nill, 1976). Visual target recognition has
been found to be related to image contrast in a much more complicated
fashion. A general finding is that supra-threshold display contrast has
a minimal effect on observer performance (Humes and Bauerschmidt, 1968
and Johnson, 1968).

There are two major experimental questions addressed in Study I.

1. Do the information density measures correlate positively
    with display dynamic range? Information density should
    decrease with decreasing dynamic range. This should occur for
    all three classes of measurements. If the assumption of
    display symmetric response is valid, differences in the three
    bar pattern orientation should not produce significantly
    different results.

55

2. Do the information density measures correlate positively
   with measures of observer target recognition performance?

In general, it is expected that recognition performance will improve
with increasing information density. This relationship, however, may be
complicated by interaction with the viewer's perceptual capabilities.
The human perceptual system may be limited in its capacity to process
image information. Information density values beyond that level would
not be expected to produce further improvements in performance. At the
other extreme, perceptual contrast thresholds may limit the information
available to the observer. The assumption made here is that the image
information is limited by display noise rather than by observer thres-
hold. If this assumption is not valid, the resulting information density
values will be excessive.

Subjects

Eight male subjects whose ages ranged from 35 to 60 were used in this
study. All were scientists with experience in imagery interpretation.
Visual acuity, tested with an American Optical Sight-Screener, was 20/20
or better for all subjects.

Performance Task

Subjects were required to perform a target recognition task using five
vehicle-type targets. Targets were viewed binocularly on a 525-line,
black and white, 19 inch CRT monitor. At the start of a trial the
target appeared as a small object in the center of the screen. The
target increased in size until the subject was able to recognize which
of the five targets was being displayed. The subtended angle of the
diagonal dimension of the target at recognition was used as the measure
of observer performance.

Stimulus Materials

Still photographs of model tactical-type targets placed on a floor tile
background provided the source from which 16mm zoom movies were produced
for each target. There were five target models used: tank, mobile gun,

56

half-track, open truck, and covered truck. The models were photographed while mounted on a rectangular, pseudo-random background floor tile. A separate sequence was filmed for each of four orientations. The longitudinal axis of the target was always aligned diagonally against the square background of tile. Each zoom sequence in the original film covers a magnification range of 10:1 and consists of approximately 380 individual frames.

Only two of the four orientations were used for this study. The front of the target vehicle was either to the upper right or lower left of the frame. Twenty-five frames were selected from each of the ten sequences. Every twelfth frame was used. The selected frames covered a magnification range of 8:1. A sampling of the original film sequence was necessary because of the limited capacity of the video disc recorder. Each selected frame was projected by a 16mm projector on a ground glass screen and imaged by a television camera. The camera output was recorded on a video disc. A total of twenty-five frames for each of the ten sequences were recorded on the disc. Targets for information density measures were also recorded on the disc. These included a random dot pattern, a bar pattern at horizontal, vertical, and diagonal orientations, and uniform grey patches for calibration and noise measurements.

Equipment

Stimulus preparation and observer performance testing used the Advanced Sensor Analysis and Display facility located at the Boeing Space Center. The equipment used to generate and store the stimulus material and that used for subject performance testing is diagrammed in Figure 16. A 16mm projector in the single frame mode was used to project the selected frames on a ground glass rear projection screen. This image was picked up by the television camera (Sierra Scientific - Model LSV, 1.5 inch, Type C23187 vidicon), and fed through the disc controller of the video disc. The controller conditions the video signal for recording and routes the information to the selected track on the disc. Storage is on a 16-inch diameter magnetic disc with a maximum capacity of 317 video frames. The coordinate measuring capability of the image analyzer was
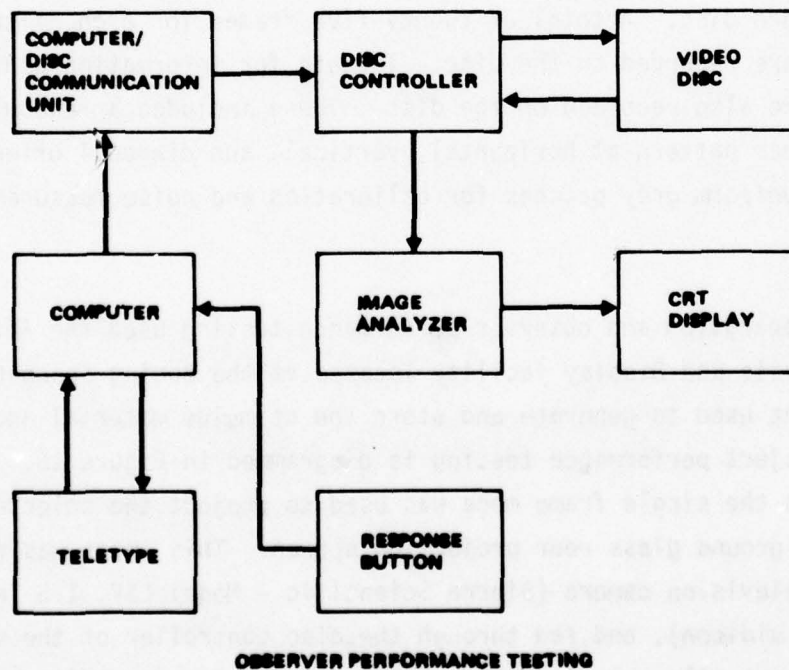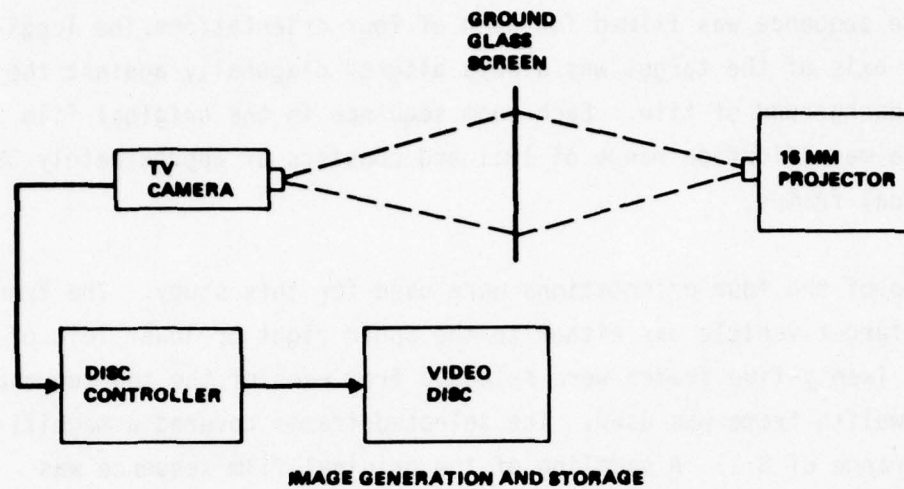
57

GROUND GLASS SCREEN

TV CAMERA

16 MM PROJECTOR

DISC CONTROLLER

VIDEO DISC

IMAGE GENERATION AND STORAGE

COMPUTER/ DISC COMMUNICATION UNIT

DISC CONTROLLER

VIDEO DISC

COMPUTER

IMAGE ANALYZER

CRT DISPLAY

TELETYPE

RESPONSE BUTTON

OBSERVER PERFORMANCE TESTING

Figure 16. Schematic Diagram of Equipment Used for Image Generation and Storage and for Observer Performance Testing.

used to measure the target diagonal dimension for each of the stored frames. These values were then scaled to the actual size on the monitor used for testing.

For performance testing, the Varian computer and disc controller allow the experimenter to select any order of presentation of the individual sequences to be read out of the disc and displayed on the CRT monitor. The disc controller also allows the selection of the desired video frame rate. The CRT monitor is a Conrac, Model SNA, 19 inch, 525 line, black and white display. The screen was masked with light grey material except for a 2-1/2 inch square area at the center of the screen. Communications with the computer operator were provided by an intercom system. The response button provided a command to the computer to terminate the display sequence and to print out the number of the last frame displayed.

Power spectrum measurements used for the calculation of information density values were made on a Recording Optical Spectrum Analyzer manufactured by Recognition Systems, Inc. This equipment is described in Section III. Film recording of the CRT display was accomplished with a Vivitar, 220/SL, 35mm camera equipped with a Macro-Takumar 1X to 4X, f4.0 lens. All photometric measurements were made with a Gamma Scientific Company, Model 700, photometer equipped with a fiber optics probe.

CRT Calibration
Four display conditions were used in this study. The conditions resulted from four different settings of the CRT contrast control accompanied by adjustment of the brightness control to maintain a constant maximum screen luminance of 15 fL. The video transfer curves for the four conditions are shown in Figure 17. A grey step pattern was used before each testing session to calibrate the display control settings. The four conditions provided dynamic range values (max luminance/ min luminance), of 37.5:1, 10:1, 5.4:1, and 2.5:1. The five targets, as they appeared at the maximum dynamic range, are shown in Figure 15. The mobile gun is shown in Figure 18 as it appeared at each CRT dynamic range condition.
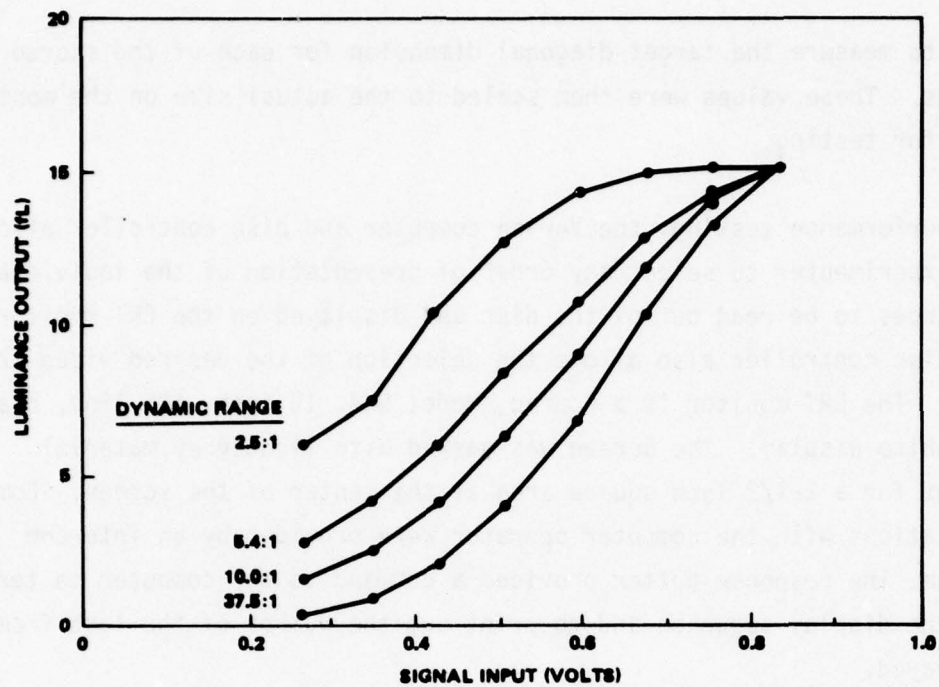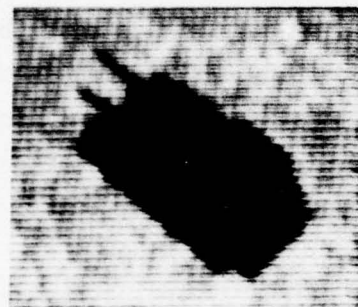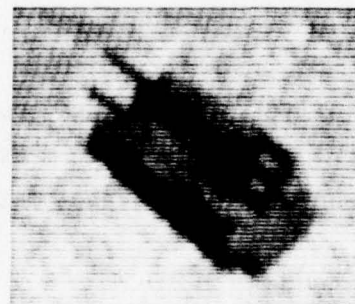
59

Figure 17.   *Video Transfer Curves for the 4 CRT Dynamic Range Conditions Used in Study I*
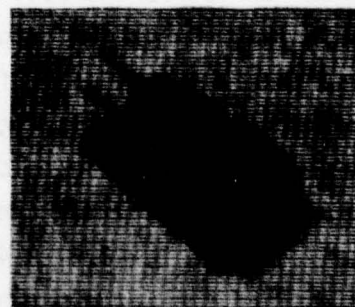

37.5:1

10.0:1

5.4:1

2.5:1

Figure 18 .   *Study I—Dynamic Range Conditions*

Information Density Measurements

Information density measurements were made for the following images under each display condition:

- random dot pattern,
- random bar pattern at horizontal, vertical and diagonal orientations, and
- the largest image of each vehicle target at each of the two orientations presented.

The procedures used for these measurements are described in Section III. Film recording used Kodak Tri-X, 35mm film with an exposure time of 1/8 seconds. The film was developed in D-19 for 10 minutes at 68°F. The resulting gamma value was 0.91. The photographic scale was 1:6.4. A 3/8 inch diameter aperture was used for power spectrum measurements of the dot and bar test patterns. A 1/4 inch diameter aperture was used for the vehicle images in order to minimize the effect of extraneous content in the image. This aperture size was slightly larger than the largest vehicle diagonal.

Test Design

Each of the eight subjects viewed two replications of all targets and orientations under each of the four display conditions. Each subject, therefore, responded to a total of $2 \times 5 \times 2 \times 4 = 80$ individual target sequences. The orders of target presentations were randomized. The orders of display conditions were counterbalanced and subjects assigned at random to these orders.

The dependent variable was the visual angle of the target diagonal at the time of recognition. The independent variables were display dynamic range (4 levels), targets (5), orientation (2), and subjects (8). A $4 \times 5 \times 2 \times 8$ replicated, mixed model analysis of variance was used to analyze the performance data. Subjects were treated as a random variable in this design.

61

Viewing Conditions

Subjects were seated at a 36 inch viewing distance from the display
screen. The 2-1/2 inch square unmasked portion of the screen subtended
4 degrees on a side and 6 degrees on the diagonal. Target size at the
beginning of a series was about 0.3 degrees of visual angle and grew to
about 2.3 degrees at maximum size. The target sizes were established
with a brief pilot study to ensure a proper range for the display condi-
tions tested. The 25 frames were presented at a rate of 2 frames per
second. This provided the same rate of size increase as the original
film strips when projected at 24 frames per second.

The ambient illumination in the testing room was controlled to provide
an average background luminance of 4 fL. Maximum luminance on the CRT
was 15 fL under all display conditions.

Performance Testing Procedure

After visual acuity testing, each subject was briefed on the objective
of the experiment. Specific instructions were given verbally. Pictures
of the five targets at both orientations were studied by the subject
until he was easily able to identify each by name. The pictures were
available for reference by the subject throughout the testing session.
Several runs were presented to familiarize the subject with the general
appearance of the stimulus material. Each subject was then trained at
the largest dynamic range display condition until his performance improve-
ment on three successive trials was less than 10%. This took, on the
average, 80 individual target presentations.

Subjects were instructed to respond when they were "virtually certain"
that they could recognize the target. This instruction, based on a
previous Air Force study by Martin and Task (1976), was designed to
minimize guessing, yet still provide motivation for identifying the
target early in the run. The subject pressed his response button when he
thought he could recognize the target. This stopped the display sequence
and blanked the screen. The subject then named the target and his
response was recorded by the experimenter. At the same time the computer

62

printed out the frame number at recognition. Frame numbers were transformed into target angular size through the measurements made previously on the image analyzer.

Results
Information Density vs. Dynamic Range

Information density values for the dot pattern are shown in Figure 19. As expected, information density increases with increasing dynamic range. Furthermore, as suggested by equation (14), the relationship is linear with log dynamic range (correlation coefficient = .997).

The bar pattern information density values are, for the most part, consistent with the dot pattern results. As shown in Figure 20, the relationships are linear with log dynamic range. The correlation coefficients for the vertical, diagonal and horizontal bars are .997, .993 and .94 respectively. An analysis of variance test of these data (see Appendix B) shows that the effect of bar orientation is not statistically significant. This finding supports the assumption of uniform display performance as a function of orientation (radial symmetry). The discrepant reading for the horizontal bar orientation is repeatable but attempts to identify the cause have not been successful.

Figure 21 presents the information spectra for the vehicle image ensembles. Each curve is the result of an averaging of the ten images (5 targets at 2 orientations) presented at each dynamic range condition. Frequency is shown in units of cycles per degree of visual angle as well as cycles per vehicle width. The latter units are useful for relating information levels to vehicle image content. Considerable caution, however, is required in the interpretation of these curves. The measuring aperture and center spot spread effects discussed earlier raise serious questions about the validity of the low frequency values. In this plot, for example, values below 2 cycles per vehicle width are suspect. The values between 2 cycles and 6 cycles are properly ordered as a function of dynamic range. The decline in the spectra at the higher frequencies illustrates the effect of high frequency roll-off in the display system's performance.
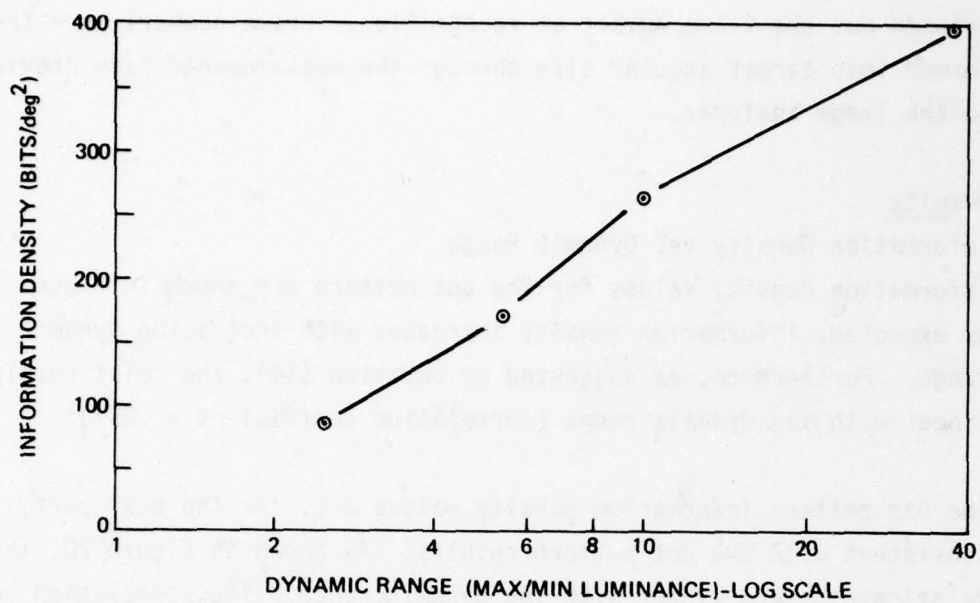
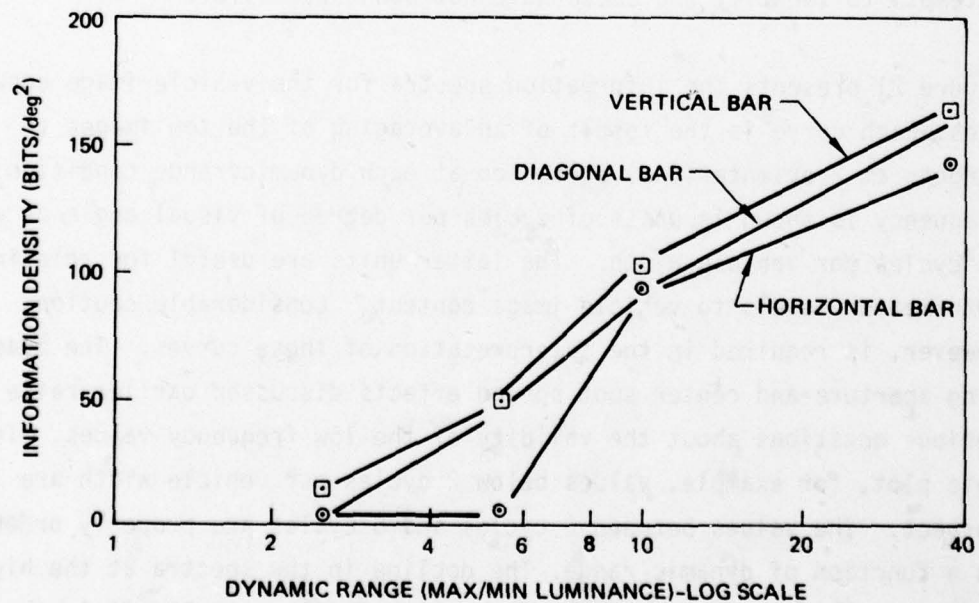*Figure 19.* Dot Pattern Information Density Values for Dynamic Range Conditions in Study I.

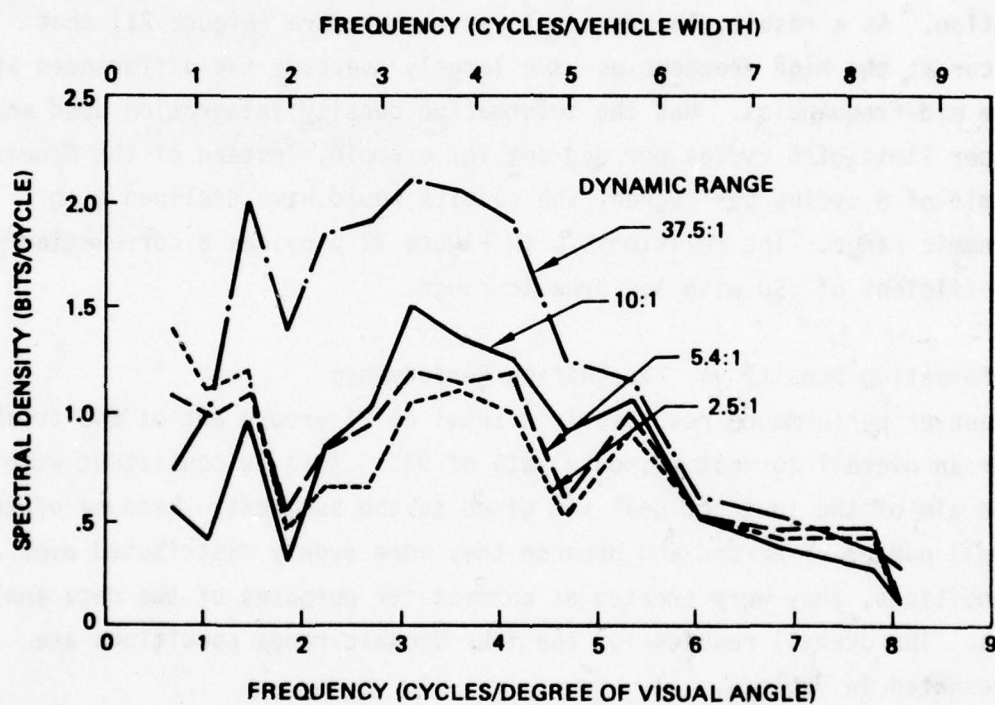*Figure 20.* Bar Pattern Information Density Values for Dynamic Range Conditions in Study I.

64

FREQUENCY (CYCLES/VEHICLE WIDTH)

SPECTRAL DENSITY (BITS/CYCLE)

DYNAMIC RANGE

37.5:1

10:1

5.4:1

2.5:1

FREQUENCY (CYCLES/DEGREE OF VISUAL ANGLE)

Figure 21.   Information Spectra for Vehicle Image Ensembles in Study I.

The information density values calculated from the spectra in Figure 21 display a somewhat different relationship with dynamic range from that found for the dot or bar patterns (Figure 22). In spite of the separation at the mid-frequencies, the integrated values (information density) show little change for the lower dynamic range values. This situation illustrates an important concern for the use of the information density metric. The formulation (equation 17) of the information density value weights the integration by frequency. The higher frequencies, therefore, contribute proportionately more to the information density calculation. As a result, the reversals in the spectra (Figure 21) that occur at the high frequencies have largely overcome the differences at the mid-frequencies. Had the information density integration used an upper limit of 5 cycles per degree, for example, instead of the Nyquist limit of 8 cycles per degree, the results would have declined with dynamic range. The relationship in Figure 22 provides a correlation coefficient of .90 with log dynamic range.

Information Density vs. Recognition Performance

Observer performance resulted in a total of 21 errors out of 640 trials for an overall correct response rate of 97%. This is consistent with the aim of the instructional set given to the subjects. Because of the small number of errors and because they were evenly distributed over all conditions, they were treated as correct for purposes of the data analysis. The overall results for the four dynamic range conditions are presented in Table 4.

Table 4: Observer Performance Results

Dynamic Range	Mean Subtended Angle (degrees)	Standard Deviation (degrees)
37.5:1	1.17	0.38
10.0:1	1.25	0.35
5.4:1	1.24	0.36
2.5:1	1.52	0.42
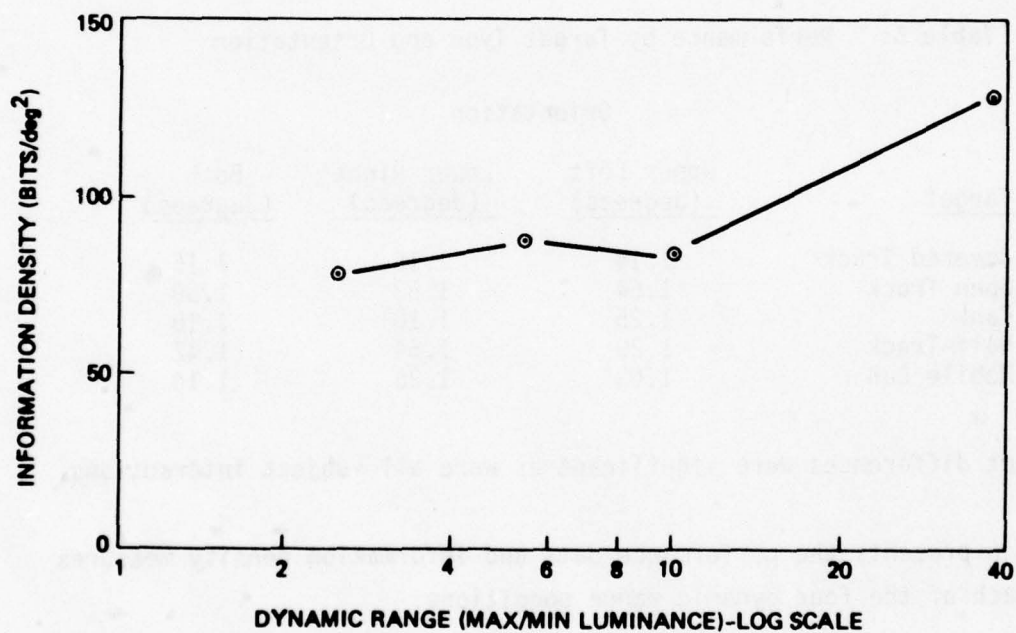
Figure 22. Vehicle Ensemble Information Density Values for Dynamic Range Conditions in Study I.

These data are plotted as a function of display dynamic range in Figure
23. In this and subsequent plots the recognition performance data are
plotted as the reciprocal of the vehicle angular size at recognition. This
provides increasing values with improving performance and also improves
the linearity of the relationships of interest. The results of the
analysis of variance show the main factors of display condition and
target to be significant at the .01 level. Orientation itself was not
significant but the target-by-orientation interaction was. This indi-
cates that orientation does have an effect but that the same orientation
is not best for all targets. This is evident from the results shown in
Table 5.

Table 5:   Performance by Target Type and Orientation

Orientation

Target	Upper Left (degrees)	Lower Right (degrees)	Both (degrees)
Covered Truck	1.14	1.15	1.15
Open Truck	1.54	1.63	1.59
Tank	1.25	1.10	1.18
Half-Track	1.29	1.54	1.42
Mobile Gun	1.03	1.25	1.14

Subject differences were significant as were all subject interactions.

Table 6 presents the performance data and information density measures
for each of the four dynamic range conditions.

Table 6:   Study I Performance and Information
Density Measures

Dynamic Range	Vehicle Recognition Performance (deg)	Dot (bits/deg^2)	Information Density			
			Vertical Bar (bits/deg^2)	Diagonal Bar (bits/deg^2)	Horizontal Bar (bits/deg^2)	Vehicles (bits/deg^2)
37.5:1	1.17	395	164	161	143	128
10.0:1	1.25	262	102	93	93	83
5.4:1	1.24	169	49	47	5	88
2.5:1	1.52	85	14	4	3	78
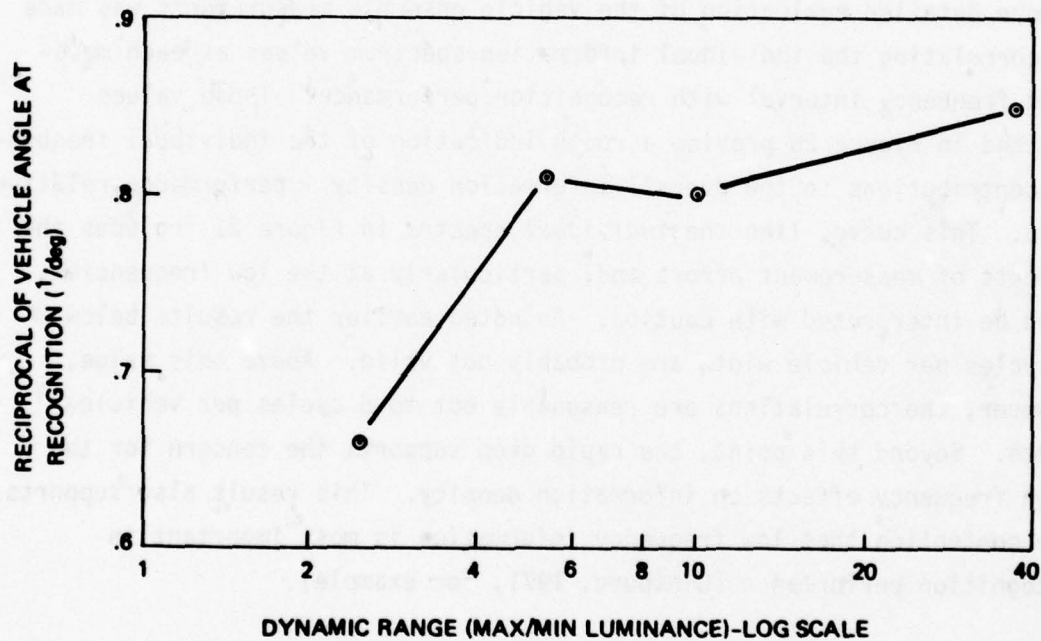
Figure 23. *Observer Performance Scores for Dynamic Range Conditions in Study I.*

Relationships for the dot pattern and vehicle ensemble measurements are plotted in Figures 24 and 25. Although the vehicle ensemble measures are properly ordered according to performance, neither set of measurements appear to properly reflect the large drop in performance at the low dynamic range condition. Pearson product-moment correlation coefficients for the relationships between vehicle recognition performance and the dot and vehicle ensemble measurements are 0.84 and 0.69 respectively. Since these values are based on only four sets of measurements they should be treated only as rough indicators of the strength of the relationships.

A more detailed evaluation of the vehicle ensemble measurements was made by correlating the individual information spectrum values at each measured frequency interval with recognition performance. These values plotted in Figure 26 provide a rough indication of the individual frequency contributions to the overall information density - performance relationship. This curve, like the individual spectra in Figure 21 includes the effects of measurement errors and, particularly at the low frequencies, must be interpreted with caution. As noted earlier the results below 2 cycles per vehicle width are probably not valid. Above this value, however, the correlations are reasonable out to 6 cycles per vehicle width. Beyond this point, the rapid drop supports the concern for the high frequency effects on information density. This result also supports the contention that low frequency information is most important in recognition performance (Ginsburg, 1971, for example).

Discussion
The standardized targets (dot and bar patterns) provide information density values that are in excellent agreement with the expected results of the display conditions used. Measurements based on the vehicle image ensembles were less successful. The information density - observer performance relationship was also better for the dot pattern than for the vehicle image ensemble. There are several factors that probably contribute to this discrepancy.
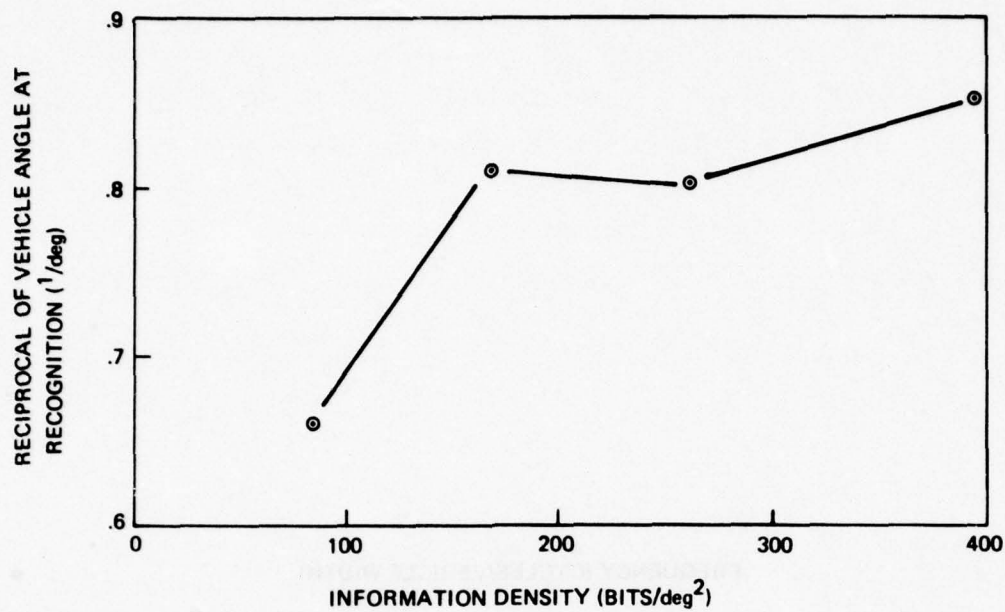
70

Figure 24. Relationship Between Dot Pattern Information Density and Observer Performance Scores for Study I.
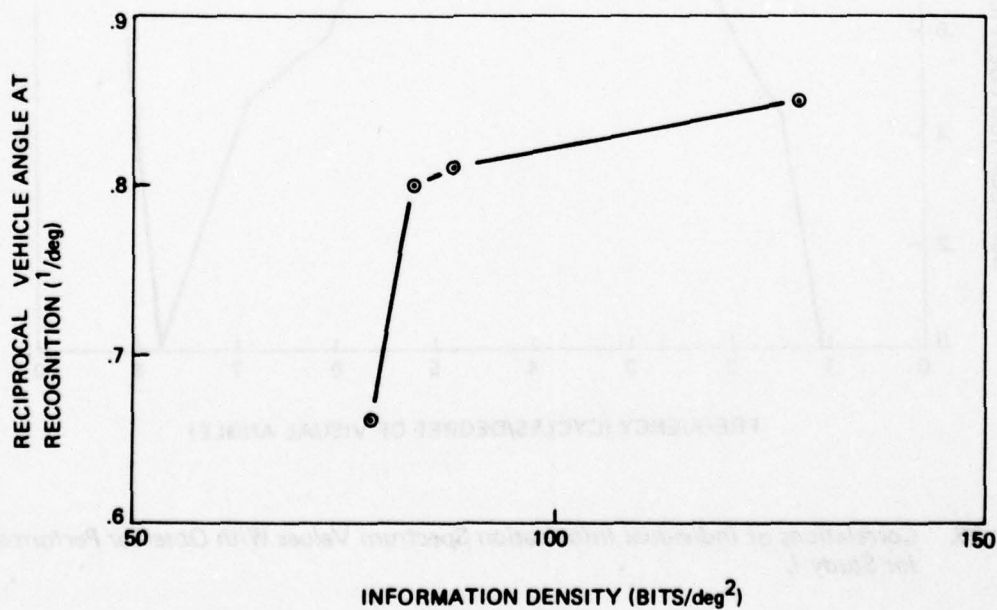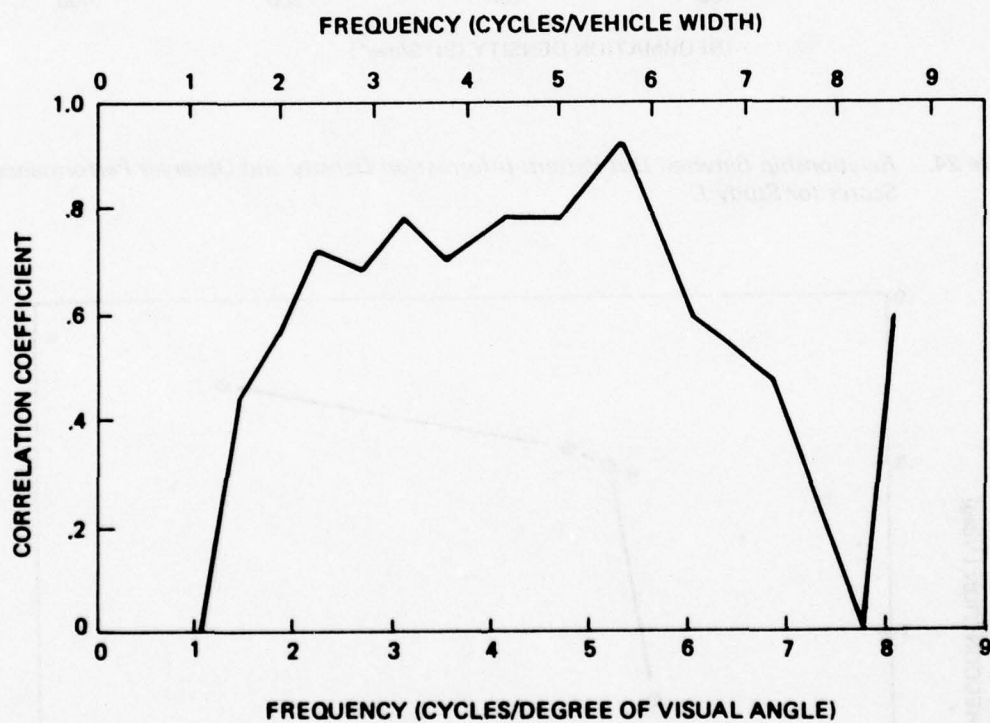

Figure 25. Relationship Between Vehicle Ensemble Information Density and Observer Performance Scores for Study I.

71

FREQUENCY (CYCLES/VEHICLE WIDTH)

Figure 26. Correlations of Individual Information Spectrum Values With Observer Performance for Study I.

72

1. The standardized targets are of much higher contrast than the vehicle images. This provides a much better signal-to-noise ratio for the optical power spectrum measurements. Marginal signal levels were found at the high frequencies for the vehicle imagery.

2. The standardized targets are larger which permits the use of a larger aperture in the power spectrum measurements. This is likely to reduce the low frequency errors noted in the results.

The high frequency contribution in the vehicle image information density calculations clearly degrades the relationship with observer performance. If a lower integration limit had been used, the correlation between vehicle information density and observer performance would have been significantly increased. Such a reduced limit might occur if visual perceptual thresholds were incorporated in the information density calculations.

STUDY II - CRT BANDWIDTH AND NOISE

Objective

The primary objective in the second study is to evaluate information density measurements under conditions that clearly violate the assumption of radial symmetry. The reduction of CRT bandwidth reduces the display resolution along the scan lines, i.e,. horizontal resolution, without altering the vertical resolution. Thus, as bandwidth is reduced, the difference in display performance as a function of orientation is increased. This problem is complicated further by the introduction of vertical, horizontal and diagonal orientations of the major dimension of the vehicle images. It is expected that, under conditions of reduced bandwidth, significant interactions will occur with vehicle orientation. The effect of random Gaussian noise is also considered by adding noise to existing system levels as an additional display condition. Another important difference, based on the results of Study I,

73

is a decrease in the film recording scale. The scale has been reduced from 1:6.4 to 1:13. This means that the images photographed from the CRT are about one-half the size of those used in Study I. As a consequence, the optical power spectrum estimates are based on a greater number of sampling intervals.

The specific hypotheses here are that;

(1) Both information density and recognition performance will decrease as a function of decreasing CRT bandwidth, and

(2) Both information density and recognition performance will decrease as a function of increasing noise.

Subjects

Six subjects from the previous study were used here. Visual acuity was retested before each session.

Performance Task

The performance task was identical to that used in Study I.

Stimulus Materials

Because of the limited capacity of the disc recorder, 20 frames were selected from the original sequence for each target. These 20 frames were selected such that each frame provided a constant proportional increase in visual angle. The size range covered performance levels for all display conditions. The sequence used covered a magnification range of 4.2:1. Only one original image orientation was used for each target. All frames, however, were recorded at three orientations, (horizontal, vertical, and diagonal), by rotating the TV camera. The random dot and bar patterns and uniform grey level frames were also recorded. The half-track target at the three bandwidth levels is shown in Figure 27.

74
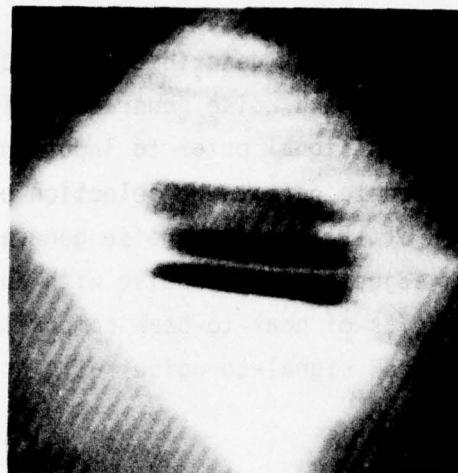
0.4 MHz
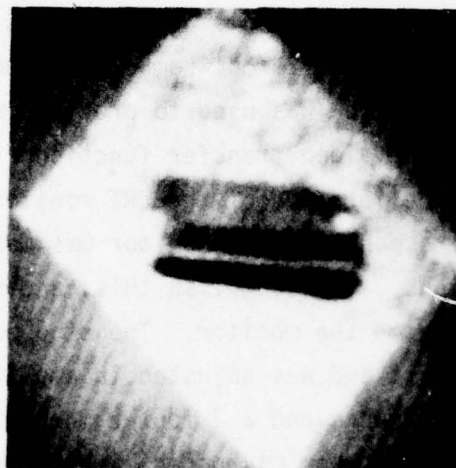
1.0 MHz

4.0 MHz

Figure 2 7   . Study II—Bandwidth Conditions

Equipment

The same equipment was used as that described for Study I with the addition of a bandwidth filter and noise generator. The added items were used to modify the video signal prior to input to the CRT. The bandwidth filter is designed to permit the selection of 4.0, 1.0 or 0.4 MHz bandwidths, (measured at -3 dB). The noise generator is a General Radio Model 1383 and was adjusted to add noise with an rms amplitude of 0.162 volts to the 0.91 volts of peak-to-peak composite video. This provides an approximate 15 dB signal-to-noise ratio as compared with a nominal system level of 43 dB.

CRT Calibration

The CRT brightness and contrast controls were adjusted to provide a 100 foot-Lambert maximum output and a 2 foot-Lambert minimum. A Hewlett Packard 3310B function generator was used to provide inputs for measurement of the resulting video transfer function (Figure 28). In addition to the repeated calibration of the CRT monitor video transfer function, the sine wave response of the monitor was measured under each of the bandwidth conditions. To accomplish this, a sine wave from the function generator was fed to the monitor. The sine wave was synchronized to the horizontal line start and was adjusted in amplitude to provide 100 foot-Lamberts peak luminance and a 2 foot-Lambert minimum luminance at the DC condition. A 12.5 power microscope imaged the monitor screen onto a vertical aperture slit whose width was 30% of the monitor spot size and whose height covered 10 scan lines. A photomultiplier was positioned to sense the light passing through the aperture. A neutral density filter attenuated the light to provide absolute calibration in foot-Lamberts. This assembly was scanned across the monitor face while the output of the photomultiplier was recorded on a X-Y recorder. The modulation contrast was calculated from the strip chart deflections. This procedure was repeated for several spatial frequencies until the complete sine wave response curve was generated. The equipment set-up for this measurement is shown in Figure 29. The resulting curves are plotted in Figure 30. The response curve with the bandwidth filter bypassed is included for comparison.
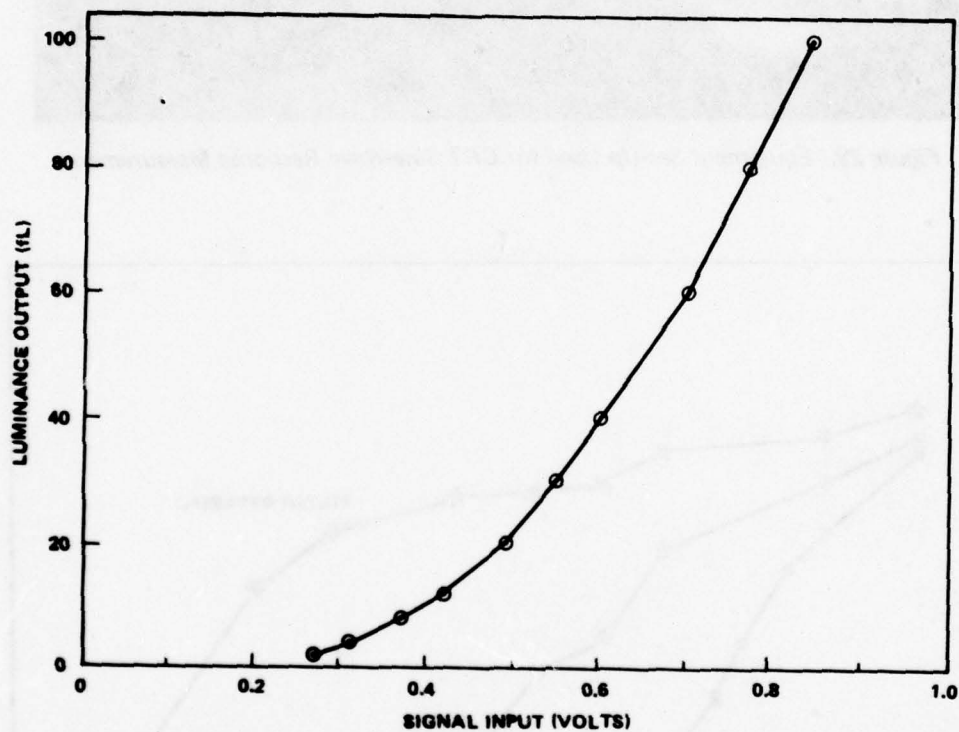
76

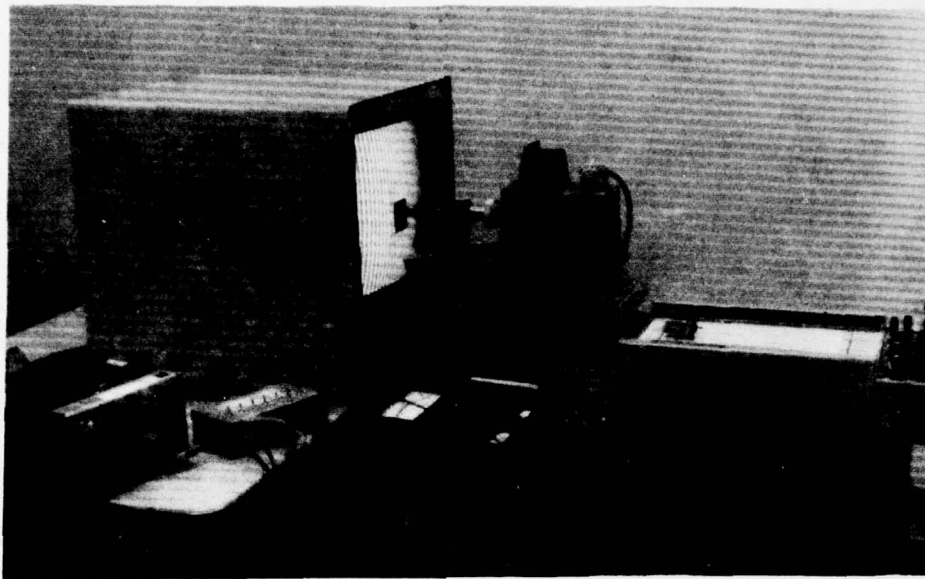Figure 28.   Video Transfer Function Used for All Study II CRT Display Conditions

77

Figure 29. Equipment Set-Up Used for CRT Sine-Wave Response Measurement
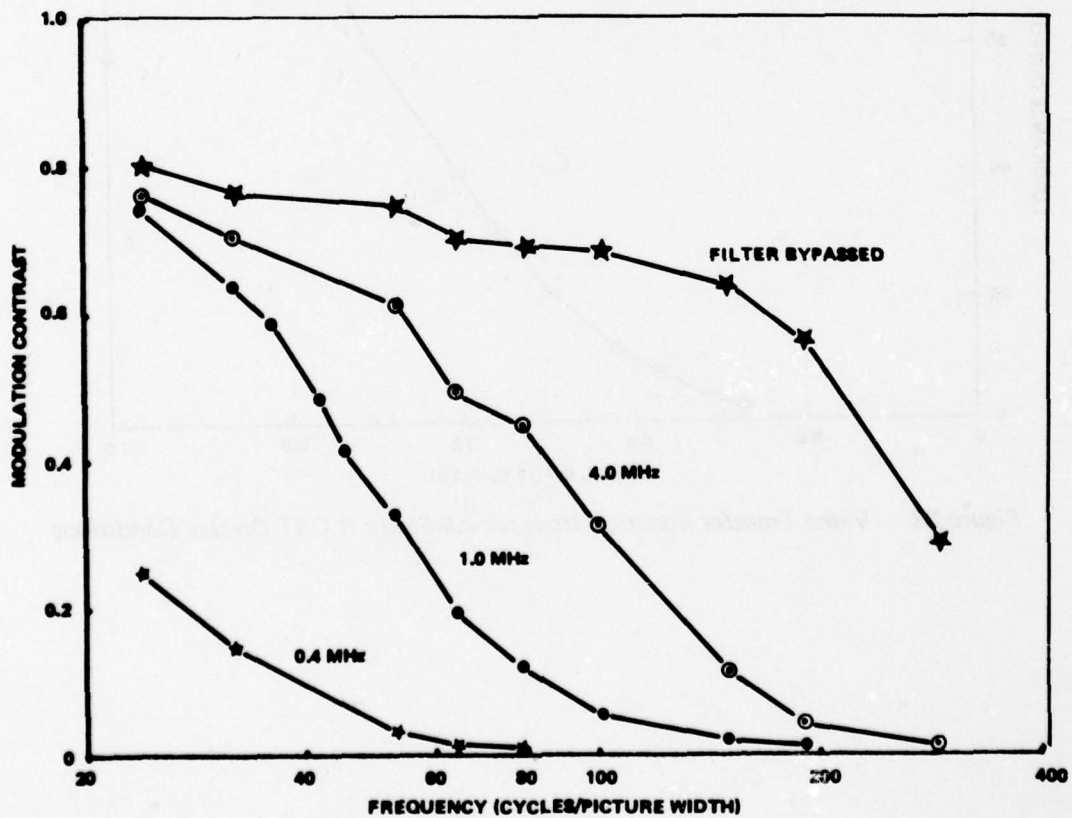

Figure 30. CRT Sine-Wave Response Curves for the Bandwidth Conditions Used in Study II.

78

Information Density Measurements

Information density measurements were made for the random patterns and the largest vehicle target image for each bandwidth by noise condition. Measurements were made for each target at each orientation. This provided 15 vehicle target measurements for each of the six display conditions. Each set of 15 power spectrum estimates was then averaged to provide the vehicle ensemble used for the information density calculations.

Except for scale, the film recording procedures were identical to those used in Study I. Experience with the vehicle target optical power spectrum measurements in Study I suggested that improved results might be obtained with a smaller image on the film. A smaller image involves higher spatial frequencies and makes better use of the existing ROSA detector frequency range. Consequently, the film recording was accomplished at a scale of 1:13. This scale is consistent with the recommendations in Section III. Because of the smaller image it was necessary to reduce the size of the measuring aperture used in the optical power spectrum determinations. The aperture used in this study was circular with a 3/16 inch diameter.

Test Design

Each of the six subjects viewed all targets and orientations under each of the six display conditions. Each subject, therefore, responded to a total of 5 x 3 x 6 = 90 individual target sequences. The orders of target-by-orientation presentations were randomized within each display condition. These random sequences were counterbalanced across display conditions. The presentation orders of the display conditions were also counterbalanced and subjects assigned at random to these orders.

The dependent variable was the visual angle of the target diagonal at the time of recognition. The independent variables were display bandwidth (3 levels), noise (2 levels), targets (5), orientation (3) and subjects (6). A mixed-model analysis of variance was used to analyze the performance data. Subjects were treated as a random variable.

Viewing Conditions

The physical viewing conditions were the same as those used in Study I. The video transfer function of the CRT monitor as described earlier was modified for this study as was the range of target sizes presented in each sequence. Target size at the beginning of a series was about 0.7 degrees and grew to slightly over 3 degrees at maximum size. The same frame rate, (2 frames per second), was used in both studies.

Performance Testing Procedures

Except for training, the test procedures did not differ from Study I. Since all subjects were experienced with the test targets and procedures, training was reduced to 3 runs, (15 target presentations per run). Two runs were presented at the middle bandwidth condition, (1.0 MHz.), and one at the lowest condition, (0.4 MHz.). The latter was considered necessary to familiarize the observer with the very poor image quality at that level.

Results

Information Density vs. Display Performance

The bar and dot pattern information density values are shown as functions of display bandwidth in Figures 31 and 32. The bar plots represent the average of the two noise conditions. These results clearly reflect the expected effects of bandwidth reduction. The horizontal bars are a measure of vertical display performance and, as expected, show no difference in information density. The vertical and diagonal bars are subjected to the effects of bandwidth reduction and exhibit the expected decline with bandwidth. The relationship of the diagonal information density to the horizontal and vertical values is of some interest. A good fit is found from,

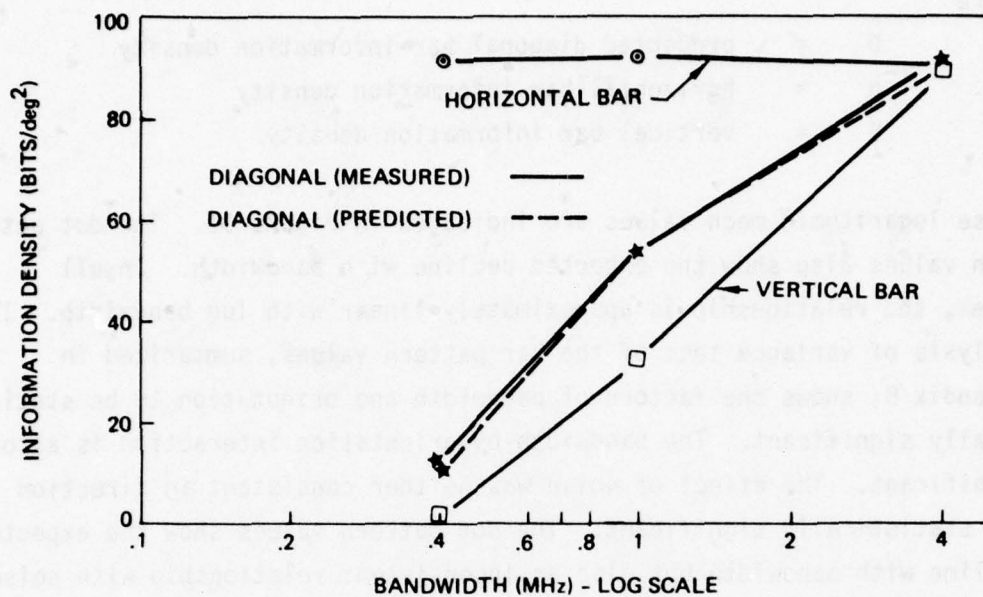$$\hat{D} = exp\left[(\ln H + \ln V)/2\right], \qquad (35)$$

Figure 31. Bar Pattern Information Density Values for Bandwidth Conditions in Study II.
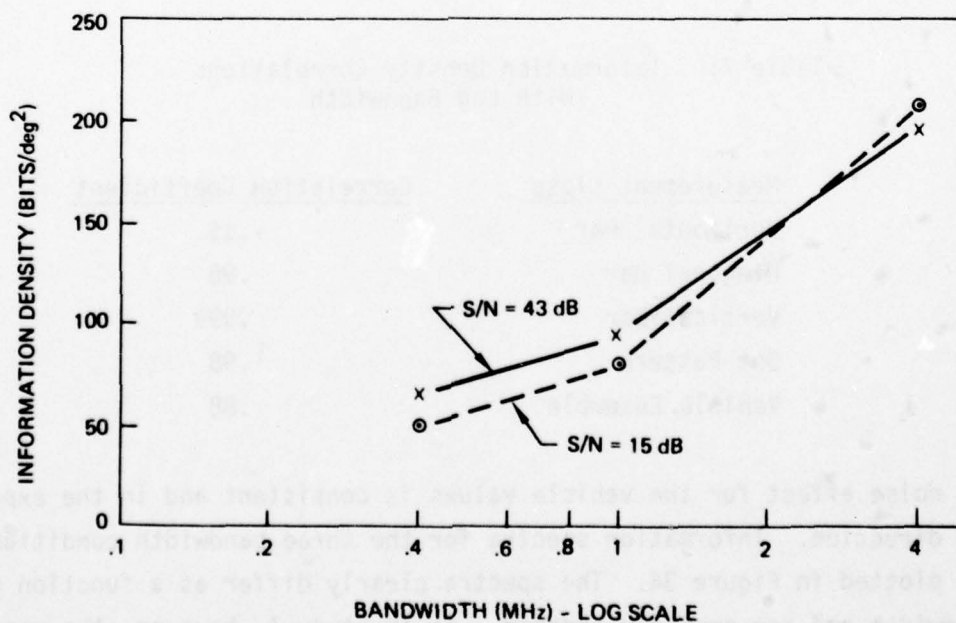Values are Averages of Both Noise Conditions

Figure 32. Dot Pattern Information Density Values for Bandwidth and Noise Conditions in
Study II.

where

$\hat{D}$ = predicted diagonal bar information density

H = horizontal bar information density

V = vertical bar information density.

These logarithmic mean values are indicated in Figure 31. The dot pattern values also show the expected decline with bandwidth. In all cases, the relationship is approximately linear with log bandwidth. The analysis of variance test of the bar pattern values, summarized in Appendix B, shows the factors of bandwidth and orientation to be statistically significant. The bandwidth-by-orientation interaction is also significant. The effect of noise was neither consistent in direction nor statistically significant. The dot pattern values show the expected decline with bandwidth but also an inconsistent relationship with noise.

The vehicle image information density values are shown in Figure 33. The general trend is consistent with that seen for dot and bar patterns. The correlations with log bandwidth for each of the measurement classes are shown in Table 7.

Table 7: Information Density Correlations
With Log Bandwidth

Measurement Class	Correlation Coefficient
Horizontal Bar	-.15
Diagonal Bar	.98
Vertical Bar	.999
Dot Pattern	.98
Vehicle Ensemble	.88

The noise effect for the vehicle values is consistent and in the expected direction. Information spectra for the three bandwidth conditions are plotted in Figure 34. The spectra clearly differ as a function of bandwidth and are properly ordered. As in Study I, however, the very low frequency values (below two cycles per vehicle width) are of questionable stability. The reduced film recording scale used in this study
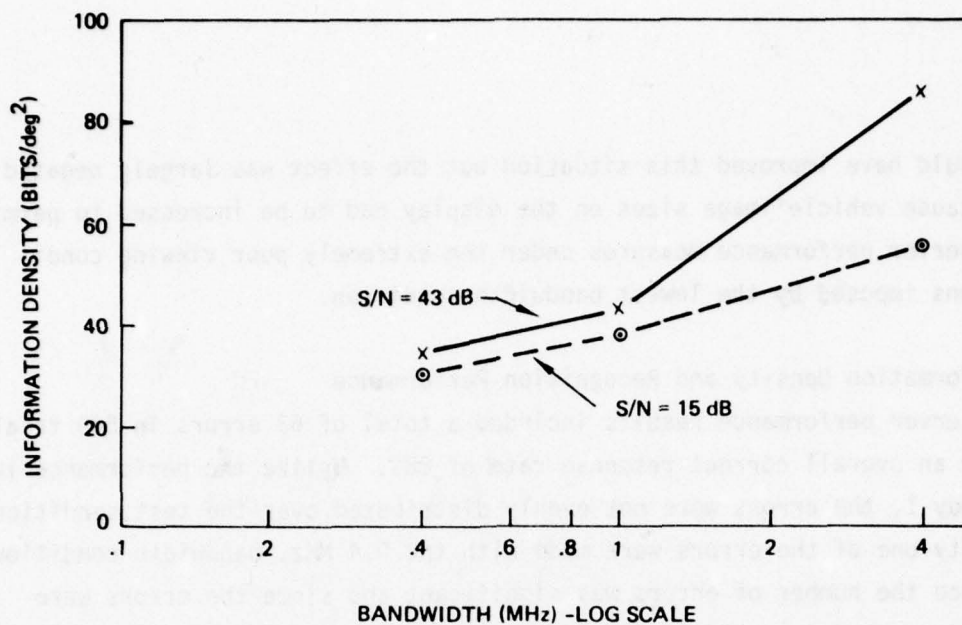
82

Figure 33. Vehicle Ensemble Information Density Values for Bandwidth and Noise Conditions in Study II.
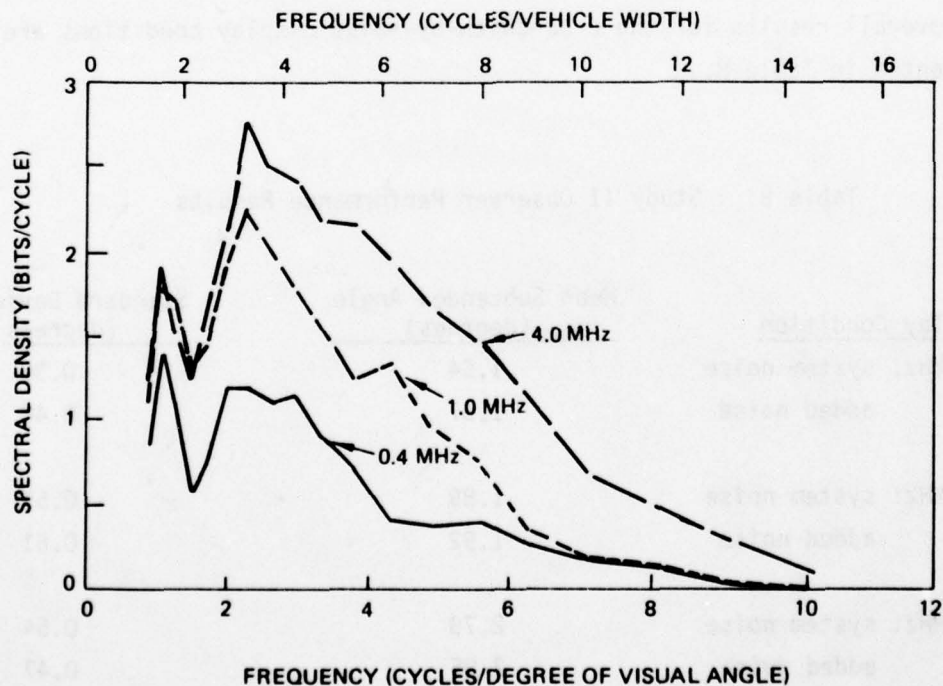

Figure 34. Information Spectra for Vehicle Ensembles at Each of the Study II Bandwidth Conditions. Values are Averaged Across Noise Conditons

83

should have improved this situation but the effect was largely negated because vehicle image sizes on the display had to be increased to permit observer performance measures under the extremely poor viewing conditions imposed by the lowest bandwidth condition.

Information Density and Recognition Performance
Observer performance results included a total of 63 errors in 540 trials for an overall correct response rate of 88%. Unlike the performance in Study I, the errors were not evenly distributed over the test conditions. Fifty-one of the errors were made with the 0.4 MHz. bandwidth condition. Since the number of errors was significant and since the errors were concentrated in a single display condition, they could not be treated in the same manner as that used in Study I. In Study II, errors were given a maximum score representing the size of the largest image presented for that target.

The overall results for the 6 bandwith-by-noise display conditions are presented in Table 8.

Table 8:   Study II Observer Performance Results

Display Condition	Mean Subtended Angle (degrees)	Standard Deviation (degrees)
4.0 MHz: system noise	1.54	0.36
added noise	1.67	0.40
1.0 MHz: system noise	1.89	0.55
added noise	1.92	0.61
0.4 MHz: system noise	2.79	0.54
added noise	2.85	0.47

84

These data are plotted as a function of bandwidth in Figure 35. The results of the analysis of variance summarized in Appendix B show the main factors of bandwidth, target, and orientation to be significant at the .01 probability level. Subject differences were significant as were all subject two way interactions. Although the effect of noise was consistent, and in the expected direction, the magnitude of the effect was not sufficient to achieve statistical significance. As in Study I, the target-by-orientation interaction was significant. These data are presented in Table 9. The vertical target orientation was the most difficult except for the covered truck. This reversal appears to result from the fact that the ribs on the truck cover are an important cue and they are most easily resolved when they are parallel with the scan lines. This occurs with the vertical target orientation.

Table 9: Study II Performance by Target Type and Orientation

Target	Horizontal (Degrees)	Vertical (degrees)	Diagonal (degrees)	All (degrees)
Covered Truck	2.04	1.68	1.99	1.87
Open Truck	2.38	2.53	2.33	2.41
Tank	1.93	2.40	1.86	2.06
Half-Track	1.99	2.28	1.99	2.09
Mobile Gun	1.86	2.49	1.98	2.11
All Targets	2.04	2.27	2.01	

Table 10 presents the performance data and information density measures for each of the bandwith-by-noise level conditions.
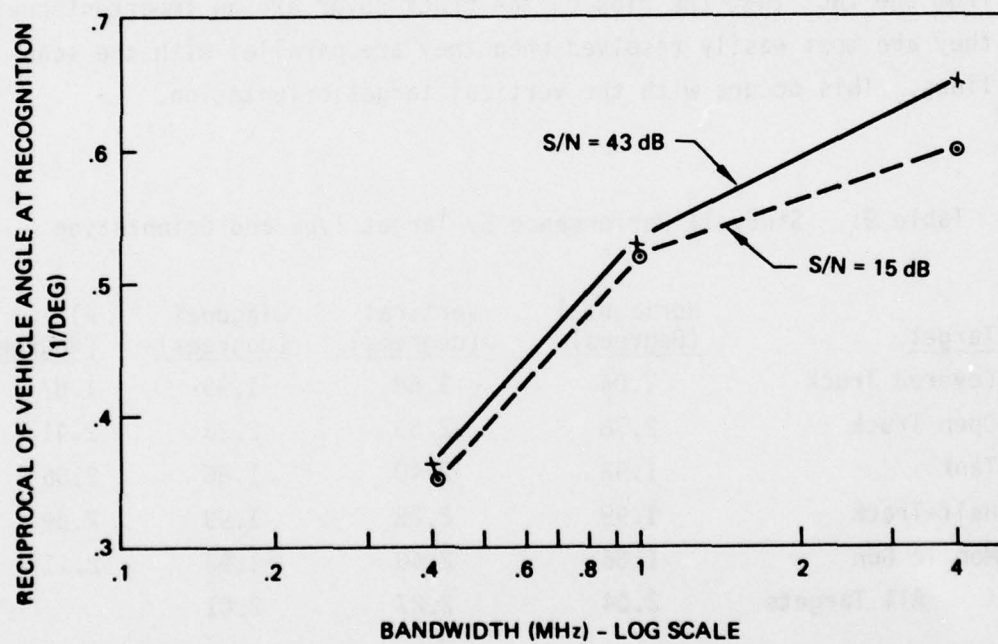
Figure 35.   Observer Performance Scores for Bandwidth and Noise Conditons in Study II.

Table 10: Study II Performance and Information Density Measures

Band-Width MHz	Signal-to-noise Level	Vehicle Recognition Performance (degrees)	Information Density (bits/deg^2)				
			Dot	Vertical Bar	Diagonal Bar	Horizontal Bar	Vehicle Ensemble
4.0	43 dB	1.54	197	87	91	89	86
	15 dB	1.67	207	91	93	90	56
1.0	43 dB	1.89	94	30	54	8?	43
	15 dB	1.92	80	34	55	95	38
0.4	43 dB	2.79	65	0	14	98	34
	15 dB	2.85	50	0	20	84	30

Relationships for the dot pattern and vehicle ensemble measurements are plotted in Figures 36 and 37. The general shape of both relationships is similar to that in Study I (see Figures 24 and 25). As plotted in Figures 36 and 37, the correlation coefficients for the dot and vehicle relationships are .87 and .85 respectively. Both relationships are improved by using log information density; correlations become .92 and .90. In all cases, however, it appears that the information density is overestimated for the poorest viewing conditions. This result supports the suggestion that the use of visual thresholds will improve the relationship between information density and observer performance.

The correlations, by frequency, between the vehicle ensemble information spectrum values and observer performance are shown in Figure 38. Although the correlations are higher, the general shape of the curve is similar to the Study I results. The correlations are highest from about 2 cycles per vehicle width through the mid-frequencies (to about 7 cycles per vehicle width in this case) and then drop at the higher frequencies.
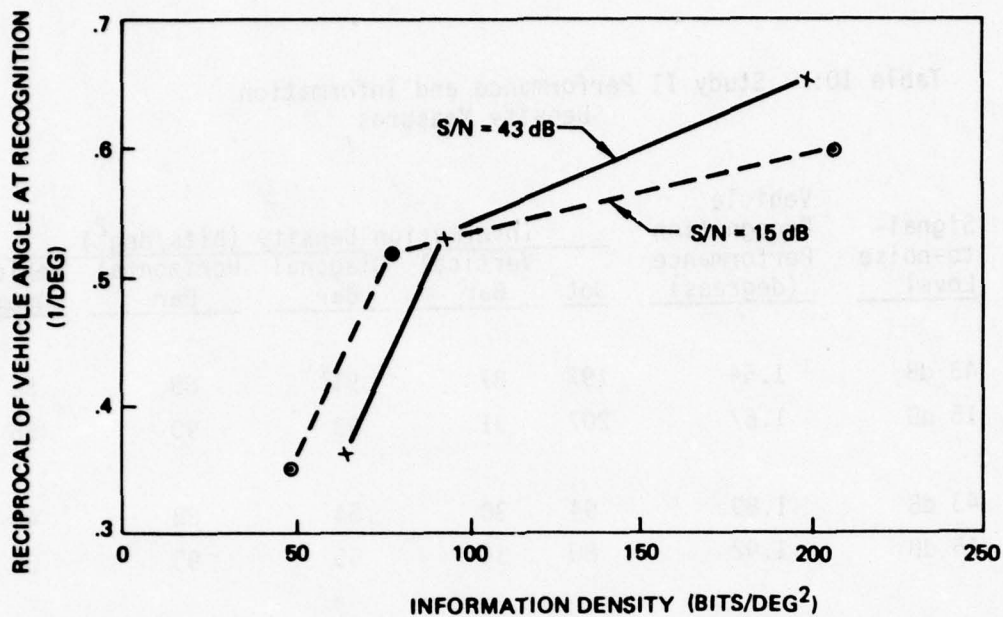
87

Figure 36. Relationship Between Dot Pattern Information Density and Observer Performance Scores for Study II.
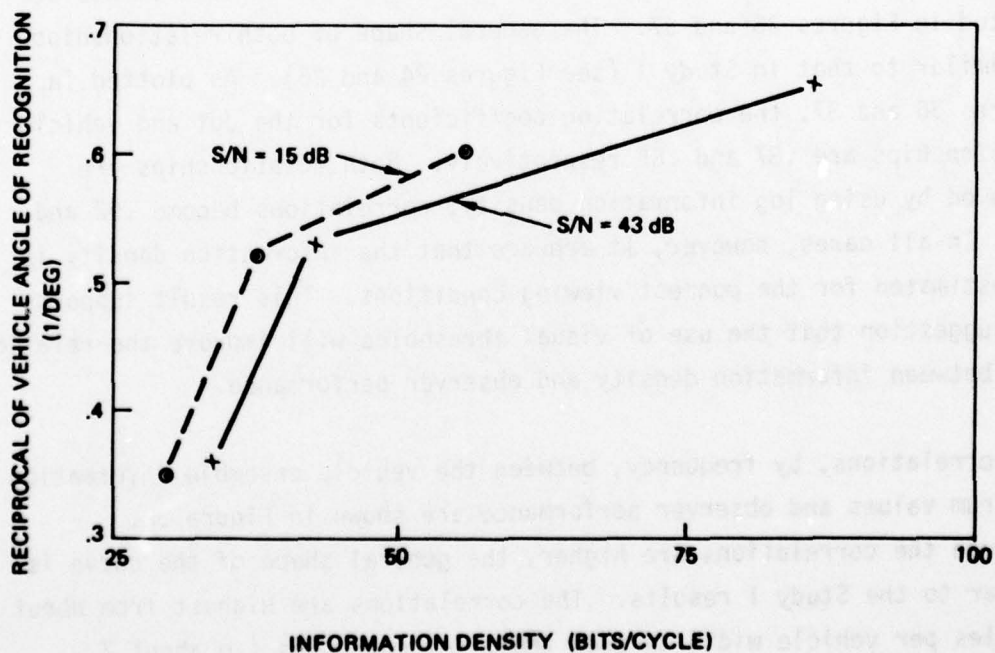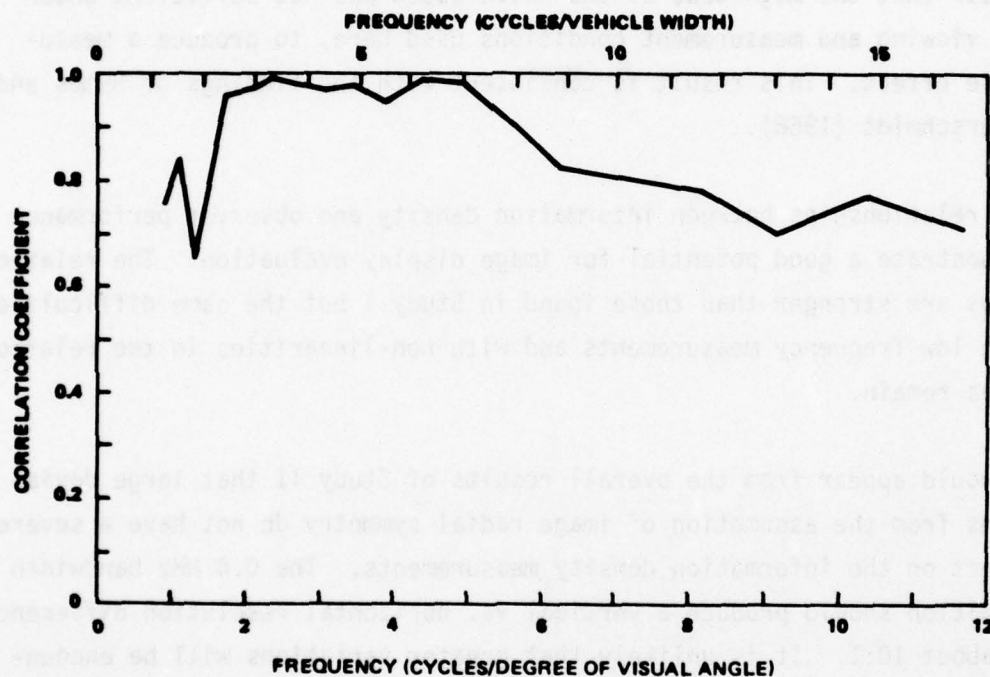

Figure 37. Relationship Between Vehicle Ensemble Information Density and Observer Performance Scores for Study II.

Figure 38. Correlations of Individual Vehicle Ensemble Information Spectrum Values With Observer Performance for Study II

<u>Discussion</u>. The information density relationships with bandwidth show excellent agreement with the expected effects on display system performance. As in Study I, the standardized images (dot and bar patterns) provide the best results.

The effects of noise level are small and non-significant for both the observer performance and the information density measures. It would appear that the magnitude of the noise added was not sufficient under the viewing and measurement conditions used here, to produce a measurable effect. This result is consistent with the findings of Humes and Bauerschmidt (1968).

The relationships between information density and observer performance demonstrate a good potential for image display evaluation. The relationships are stronger than those found in Study I but the same difficulties with low frequency measurements and with non-linearities in the relationships remain.

It would appear from the overall results of Study II that large deviations from the assumption of image radial symmetry do not have a severe effect on the information density measurements. The 0.4 MHz bandwidth condition should produce a vertical vs. horizontal resolution difference of about 10:1. It is unlikely that greater variations will be encountered in practice.

STUDY III - MATRIX CAMERA AND GREY LEVEL CODING

<u>Objective</u>. The test conditions in this study utilize matrix element sampling of the image rather than the line sampling of the conventional TV system used in the previous studies. In addition, the image luminance values are sampled at discrete levels rather than the continuous sampling previously used. These conditions are representative of digital video imagery as opposed to the analog imagery in the previous two studies.

The sampling matrix used here is considerably more coarse than the conventional TV vidicon. The resolution of the displayed imagery in this study is, therefore, reduced from that under the full bandwidth conditions in the previous studies. The sampling matrix has 244 vertical elements and 188 horizontal elements, so vertical resolution is about one-half of the previous displays along with a reduction to about one-third in the horizontal resolution. These conditions, as in Study II, represent a violation of the radial symmetry assumption in the formulation of the information density measurement.

The luminance level sampling or quantization, as noted in Section II, requires a different treatment of "noise" in the calculation of informational density. This approach, defined by equation 23 in Section II, is evaluated here. The number of quantization levels is used as the primary variable in this study.

The results here are expected to show a declining level of both information density and operator performance as the number of quantization levels is reduced.

Subjects
Nine male subjects with an age range of 35 to 60 were used in this study. Eight of these subjects had participated in at least one of the previous studies. Visual acuity was tested as noted for Studies I and II.

Performance Task
The performance task for the observers was identical to that used in the previous two studies.

Stimulus Materials
The same original materials as used in the previous studies were used to generate 10 sequences, (5 targets at 2 orientations each). Each sequence included 20 frames selected as in Study II. The orientations are those used in Study I, (i.e., target pointed to the upper right or lower left). Each sequence was recorded on the video disc.

91

Equipment

This study used the same equipment and configuration as described for Study I except for the video recording camera and a real time PCM* encoder. The vidicon in Study I was replaced with a General Electric Charge Injection Device (CID) camera. The image sensor in this camera is a two-dimensional solid state array with 188 horizontal elements and 244 vertical elements. The PCM encoder digitizes the output from the video disc, encodes the signal at the appropriate grey step, and converts the signal back to analog for input to the CRT monitor. Encoding was commanded at 8, 5, or 4 bits, representing 154, 20, or 10 grey levels for the sensor video portion of the composite signal. The PCM transfer functions for the three bit level conditions are shown in Figure 39. Examples of these display conditions are shown in Figure 40.

CRT Calibration

The CRT video transfer function was adjusted as in Study II, (see Figure 28). As in the other studies, the transfer function was monitored and adjusted as necessary throughout the testing sessions. Since the bandwidth filter was not used in this study, the "bandwidth filter bypassed" sine wave response curve in Figure 30 applies here. The curve, however, applies only to the CRT. The total imaging response is well below these levels.

Information Density Measurements

Information density measurements used the same film recording techniques as discussed for Study II. Vehicle target measurements were made for each target at each orientation and at each PCM level display condition. This resulted in 10 vehicle target measurements for each of the 3 display conditions.

A major difference from the previous studies, however, was incorporated because of the nature of the PCM process. The translation of the video signal into discrete grey levels has a very significant impact on the
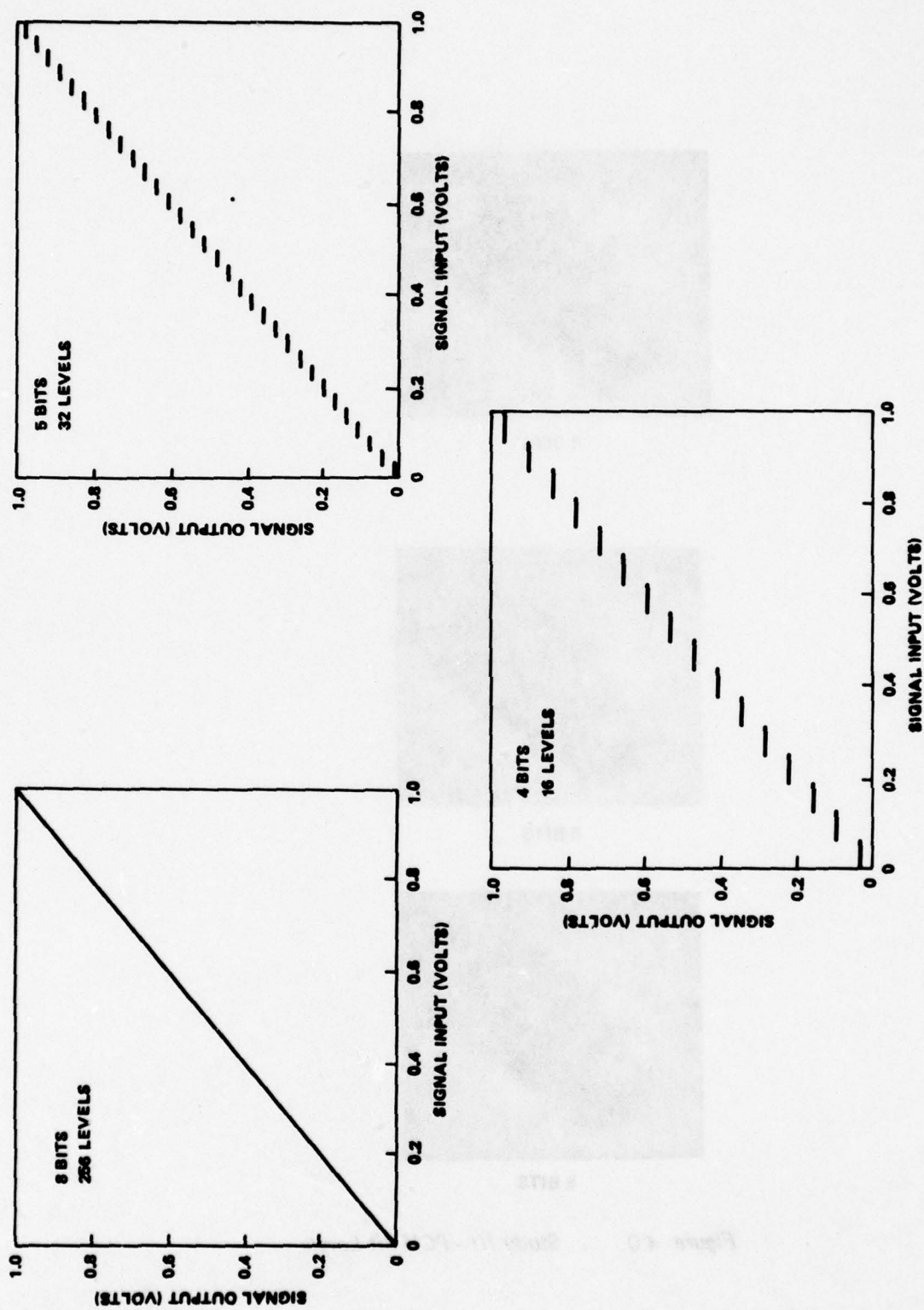
*Pulse Coded Modulation
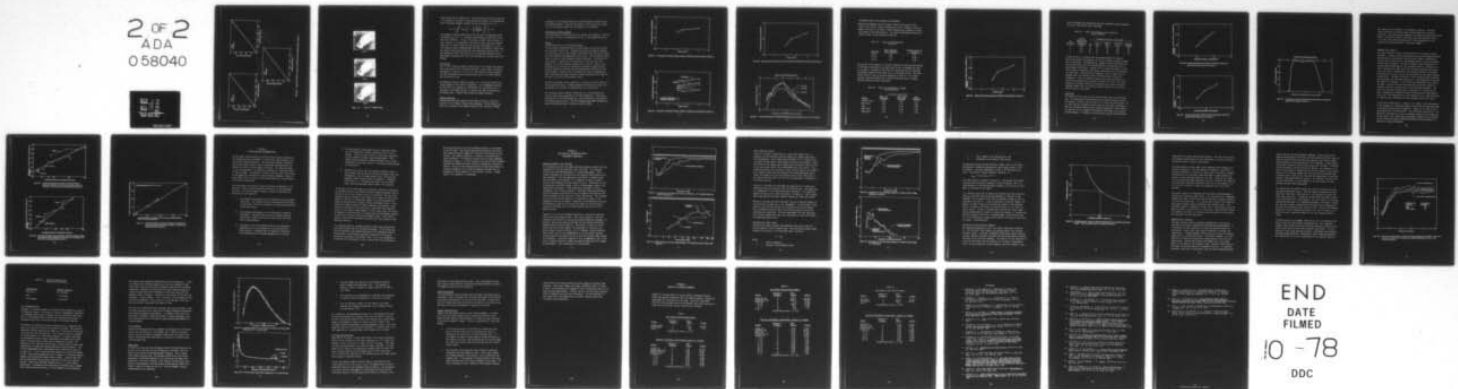
Figure 39. Quantizer Transfer Functions for PCM Bit Level Conditions Used in Study III

93

4 BITS

5 BITS

8 BITS

Figure 4 0 . Study III— PCM Bit Levels

nature and effect of image noise. The noise model described by equation 17 in Section II and used in the previous two studies is not appropriate here. The proper approach involves the use of equation 23, i.e.,

$$D = 2\pi \int_{0}^{R} \log_2 \left[1 + \left(\frac{P_S(r)}{P_{\Delta S}(r)} \right)^{\frac{1}{2}} \right] r\, dr.$$

This approach requires power spectra for the just discriminable signal difference, $P_{\Delta S}(\rho)$, i.e., one grey step difference, under each of the PCM level conditions. It was not possible to obtain valid measures of these spectra. As a compromise, the uniform signal image was measured under each of the PCM conditions and used as an estimate of $P_{\Delta S}(\rho)$. This approach tends to underestimate the just discriminable signal level and, hence, should overestimate the true information density level. If the magnitude of this error proves to be significant, improved "noise" measurement techniques will have to be developed for discrete grey level imagery.

Test Design

Each of the 9 subjects viewed 2 replications of all targets and orientations under each of the 3 display conditions. Each subject, therefore, responded to a total of 2 x 5 x 2 x 3 = 60 individual target sequences. The same randomization and counterbalancing used in the other studies were incorporated here.

The dependent variable remains the same, i.e., the visual angle of the target diagonal at the time of recognition. The independent variables are PCM level (3), targets (5), orientation (2), and subjects (9). A replicated, mixed-model analysis of variance was used to analyze the performance data. Subjects were treated as random variables.

Viewing Conditions

Viewing conditions were identical with those of Study II, with the exception of the range of target sizes presented. A pilot study indicated that, because of the reduced resolution with the matrix camera,

95

increases in the displayed target size were necessary to provide valid performance measures. Based on the results of the pilot study, target size on the display ranged from .98 degrees to 3.80 degrees.

Performance Testing Procedure

Testing procedures for the two previous studies were repeated. Training consisted of 3 runs, (20 sequences per run), at the highest PCM level.

Results

Information Density vs. Display Performance

The dot pattern information density values show a very small variation with bit level (Figure 41). Although the values are properly ordered the differences are of questionable significance since they are at about the level expected from measurement error alone. The bar pattern values shown in Figure 42 show somewhat greater differences. The overall bit level effect is significant in the analysis of variance test (see Appendix B) but the difference between the 4 and 5 bit levels is not. Differences as a function of orientation are highly significant and properly ordered as expected from the differential resolution of the matrix camera. Figure 42 also illustrates the level of agreement between the measured diagonal values and those predicted by the logarithmic mean of vertical and horizontal results.

The vehicle ensemble values, depicted in Figure 43, are very similar to the dot pattern results. Although properly ordered by bit level, the differences are too small to consider this as a valid effect.

The individual vehicle spectra (Figure 44), as in the previous two studies, show a good separation in the mid-frequencies. Cross-overs, particularly at the high frequencies, create problems for the over-all information density values. The low frequency measurement problems are again evident below about 2 cycles per vehicle width.
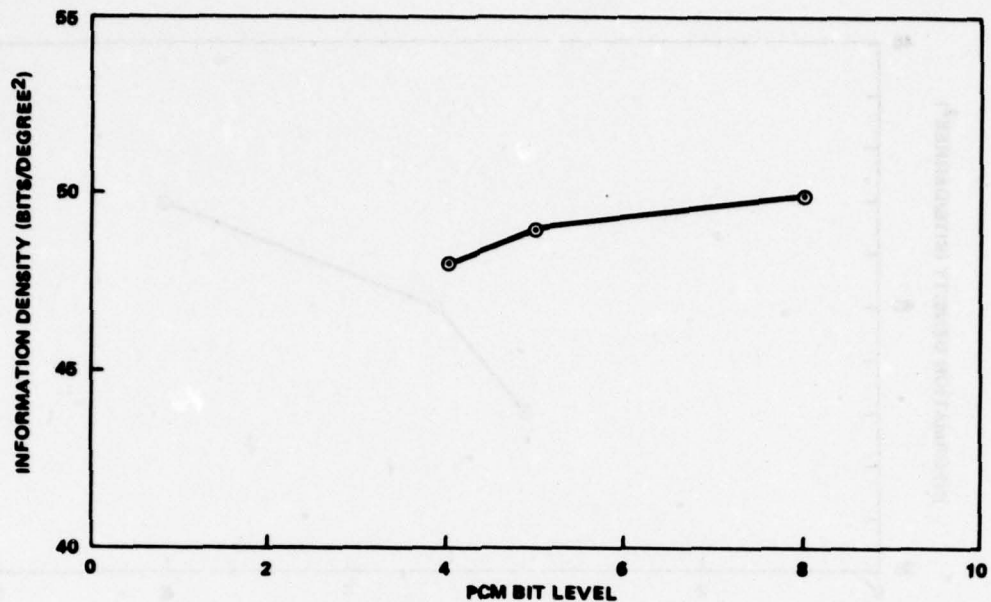
96

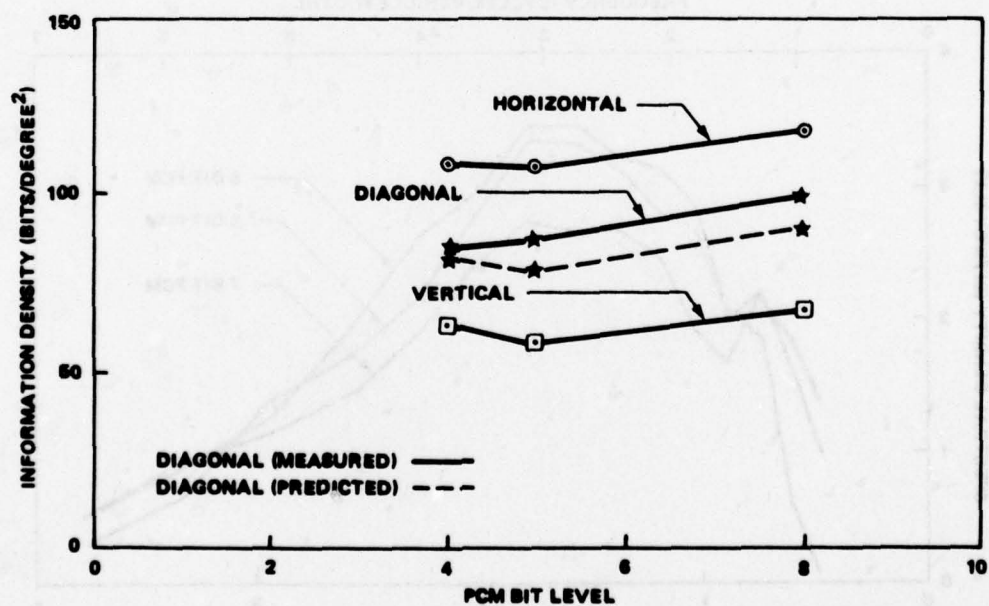*Figure 41. Dot Pattern Information Density Values for PCM Bit Level Conditions in Study III*

Figure 42. Bar Pattern Information Density Values for PCM Bit Level Conditions in Study III
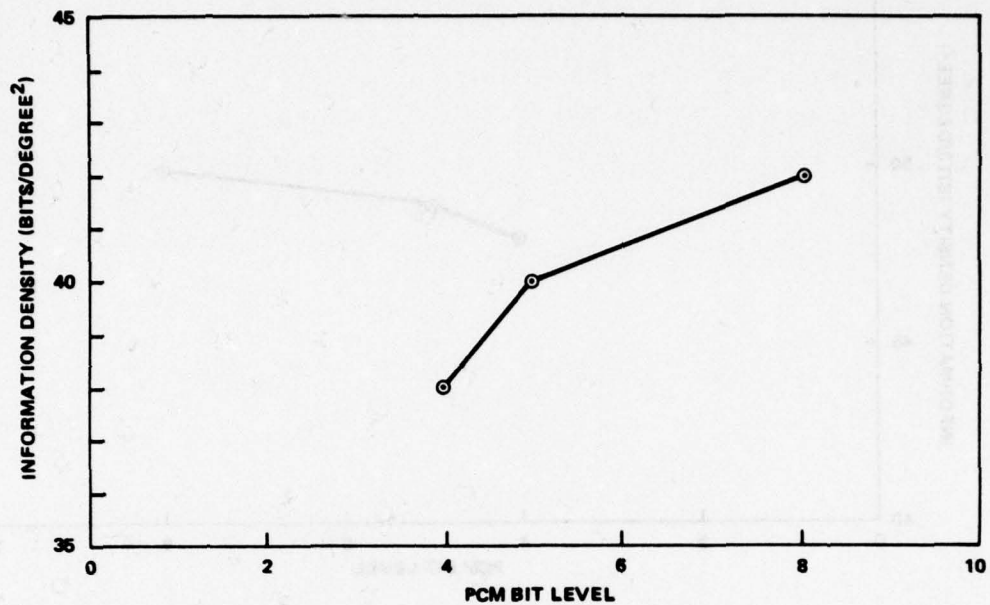
97

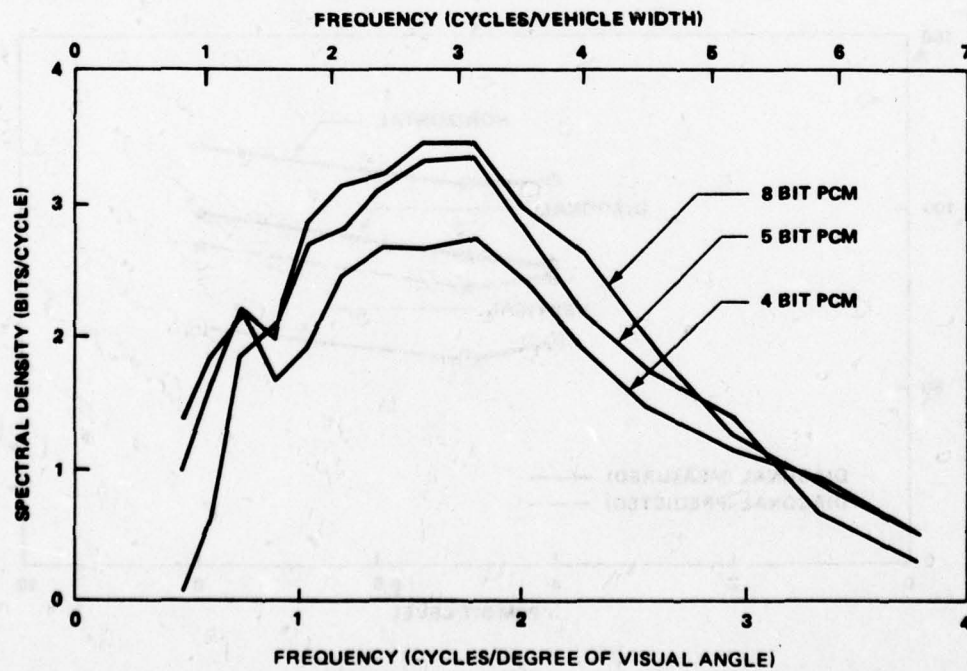*Figure 43. Vehicle Ensemble Information Density Values for PCM Bit Level Conditions in Study III*

Figure 44. Information Spectra for Vehicle Ensembles at Each of the Study III Bit Level Conditions

Information Density and Recognition Performance

Observer performance results included a total of 18 errors in 540 trials for an overall correct response rate of 97%. Because of the low number of errors, as in Study I, these responses were treated as correct for purposes of the data analysis. The overall performance results are listed in Table 11 and plotted in Figure 45.

Table 11: Study III Performance by
PCM Level

PCM Level	Mean Subtended Angle (degrees)	Standard Deviation (degrees)
8 bits	3.08	0.73
5 bits	3.20	0.88
4 bits	3.37	0.82

The results of the analysis of variance (Appendix B) show the main effects of PCM level and targets to be significant at the .01 probability level. As in Study I, orientation itself was not significant but the target-by-orientation interaction was found to be a significant effect. The interaction effect is seen in the data presented in Table 12. As in both previous studies performed here, subject differences and all subject two-way interactions were significant.

Table 12: Study III Performance by Target
and Orientation

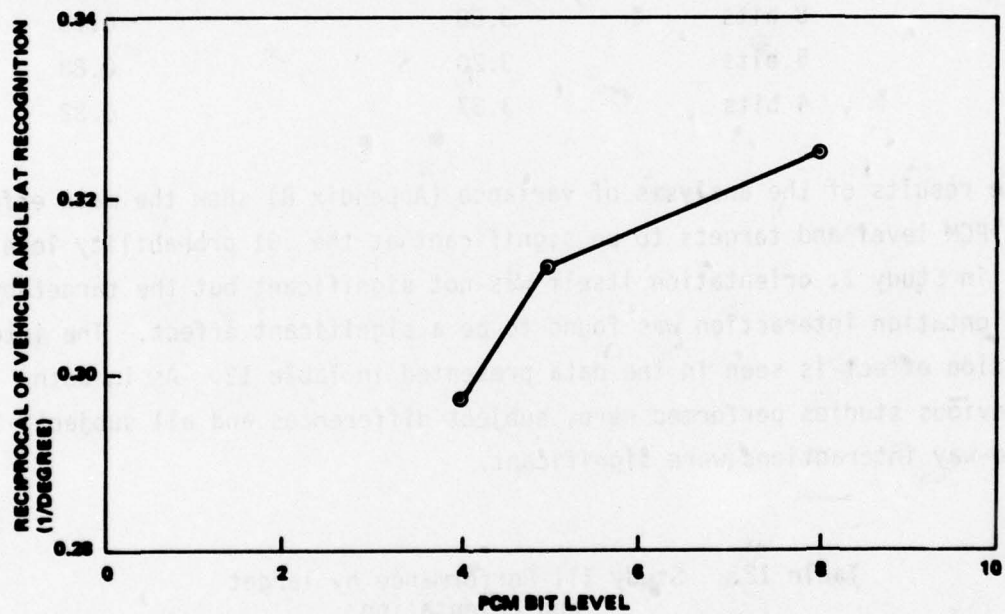|	Orientation		
Target	Upper Left (degrees)	Lower Right (degrees)	Both (degrees)
Covered Truck	3.02	3.21	3.11
Open Truck	3.67	3.70	3.69
Tank	3.15	2.74	2.95
Half-Track	3.16	3.14	3.15
Mobile Gun	3.12	3.27	3.20

99

Figure 45. Observer Performance Scores for PCM Bit Level Conditions in Study III

Table 13 presents the performance data and information density measures for each of the PCM bit level conditions.

Table 13: Study III Performance and Information
Density Measures

PCM Bit Level	Vehicle Recognition Performance (degrees)	Information Density (bits/deg^2)				
		Dot	Vertical Bar	Diagonal Bar	Horizontal Bar	Vehicle Ensemble
8	3.08	50	68	100	118	42
5	3.20	49	58	87	108	40
4	3.37	48	63	84	109	38

Figures 46 and 47 illustrate the relationship between information density and observer performance for the dot pattern and vehicle ensemble, respectively. As noted earlier, however, these relationships may well be fortuitous since the information density differences are of questionable significance. Because of this problem and because of the small number of conditions, correlation coefficients are not presented for these data. Correlations by frequency, shown in Figure 48, are somewhat more valid because larger differences exist at the mid-frequencies. They are, however, based on only three conditions and should be considered only as general indicators of trend. As in the previous two studies, effective relationships exist only in the mid-frequency range (from 1.6 cycles per vehicle width to 4.6 cycles per vehicle width in this case).

Discussion

The results of this study are less positive than those of the previous two. The questionable significance of the information density values differences is likely to be the result of at least two difficulties. It is clear from the information spectra and the individual correlations that the information density metric imposes integration limits that are not optimum for the frequency relationships that appear to exist with the measurements. In addition, the technique used here to approximate
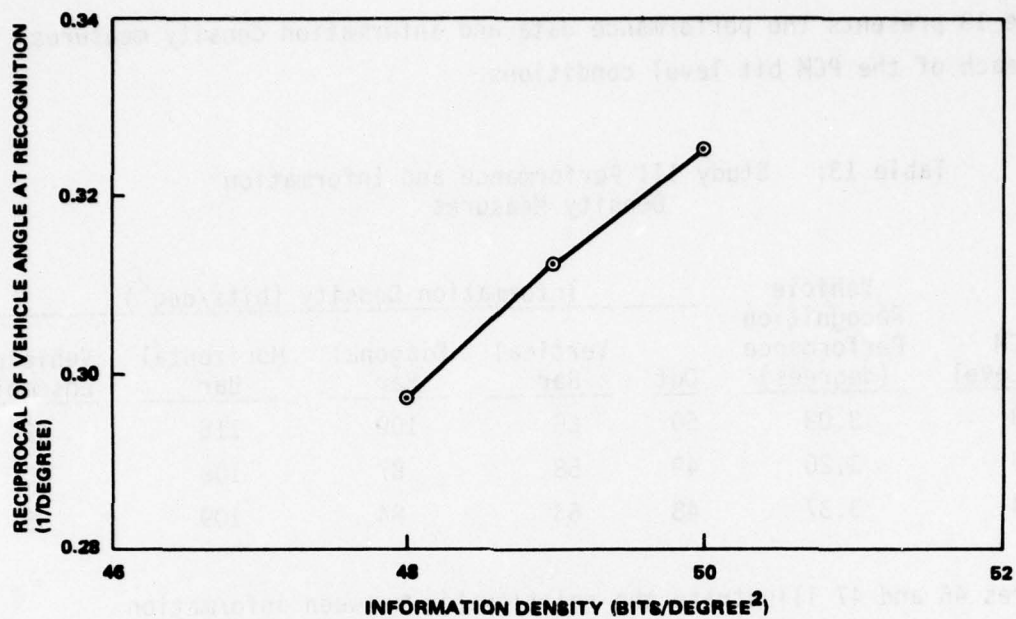
101

Figure 46. Relationship Between Dot Pattern Information Density and Observer Performance Scores for Study III
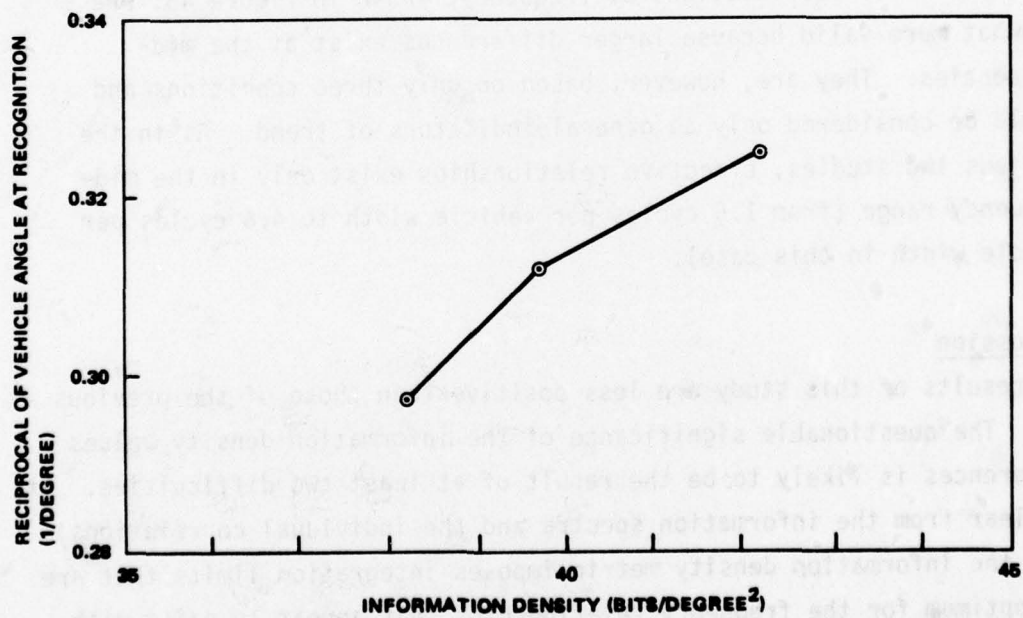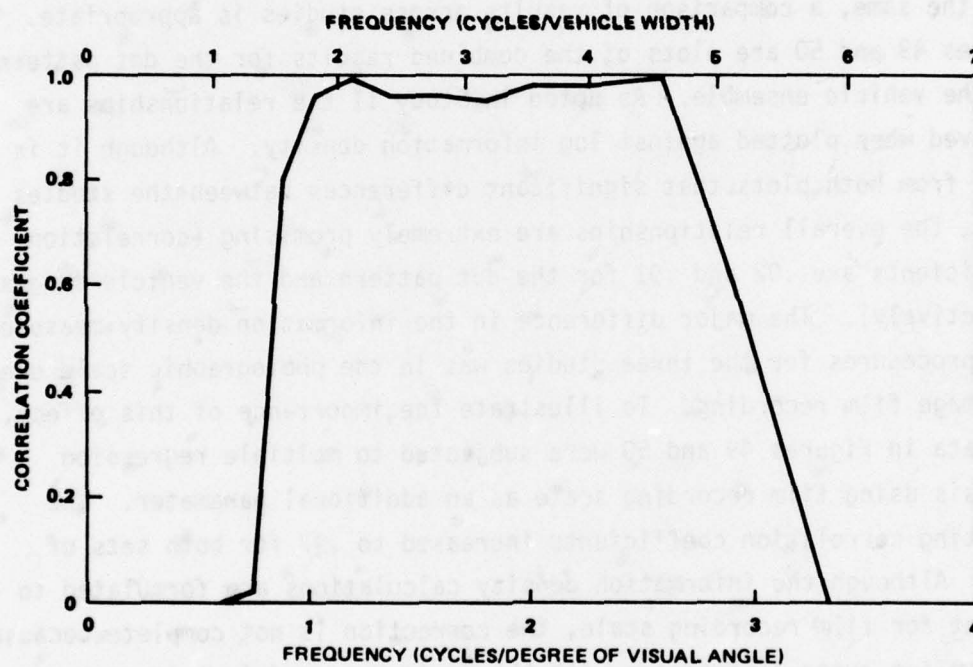

Figure 47.   Relationship Between Vehicle Ensemble Information Density and Observer Performance Scores for Study III

Figure 48. Correlations of Vehicle Ensemble Individual Spectrum Values With Observer Performance for Study III

103

the image noise distribution is not properly effective. There was
little difference in the noise power spectra among the 3 bit-level
conditions. Had these spectra adequately reflected the quantization noise
effects, information density differences would have been much larger.
It is clear that improved techniques for noise measurement will be
required for proper evaluation of digitized imagery.

COMBINED STUDY RESULTS

The three individual studies involved variation of different display
parameters. However, since the performance task and performance measures
were the same, a comparison of results across studies is appropriate.
Figures 49 and 50 are plots of the combined results for the dot pattern
and the vehicle ensemble. As noted in Study II the relationships are
improved when plotted against log information density. Although it is
clear from both plots that significant differences between the studies
exist, the overall relationships are extremely promising (correlation
coefficients are .92 and .91 for the dot pattern and the vehicle images,
respectively). The major difference in the information density measure-
ment procedures for the three studies was in the photographic scale used
for image film recording. To illustrate the importance of this effect,
the data in Figures 49 and 50 were subjected to multiple regression
analysis using film recording scale as an additional parameter. The
resulting correlation coefficients increased to .97 for both sets of
data. Although the information density calculations are formulated to
correct for film recording scale, the correction is not complete because
of sampling error differences with the equipment used in this work.

An additional finding that is common to all studies is the relationship
of the diagonal bar information density values with the logarithmic mean
of the horizontal and vertical measures. Figure 51 is a plot of this
relationship for all three studies. The correlation coefficient is .98.
While this relationship is only of secondary interest to the objectives
of this effort, this result adds considerable evidence for the validity
of the diffraction pattern sampling/information density approach as a
measure of display performance.

104

Figure 49. *Relationship Between Dot Pattern Information Density Values and Observer Vehicle Recognition Performance for All Studies. The Solid Line Is the Least-Squares Linear Fit*
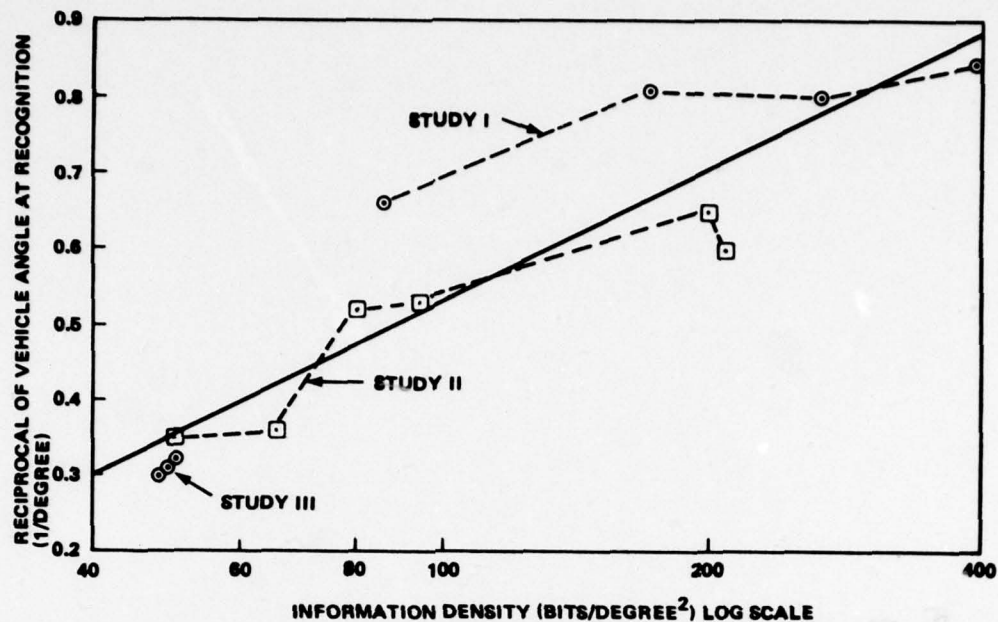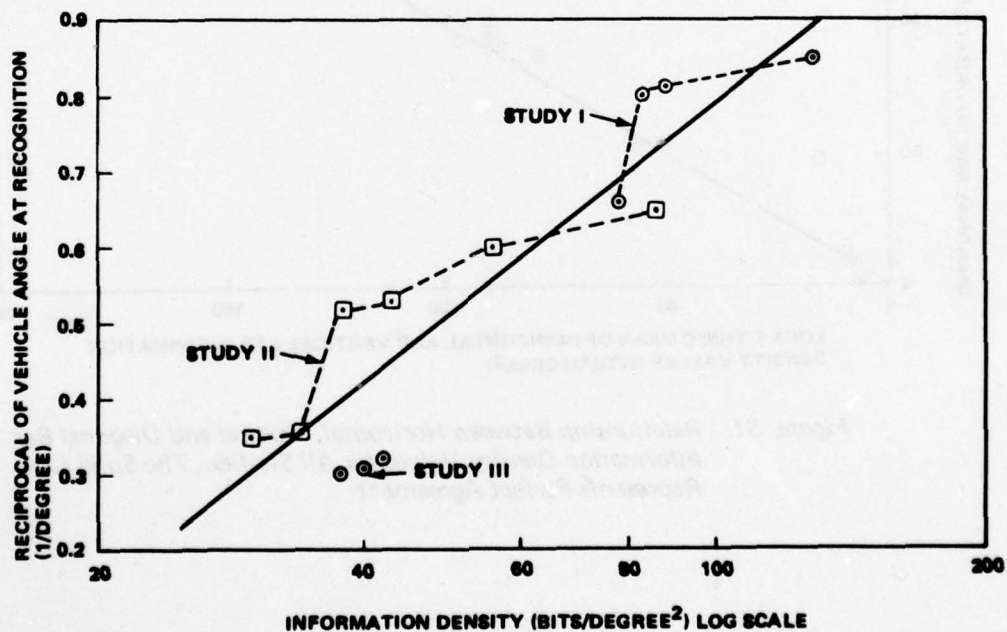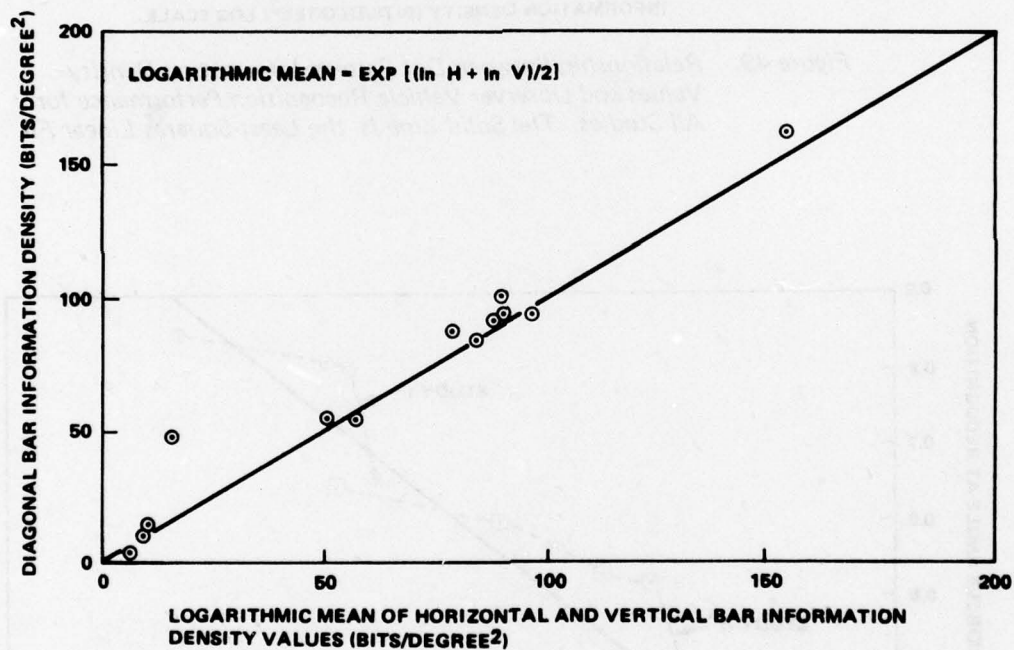

Figure 50. *Relationship Between Vehicle Ensemble Information Density Values and Observer Vehicle Recognition Performance for All Studies. The Solid Line Is the Least-Squares Linear Fit*

105

Figure 51. Relationship Between Horizontal, Vertical and Diagonal Bar Information Density Values for All Studies. The Solid Line Represents Perfect Agreement

SECTION V
CONCLUSIONS AND RECOMMENDATIONS

Optical power spectrum analysis using diffraction pattern sampling and
the information theory framework is found to be a very promising tool
for display imagery evaluation. The relationship between information
density and display dynamic range and bandwidth show good promise for
display calibration and performance evaluation. The speed and simpli-
city of this approach is an important consideration in the application
of these findings. The approach is found to be very robust with respect
to the theoretical assumption of image rotational symmetry. Relation-
ships remain stable in spite of very large differences in performance as
a function of orientation.

The relationships with observer target recognition performance is sub-
stantial in spite of several apparent deficiencies in the techniques
used here. The results suggest a number of areas for improving the
application of this approach.

1) Low frequency measurements are not acceptable with the present
   techniques. This problem must be corrected with better image
   scaling and/or correction techniques for measuring aperture and
   center spot scatter.

2) High frequency measurements do not relate well to observer
   performance. The application of visual threshold data may
   significantly enhance the predictive validity of the infor-
   mation theory approach.

3) Variations in the film recording scale are not completely
   compensated for in the procedures for calculating infor-
   mation density. Procedures must be improved or recording
   scale standardized for improved comparability of results.

107

4)   The measurement of quantization noise in digitized imagery
     must be improved for a proper evaluation of this class of
     imagery. The most direct solution is the proper preparation
     of noise samples for power spectrum measurement. These
     samples should represent a random dot pattern with a signal
     range equal to one step interval in the coding scheme employed
     in digitization.

5)   Although less obvious than the preceding problems, there is
     some evidence that at very low display performance levels and
     consequently, very low image content levels, the measuring
     equipment signal-to-noise levels are marginal. Increased
     light levels i.e., increased laser power, for the optical
     power spectrum measurement should improve this situation.

The results of this effort bear on an additional question of importance
to the application of the diffraction pattern sampling approach; what is
the best class of input imagery to use for evaluation? The use of the
random bar pattern, because of the capability to measure display perfor-
mance as a function of orientation, appears to be the preferred tech-
nique for the evaluation of general display performance levels. Evalu-
ation with respect to observer target recognition performance is most
effective, according to the results here, with either the random dot
pattern or the vehicle image ensemble. On this basis alone, the random
dot pattern is preferred since it requires only one measurement compared
to the 10 or 15 used for the vehicle ensemble values. These results,
however, should not be considered conclusive until the problems listed
above are resolved.

In a separate analysis, information density values were calculated for
each vehicle rather than for the vehicle ensemble. It was noted that,
with one exception, the standard deviation of the information density
values within a given display condition related well with observer
recognition performance (correlation = .95). This is not unexpected if
we consider that the observer's task is really that of discrimination.

108

He must decide which of the five candidate vehicles is represented by the CRT image. The display condition that maximizes the differences among the vehicle images will provide for the easiest discrimination. The standard deviation is a measure of the magnitude of those differences. The exception occurred for the lowest bandwidth condition in Study II. In this condition, the lack of radial symmetry inflated the standard deviation because of exaggerated orientation effects. The use of the standard deviation or some other measure of variability appears to be a promising approach provided that the assumption of radial symmetry is not seriously violated. Further study of this approach is recommended.

109

APPENDIX A
EVALUATION OF INFORMATION DENSITY
MEASUREMENT PROCEDURES

MEASURING APERTURE SIZE AND SHAPE

It is necessary to limit the image area being measured, usually with the insertion of a limiting aperture at the film plane. This aperture distorts the resulting measurement in a complicated manner. Satisfactory techniques for correcting for this aperture effect have not yet been developed. Since the magnitude of the effect is related to the size and shape of the aperture, it is important to select a configuration that introduces the least amount of error. The effects of size and shape were evaluated through a series of measurements taken on the random level dot pattern. Three shapes were considered; circular, rectangular, and "circular Gaussian." The latter shape was achieved by using the intensity distribution of the collimated laser beam and limiting the diameter at the first null of that distribution. The influence of size for the circular aperture is illustrated in Figure A-1 for diameters of 1/4 and 3/4 inches. Comparison of the measured curves with the theoretical level of 4 bits per cycle shows the fall-off below 2 cycles per millimeter that is at least partially the result of the aperture effect.

Figure A-2 is a plot of information density as a function of aperture area for the three shapes tested. The circular aperture is the most convenient and practical to use with the present measuring equipment. In addition, the circular aperture provides the anticipated relationship between aperture area and capacity. The results in Figure A-2 do not justify the use of other shapes. The advantages of increasing size decline above an area of 285 mm^2, (3/4 in. diameter circular aperture). These results lead to the recommendation to use the largest possible circular aperture consistent with the size of the relevant image content to be measured. A possible exception to this recommendation lies in the use of a smaller aperture to sample the desired image area with a number of measurements. This consideration is treated below.
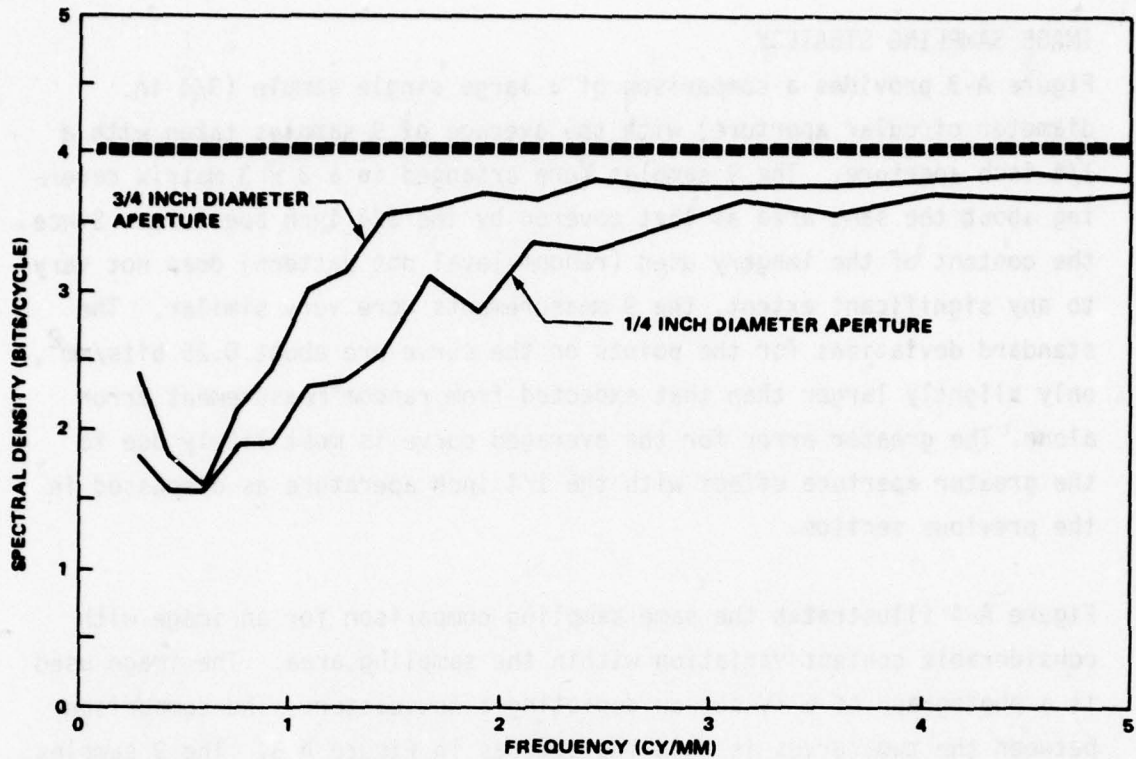
Figure A-1. *Comparison of Two Measurement Aperture Diameters. The Theoretical Spectrum is Flat at 4 Bits/Cycle.*
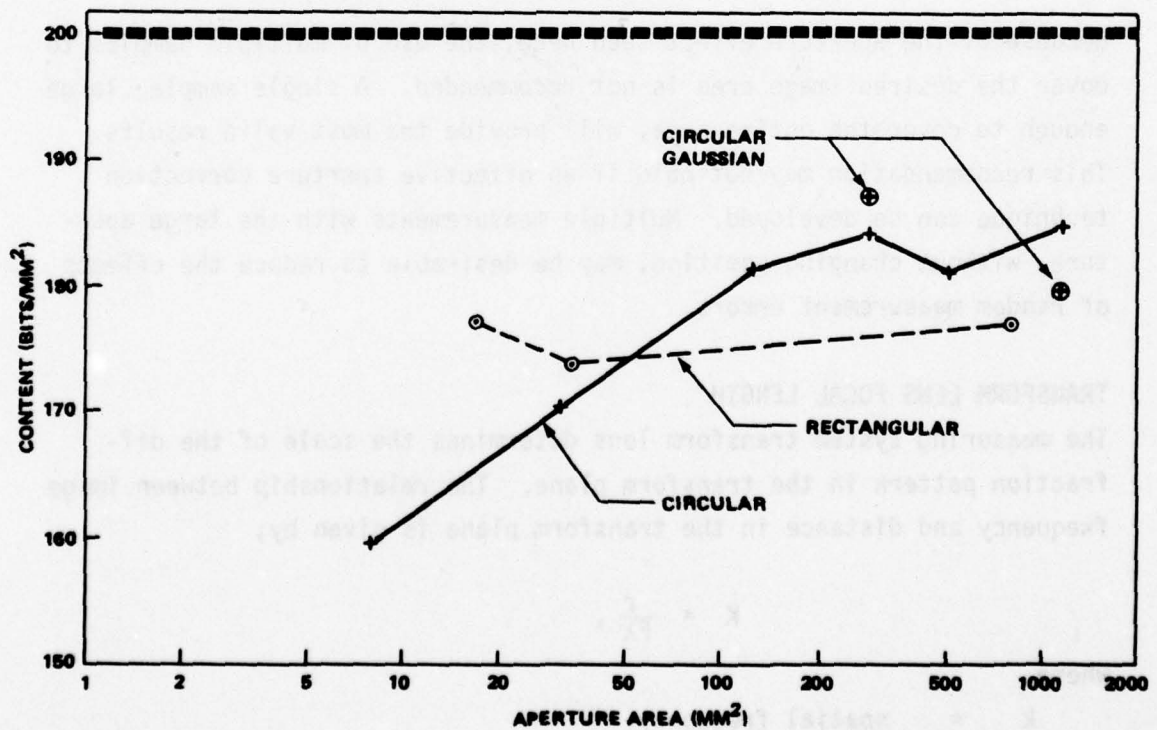

Figure A-2. *Effects of Aperture Area for Several Shapes. The Theoretical Content Value is 200 Bits/mm²*

IMAGE SAMPLING STRATEGY

Figure A-3 provides a comparison of a large single sample (3/4 in. diameter circular aperture) with the average of 9 samples taken with a 1/4 inch aperture. The 9 samples were arranged in a 3 x 3 matrix covering about the same area as that covered by the 3/4 inch aperture. Since the content of the imagery used (random-level dot pattern) does not vary to any significant extent, the 9 measurements were very similar. The standard deviations for the points on the curve are about 0.25 bits/mm^2, only slightly larger than that expected from random measurement error alone. The greater error for the averaged curve is most likely due to the greater aperture effect with the 1/4 inch aperature as discussed in the previous section.

Figure A-4 illustrates the same sampling comparison for an image with considerable content variation within the sampling area. The image used is a photograph of a TV screen depicting a newscaster. The comparison between the two curves is much the same as in Figure A-3. The 9 samples show a much greater variation, however, because of content differences.

Because of the aperture effect seen here, the use of multiple samples to cover the desired image area is not recommended. A single sample, large enough to cover the entire area, will provide the most valid results. This recommendation may not hold if an effective aperture correction technique can be developed. Multiple measurements with the large aperture, without changing position, may be desirable to reduce the effects of random measurement errors.

TRANSFORM LENS FOCAL LENGTH

The measuring system transform lens determines the scale of the diffraction pattern in the transform plane. The relationship between image frequency and distance in the transform plane is given by;

$$K = \frac{r}{F\lambda} ,$$

where,

k = spatial frequency,

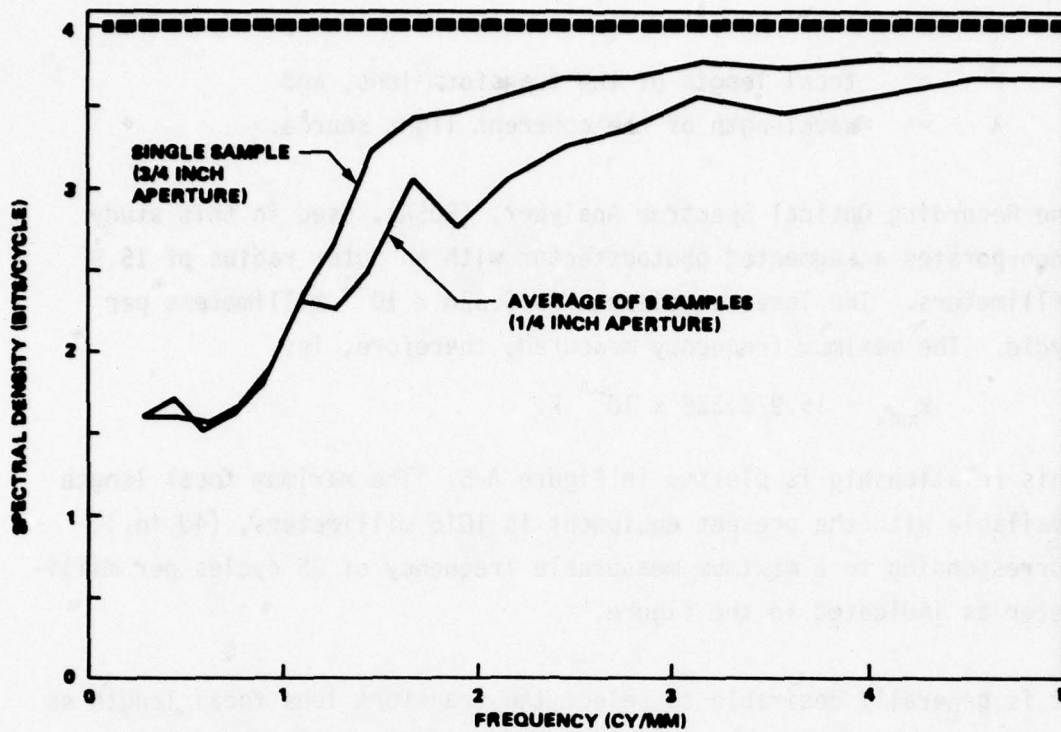r = distance in the transform plane,

112

Figure A-3. Comparison of Two Sampling Strategies for a Uniform Content Image
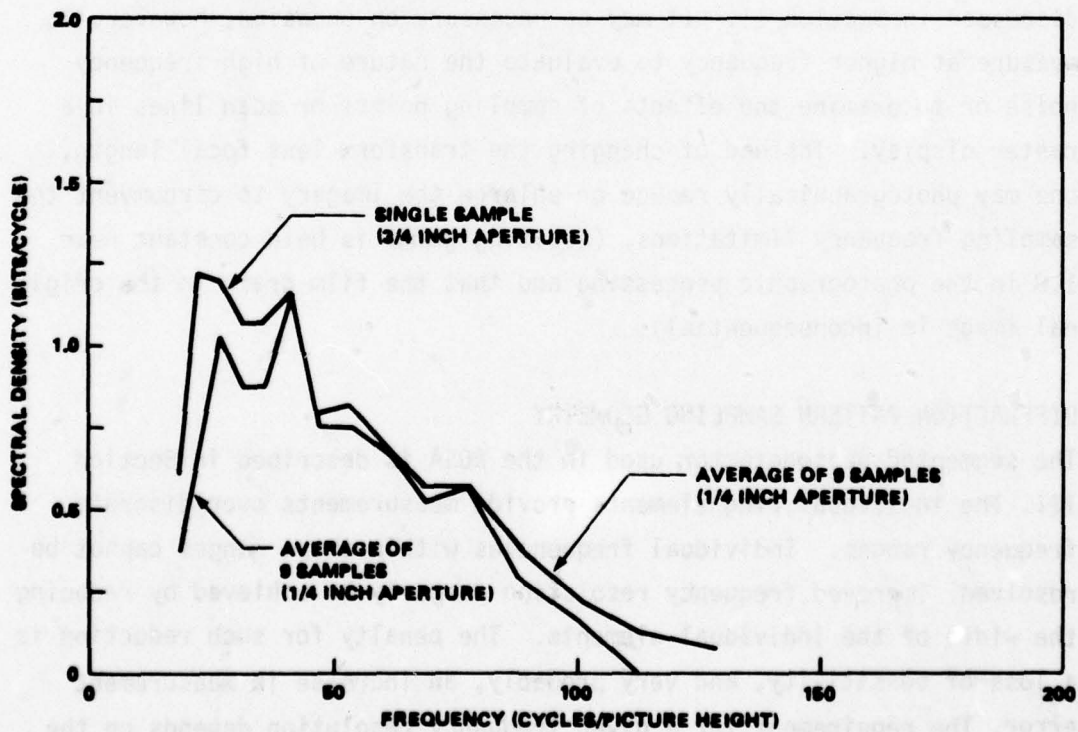(Random Dot Pattern).

Figure A-4. Comparison of Two Sampling Strategies for a Variable Content Image
(T.V. Newscaster).

113

F   =   focal length of the transform lens, and

λ   =   wavelength of the coherent light source.

The Recording Optical Spectrum Analyzer, (ROSA), used in this study incorporates a segmented photodetector with an outer radius of 15.9 millimeters. The laser wavelength is 6.328×10^{-4} millimeters per cycle. The maximum frequency measured, therefore, is;

$$k_{max} = 15.9/6.328 \times 10^{-4} \; F.$$

This relationship is plotted in Figure A-5. The maximum focal length available with the present equipment is 1016 millimeters, (40 in.), corresponding to a maximum measurable frequency of 25 cycles per millimeter as indicated in the figure.

It is generally desirable to select the transform lens focal length so that k_{max} coincides with the maximum frequency of interest in the imagery. This is generally the limiting frequency or Nyquist limit as discussed in Section II. It may be necessary on occasion, however, to measure at higher frequency to evaluate the nature of high frequency noise or to examine the effects of sampling points or scan lines in a raster display. Instead of changing the transform lens focal length, one may photographically reduce or enlarge the imagery to circumvent the sampling frequency limitations, (assuming gamma is held constant near 1.0 in the photographic processing and that the film grain in the original image is inconsequential).

DIFFRACTION PATTERN SAMPLING GEOMETRY

The segmented photodetector used in the ROSA is described in Section III. The individual ring elements provide measurements over discrete frequency ranges. Individual frequencies within these ranges cannot be resolved. Improved frequency resolution can only be achieved by reducing the width of the individual elements. The penalty for such reduction is a loss of sensitivity, and very probably, an increase in measurement error. The requirement for a given frequency resolution depends on the

114
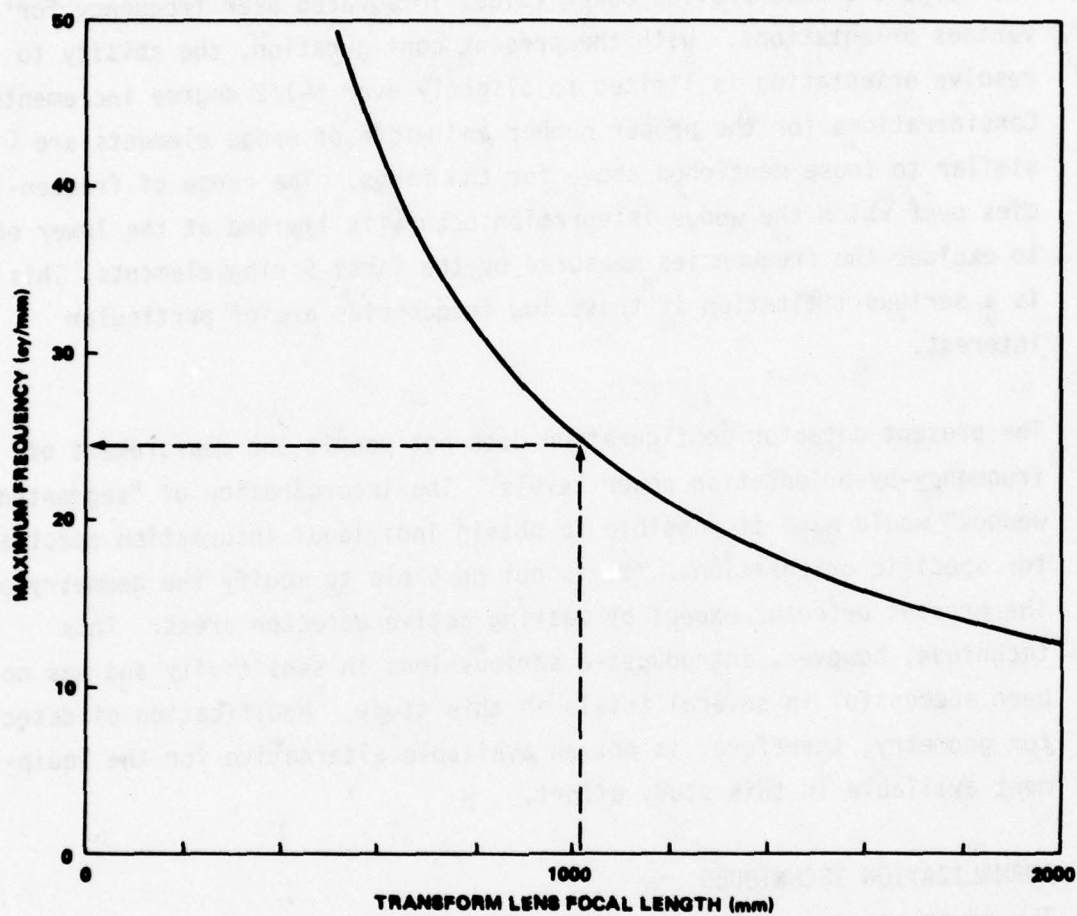
Figure A-5. *OPS Measurement Frequency Range as Determined by the Transform Lens Focal Length. The Focal Length Used in This Study is 1016 mm.*

objectives of the power spectrum measurements. With our present state of knowledge, determination of such requirements is largely a matter of experience gained in specific applications.

The wedge elements provide power values integrated over frequency for various orientations. With the present configuration, the ability to resolve orientation is limited to slightly over 5-1/2 degree increments. Considerations for the proper number and width of wedge elements are similar to those mentioned above for the rings. The range of frequencies over which the wedge integration occurs is limited at the lower end to exclude the frequencies measured by the first 5 ring elements. This is a serious limitation if these low frequencies are of particular interest.

The present detector configuration does not permit the measurement of frequency-by-orientation power levels. The incorporation of "segmented wedges" would make it possible to obtain individual information spectra for specific orientations. It is not possible to modify the geometry of the present detector except by masking active detector areas. This technique, however, introduces a serious loss in sensitivity and has not been successful in several trials in this study. Modification of detector geometry, therefore, is not an available alternative for the equipment available in this study effort.

NORMALIZATION TECHNIQUES

The power spectrum values are directly proportional to the average intensity of the light transmitted by the image during measurement. It is necessary, in most instances, to correct the spectrum values for differences in laser light level and/or differences in average film transmission. A common approach involves the use of the zero frequency power level as a normalizing factor. In practice, however, it is very difficult to obtain an accurate and reliable measure of the zero frequency value. Detector positioning, for example, has a very large effect on the measured zero frequency value. Control of positioning to the levels of accuracy required is extremely difficult. An alternate technique, often used in electronics, uses the total transmitted energy

rather than only the zero frequency component. Total energy can be measured with greater reliability, and since normalization will apply to both the signal spectrum and the noise spectrum, only relative energy need be measured. During evaluation of this technique, a simple method was devised to measure relative total energy with the ROSA. A "perfect" diffuser produces a uniform diffraction pattern. The intensity in any area in this pattern is proportional to the total energy in the pattern. Insertion of a diffuser between the film plane and the transform lens provides values in each of the rings that are proportional to the total energy in the image diffraction pattern. The outermost ring (Ring 32), has been selected for use here because it has the largest area and provides the most stable measurement.

The random-level dot pattern images were carefully controlled to have the same transmittance values. When the images are measured with the same laser light level, normalization is not necessary to control for light level variations. A comparison was made among the three normalization conditions; none, zero frequency, and total energy. The results, representing the means of 10 repeated measurements, are shown in Figure A-6. The zero frequency normalization provides the best average agreement with the theoretical value of 200 bits/mm^2. However, the standard deviation of the 10 repeated measurements, as listed in Table A-1, is nearly an order of magnitude higher for the zero frequency normalization.

It would be best to use imagery that does not vary in transmission and thus to avoid the normalization problem entirely. This situation, however, rarely occurs outside of controlled laboratory conditions and normalization must be used in most practical applications. For the purposes of this study, absolute accuracy is considered less important than measurement precision. Consequently, total energy normalization was selected for use in this study because of its superior stability.
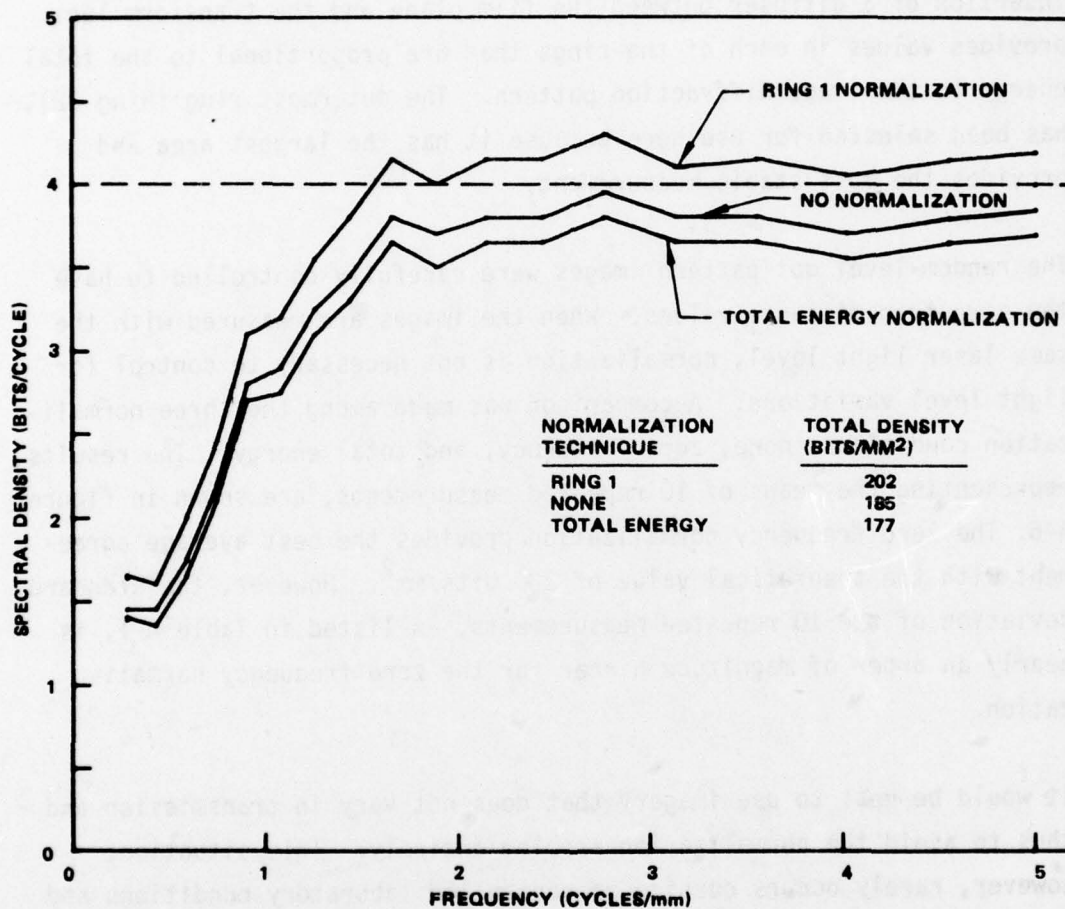
Figure A-6. Comparison of Normalization Techniques Using the Random Dot Imagery. Theoretical Values are 4 Bits/Cycle for the Spectrum and 200 Bits/Millimeter² for the Total Information Density.

Table A-1:   Stability Evaluation of
               Normalization Techniques

Normalization	Standard Deviation
Zero Freq.	16.3 bits/mm^2
None	1.7 bits/mm^2
Total Energy	1.9 bits/mm^2

CRT INTEGRATION TIME

Standard 2:1 interlace systems in the United States operate at a rate of
30 frames per second. The effects of visual or photographic integration
on information density are not obvious for CRT displays of static ima-
gery. If the display noise is random, the integration should have a
smoothing effect with a resulting increase in information density.

The effects of integration time were evaluated using a random dot pat-
tern as an input to a closed circuit television system. The television
camera was a Sierra Scientific Co. Model LSV 1.5 and the CRT display was
a 14 inch, 525 line, Mirac monitor. The TV camera output was recorded
on the disc memory of a video signal processor. To assure consistent
and representative noise inputs, measurements were made using a blank
sheet of the same paper on which the dot pattern was printed. The
luminance of this input was modified with a neutral density filter, (50%
transmission), to match the average luminance of the dot pattern. The
CRT was photographed with a 35mm camera using a 55mm Vivitar lens at a
scale of 1:27. Tri-X film was used and developed in D-19 for 10 minutes
at 68°F. The resulting gamma was 0.98, (a gamma of 1.0 provides equality
between input and obtained image contrast values). Exposure times for
both the dot pattern and the noise input were at 1/30, 1/15, and 1/8
seconds. These values provided integrations of 1, 2, and 4 frames,
respectively. The negatives were measured with the ROSA using a 1016mm
focal length transform lens and a 1/4 inch diameter circular aperture,

119

the largest usable under the constraints of the film image size. Figure A-7 presents the information spectra for the three integration times. These results show no significant differences resulting from increased integration. Examination of the three noise power spectra presented in Figure A-8 shows very little difference in the noise curves over the frequency range of interest. Variation in the "spikes" at the scan line frequency is clearly evident. This is the result of the blending of the lines with integration. Such a result is to be expected if the lines were not perfectly registered from frame to frame.

The lack of an integration effect indicates that the noise levels in the TV system used here are not sufficient to produce measurable differences with present equipment and techniques. If, however, these levels are sufficient to produce a significant effect in viewer performance, then the limited sensitivity in the optical power spectrum measurements is a serious problem.

FILM RECORDING

Selection of optimum materials, equipment and procedures for film recording of the CRT display is a very complex task. There are too many factors involved to permit a systematic study within the scope of this effort. Choices have been made largely on the basis of available knowledge and experience.

Image Scale

In order to utilize the entire frequency range of the ROSA detector, the Nyquist limit, (one-half the line frequency) as recorded on the film should coincide with the maximum measured frequency. With a 1016mm focal length transform lens, (the maximum available with the present equipment), the maximum frequency is 24.7 cycles per millimeter (see Figure A-5). With this criterion, a CRT display with 485 active lines should be photographed so that the display height measures 485/24.7x2 = 9.8mm. or about 0.4 inches on the film. There are, however, several disadvantages to this approach;
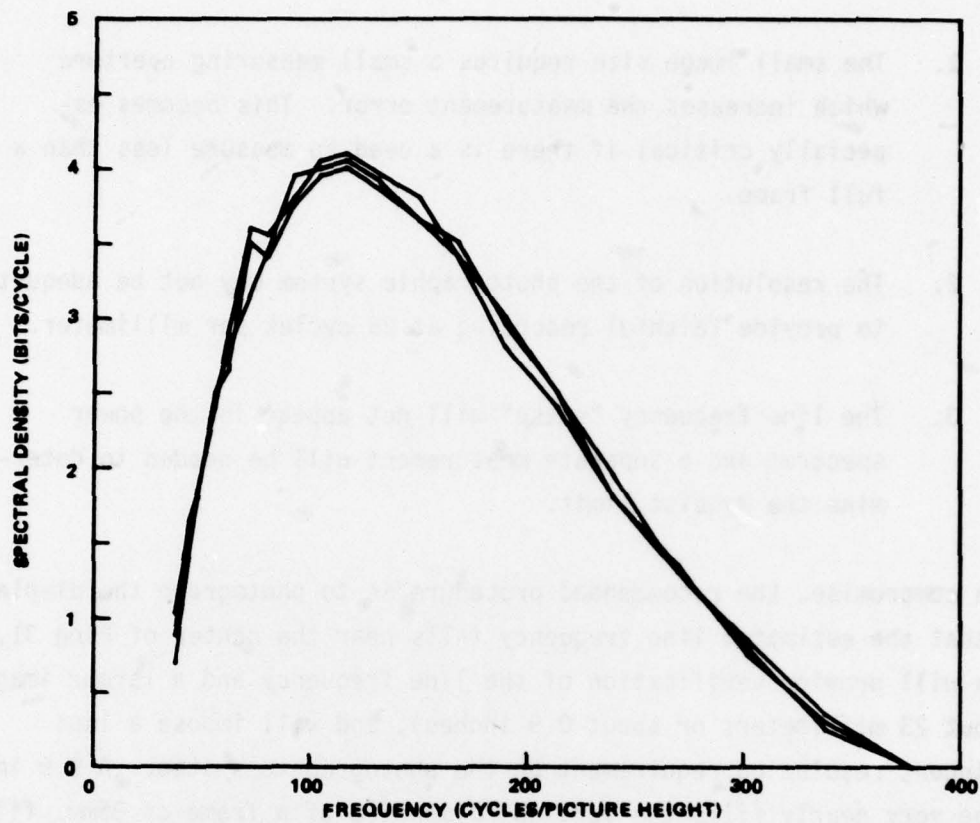
Figure A-7. Information Spectra for CRT Display of a Random Dot Pattern With Integrations of 1, 2, and 4 Frames.
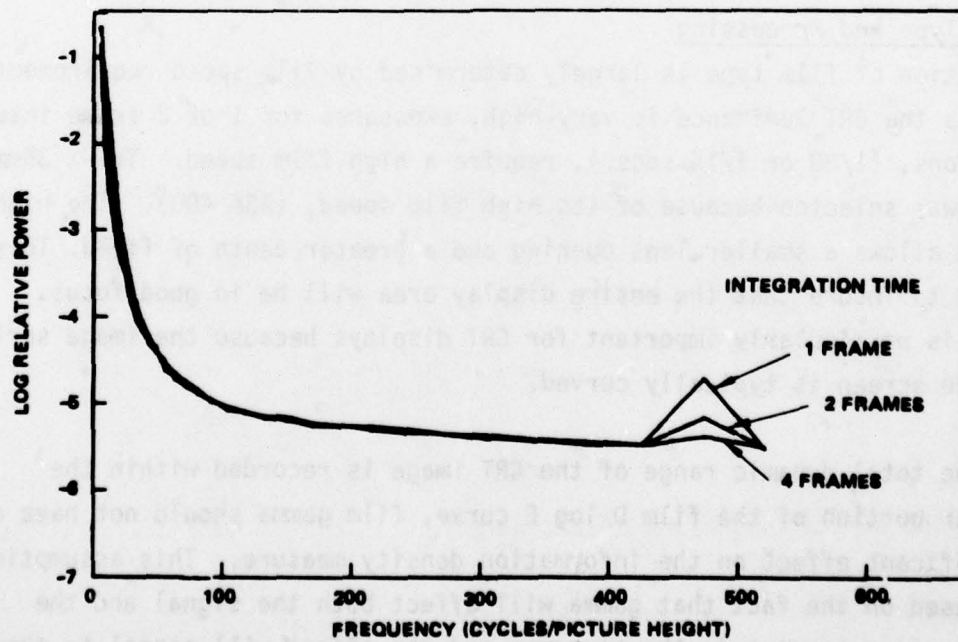

Figure A-8. CRT Noise Power Spectra With Integrations of 1, 2, and 4 Frames

121

1. The small image size requires a small measuring aperture which increases the measurement error. This becomes especially critical if there is a need to measure less than a full frame.

2. The resolution of the photographic system may not be adequate to provide faithful recording at 25 cycles per millimeter.

3. The line frequency "spike" will not appear in the power spectrum and a separate measurement will be needed to determine the Nyquist limit.

As a compromise, the recommended procedure is to photograph the display so that the estimated line frequency falls near the center of Ring 31. This will provide verification of the line frequency and a larger image, (about 23 millimeters or about 0.9 inches), and will impose a less stringent resolution requirement on the photographic system. A 0.9 inch image very nearly fills the vertical dimension of a frame of 35mm. film, (the image size on a standard 35mm "still" camera is 24 x 36 mm.).

Film Type and Processing

Selection of film type is largely determined by film speed requirements. Unless the CRT luminance is very high, exposures for 1 or 2 frame integrations, (1/30 or 1/15 secs.), require a high film speed. Tri-X 35mm film was selected because of its high film speed, (ASA 400). The high speed allows a smaller lens opening and a greater depth of field. This helps to insure that the entire display area will be in good focus. This is particularly important for CRT displays because the image surface on the screen is typically curved.

If the total dynamic range of the CRT image is recorded within the linear portion of the film D log E curve, film gamma should not have a significant effect on the information density measure. This assumption is based on the fact that gamma will affect both the signal and the noise power spectra in the same way and the effect will cancel in the

122

calculation of the signal-to-noise ratio. Since the assumptions, how-
ever, have not been verified, processing should be adjusted to provide a
film gamma as close to unity as possible.

Camera Positioning

To avoid excessive scale variation over the format, the camera must be
positioned so that its optical axis intersects the center of the display
screen and is perpendicular to the screen at that point. Screen curva-
ture will impose some scale variations, particularly in the corners, but
the effect on the total measurement is expected to be minor.

Shutter Synchronization

Ideally, the film should record in exact frame increments. To accom-
plish this, the camera shutter must be synchronized with the video
signal to open exactly at the beginning of a frame and close at the end
of the desired number of frames. Failure to synchronize will have two
effects:

1. If the exposure begins in the middle of a frame scan, only
    part of the first field will be recorded and it will be
    followed by the initial part of the succeeding field. If,
    for example, a single TV frame exposure is made and begins in
    the center of the scan, then the bottom half of the film image
    will consist of fields 1 and 2, and the top half will record
    fields 2 and 3.

2. Since shutters do not open and close instantly, variations
    in exposure over the frame will occur. Focal plane shutters
    will produce banding if the shutter is out of phase with the
    scanning spot. If the shutter is moving parallel to the scan
    lines, the band will occur along a diagonal of the image. The
    size of the band will be a function of the exposure accuracy.

123

These effects will be most serious for moving imagery and single frame exposures. With static imagery and longer integration times, (2 frames or more), these problems do not appear to have an observable effect on the power spectrum measurements. Informal testing, with and without banding, failed to demonstrate significant differences. For the conditions of this study effort, the complexities of shutter synchronization were considered to be unimportant.

124

APPENDIX B
ANALYSIS OF VARIANCE SUMMARIES

Analysis of variance tests for the bar pattern information density
values and observer performance data are summarized below. Interaction
terms above the first-order are not shown. None were significant.
Tests for the dot pattern and vehicle ensemble values were not possible
since only one value per display condition was available.

STUDY I

Bar Pattern (Fixed effects model)

Source	Degrees of Freedom	Mean Square	F-Ratio
Dynamic Range	3	13321	121.01*
Orientation	2	480	4.36
Error	6	110	

(*significant result, $\alpha \leq .05$)

Observer Performance (Mixed Model; Subjects as Random)

Source	Degrees of Freedom	Mean Square	F-Ratio
Target (T)	4	5.12	16.29*
Dynamic Range (D)	3	3.64	22.57*
Orientation (O)	1	1.08	4.44
Subjects (S)	7	1.81	39.08*
T x D	12	0.09	1.23
T x O	4	0.85	3.62*
T x S	28	0.31	6.79*
D x O	3	0.12	1.51
D x S	21	0.16	3.48*
O x S	7	0.24	5.25*

(*significant result, $\alpha \leq .05$

STUDY II

Bar Pattern (Fixed Effects Model)

Source	Degrees of Freedom	Mean Square	F-Ratio
Bandwidth (B)	2	4693.1	391.08*
Orientation (O)	2	4121.1	343.43*
Noise (N)	1	1.0	0.08
B x O	4	1289.0	107.42*
B x N	2	43.1	3.59
N x O	2	8.4	0.67
Error	4	12.5	

(*significant result $\alpha \leq$ .05)

Observer Performance (mixed model; subjects as random)

Source	Degrees of Freedom	Mean Square	F-Ratio
Target (T)	4	4.08	11.82*
Bandwidth (B)	2	72.35	146.91*
Noise (N)	1	0.70	4.08
Orientation (O)	2	3.74	22.65*
Subject (S)	5	4.30	39.95*
T x B	8	0.31	1.45
T x N	4	0.14	2.72
T x O	8	1.48	7.49*
T x S	20	0.35	3.21*
B x N	2	0.13	1.21
B x O	4	0.32	1.92
B x S	10	0.49	4.58*
N x O	2	0.01	0.08
N x S	5	0.17	1.60
O x S	10	0.17	1.53

(*significant result, $\alpha \leq$ .05)

STUDY III

Bar Pattern (Fixed effects model)

Source	Degrees of Freedom	Mean Square	F-Ratio
Bit Level	2	111.0	13.32*
Orientation	2	1785.0	214.24*
Error	4	8.3	

(*significant result, $\alpha \leq .05$)

Observer Performance (Mixed model; subjects as random)

Source	Degrees of Freedom	Mean Square	F-Ratio
Target (T)	4	8.32	11.27*
Bit-Level (B)	2	4.49	18.71*
Orientation (O)	1	0.01	.04
Subject (S)	8	5.92	58.20*
T x B	8	0.52	3.45*
T x O	4	1.50	4.17*
T x S	32	0.73	7.15*
B x O	2	0.16	3.76*
B x S	16	0.24	2.37*
O x S	8	0.40	3.89*

(*significant result, $\alpha \leq .05$)

REFERENCES

1. Armstrong, S. and Thompson, B., Comparison of Coherent and Incoherent Optical Spectrum Analysis Techniques in Image Evaluation, Proc. Soc. Photo-Optical Instr. Eng., Vol. 117, pp. 57-66, 1977.

2. Blakemore, C., Muncey, J. P. J. and Ridley, R. M., Stimulus Specificity in the Human Visual System, Vision Res., Vol. 13, pp. 1915-1931, 1973.

3. Campbell, F. W. and Robson, J. G., Application of Fourier Analysis to the Visibility of Gratings, J. Physiol., 197, pp. 551-566, 1968.

4. Dainty, J. C. and Shaw, R., Image Science - Principles, Analysis and Evaluation of Photographic Type Imaging Processes, Academic Press, New York, 1974.

5. Ditchburn, R. W., Light, 2nd Edition, Interscience Publishers, 1963.

6. Fellgett, P. B. and Linfoot, E. H., On the Assessment of Optical Images, Royal Soc. of London, Phil. Trans. Series A, Vol. 247, No. 931, pp. 369-407, 1955.

7. Ginsburg, A. P., Psychological Correlates of a Model of the Human Visual System, IEEE Proc. 1971 NAECON, pp. 283-290, 1971.

8. Ginsburg, A. P., The Perception of Visual Form: A Two Dimensional Filter Analysis, In Information Processing in the Visual System; Proc. of the IV Symposium on Sensory System Physiology (Glezer, V. D., Ed.) I. P. Pavlov Institute of Physiology, Leningrad, U.S.S.R., pp. 46-51, 1976.

9. Goodman, J. W., Introduction to Fourier Optics, McGraw-Hill Book Co., New York, 1968.

10. Harris, J. L., Resolving Power and Decision Theory, J. Opt. Soc. Amer., Vol. 54, No. 3, pp. 606-611, 1964.

11. Humes, J. M. and Bauerschmidt, D. K., Low Light Level TV Viewfinder Simulation Program. Phase B, The Effects of Television System Characteristics Upon Operator Target Recognition Performance. AFAL-TR-68-271 (AD 849 339), Air Force Avionics Laboratory, Wright-Patterson Air Force Base, Ohio, 1978.

12. Jensen, N., High Speed Image Analysis Technique, Photogrammetric Eng., Vol. 39, pp. 1321-1328, 1973.

13. Johnson, D. M., Target Recognition on TV as a Function of Horizontal Resolution and Shades of Gray. Human Factors, Vol. 10, pp. 201-210, 1968.

14. Kasdan, H. L., Optical Power Spectrum Sampling and Algorithms, Proc. Soc. Photo-Optical Instr. Eng., Vol. 117, pp. 67-74, 1977.

15. Leachtenauer, J. C., Optical Power Spectrum Analysis: Scale and Resolution Effects, Photogrammetric Eng. & Remote Sensing, Vol. 43, No. 9, pp. 1117-1125, 1977.

16. Lendaris, G. C. and Stanley, G. L., Diffraction Pattern Sampling for Automatic Pattern Recognition, Proc. of IEEE, Vol. 58, No. 2, pp. 198-216, 1970.

17. Lipson, H. and Walkley, K., On the Validity of Babinet's Principle for Fraunhofer Diffraction, Optica Acta, Vol. 15, No. 1, pp. 83-91, 1968.

18. Lukes, G. E., Rapid Screening of Aerial Photography by OPS Analysis, Proc. Soc. Photo-Optical Instr. Eng., Vol. 117, pp. 89-97, 1977.

19. Martin, W. L. and Task, H. L., Matrix Element Display Devices and Their Application to Airborne Weapon Systems. Paper presented at 33rd meeting of Aerospace Medical Panel of Advisory Group (AGARD/NATO), Athens, Greece. Also identified by Aerospace Medical Research Laboratory, WPAFB, Ohio, as AMRL-TR-76-49 (AD A027-449), 1976.

20. Nill, N., The Moment as an Image Quality Merit Factor for Scene Power Spectra, Applied Optics, Vol. 15, p. 2846, 1976.

21. Schindler, R., Optical Power Spectrum Analysis of Display Imagery Phase I: Concept Validity, AMRL-TR-76-96 (AD A035-377), Aerospace Medical Research Laboratory, Wright Patterson AFB, Ohio, 1976.

22. Schindler, R., Error Sources in Diffraction Pattern Sampling for Optical Power Spectrum Measurements, Proc. Soc. Photo-Optical Instr. Eng., Vol. 117, pp. 50-56, 1977.

23. Shannon, R. R. and Cheatham, P. S., Optical Power Spectrum Measurements, Optical Sciences Center Report, Univ. of Arizona, 1976.

24. Shaw, R., The Application of Fourier Techniques and Information Theory to the Assessment of Photographic Image Quality, Photo. Sci. and Eng., Vol. 6, No. 5, pp. 281-286, 1962.

25. Smith, F. G., and Thompson, J. H., Optics, John Wiley & Sons Ltd., New York, 1971.

26. Stark, H., Bennett, W. R. and Arm, M., Design Considerations in Power Spectra Measurements by Diffraction of Coherent Light, Applied Optics, Vol. 8, No. 11, pp. 2165-2172, 1969.

27. Swing, R. E. and Shin, M. C., The Determination of Modulation - Transfer Characteristics of Photographic Emulsions in a Coherent Optical System, Photo Sci. and Eng., Vol. 7, No. 6, pp. 350-360, 1963.

28. Task, H. L. and Verona, R. W., A New Television Quality Measure Relatable to Observer Performance, AMRL-TR-76-73 (AD A030-568), Aerospace Medical Research Laboratory, Wright Patterson AFB, Ohio, 1976.

29. Thiry, H., Power Spectrum of Granularity as Determined by Diffraction, J. Photo. Sci., Vol. 11, pp. 69-77, 1963.

30. Vander Lugt, A. and Mitchel, R. H., Technique for Measuring Modulation Transfer Functions of Recording Media, J. Opt. Soc. Amer., Vol. 57, No. 3, pp. 372-379, 1967.